FUNCTIONAL CHARACTERIZATION AND MODELING OF FACTORS INVOLVED IN HIGH GRADE SEROUS OVARIAN CARCINOMA INITIATION

A Dissertation

Presented to the faculty of the Graduate School

of Cornell University

In partial fulfillment of the requirements for the degree of

Doctor of Philosophy

By

Robert Joseph Yamulla

May 2020

© 2020 Robert Joseph Yamulla

FUNCTIONAL CHARACTERIZATION AND MODELING OF FACTORS INVOLVED IN HIGH GRADE SEROUS OVARIAN CARCINOMA INITIATION

Robert Joseph Yamulla, PhD

Cornell University 2020

ABSTRACT

High grade serous ovarian carcinoma (HGSOC) is the most lethal form of ovarian cancer and is the fifth leading cause of female death in the western world. Unlike many other cancers, few viable HGSOC screening methodologies exist. HGSOC is consequently diagnosed at an advanced stage with substantial extraovarian metastases in most cases. These late stage diagnoses have hindered discovery of screening methods due to infrequent analyses of precursor lesions and uncertainty regarding HGSOC initiation mechanisms. Both the HGSOC "cell of origin" and mutations necessary for HGSOC initiation are the subject of substantial debate. Several candidate origin tissues exist in the ovarian surface epithelium (OSE), distal fallopian tubal epithelium (TE) and stem cell subpopulation of either tissue. Mutations associated with advanced HGSOC tumors have also been identified by the Cancer Genome Atlas Research Network (TCGA). However, most HGSOC-associated mutations have not been assessed as putative cancer driver mutations or passenger mutations in several putative cells of origin. In this dissertation, I performed functional screening of random combinations of suspected HGSOC driver genes in different putative cells of origin

using a lentiviral CRISPR/Cas9 library. Results support the ovarian surface epithelial stem cell (OSE-SC) theory of HGSOC initiation and suggest that most HGSOC-associated mutations are uninvolved in OSE-SC transformation. Random screening, along with *in vitro* and *in vivo* validation experiments, demonstrate that disruption of *Trp53*, *Rb1* and/or *Pten* are minimal OSE-SC transformation requirements, and that a few other HGSOC-associated genes may enhance transformation via *Trp53* and *Rb1*-related mechanisms. These results are the first published efforts to functionally test all putative drivers of HGSOC and have direct implications for production of HGSOC developmental models. Such models may be useful tools for ascertainment of novel HGSOC screening methodologies. Growth-inhibitory mutations uncovered via screening also have value as putative druggable targets. Finally, the screening methodology employed here represents a rapid means of differentiating driver and passenger mutations in any cell type for which *in vitro* culturing exists. It may therefore serve as an important tool for elucidation of driver mutations in other cancer types.

BIOGRAPHICAL SKETCH

Robert J. Yamulla grew up in Conyngham, Pennsylvania and is the oldest of four brothers. His interest in the sciences began in childhood through a love of nature and the outdoors. He spent a substantial amount of time catching frogs or insects with his father (Robert S. Yamulla) and finding ways to sneak them into his room, much to his mother's (Ann Yamulla) dismay. His love of nature eventually developed into passions for fishing, hunting, gardening, and hiking with his dogs. Robert attended Franklin and Marshall College, where he was originally enrolled as an environmental science major. His first experience with scientific research occurred when Dr. Timothy Sipe, a Franklin and Marshall Professor of Ecology and personal mentor, asked Robert to assist with his research efforts at Allee Memorial Forest in Indiana. Robert joined Dr. Sipe in Indiana, where he developed a passion for asking scientific questions. Robert and Dr. Sipe spent several years modeling the effect of low light regimes and deer overpopulation on old growth forest ecosystems. While working on ecological endeavors, Robert developed an interest in Cancer Biology during a work study experience with Dr. David M. Roberts at Franklin and Marshall College. Robert and Dr. Roberts worked collaboratively on a research project seeking to investigate the mechanistic role of the APC tumor suppressor protein in Wnt signaling and colon cancer. This research experience led to Robert's first "first author" paper and led him to pursue a career in Cancer Biology. Robert graduated Franklin and Marshall College as a biology major and moved to Ithaca to pursue a PhD in Cancer Biology in the Schimenti Laboratory at Cornell University. Dr. John Schimenti taught Robert to think and act independently as a scientist during his PhD studying ovarian carcinoma. Robert met Eileen Shu while

working in the Schimenti lab, who convinced him that his life needed significantly more pets. Together, they raise a Pitbull (Huckleberry), Samoyed (Sydney), cat (Finn), and Chilean Ground Squirrel (Didji), and hope to adopt several chickens in the near future. Robert is applying the skillset obtained during his PhD to business management following conferral of his degree in May 2020.

ACKNOWLEDGEMENTS

This dissertation could not have been accomplished without the mentorship and guidance of John Schimenti. John was an incredible supervisor who encouraged me to become an independent thinker throughout my PhD. Rather than simply provide protocols or order experiments to be accomplished, John trusted me to independently manage projects and consult with him when advice was needed. His leadership style has allowed me to develop into a legitimate scientist.

I also want to thank Adrian McNairn for his constant assistance and guidance throughout the production of this dissertation. Adrian was the first person I'd turn to whenever I needed help or advice in the lab. Despite his incredibly busy schedule, he was always willing to provide help, and I am incredibly grateful.

Prior to beginning this dissertation, most of my scientific experience was in forest ecology, a substantially different field than cancer biology. Consequently, there were quite a few technical skills that I needed to learn. Alexander Nikitin and Andrea Flesken-Nikitin shared their substantial ovarian cancer expertise whenever needed, and I thank them for their constant openness and assistance. I also thank Claudia Fischbach for providing perspectives on my progress and results throughout my PhD.

Timothy Sipe and David Roberts of Franklin and Marshall College served as my undergraduate thesis advisors and inspired me to pursue a career in the sciences. Their mentorship taught me the value of scientific inquiry, and I would certainly not be the scientist I am today if I did not learn from their examples.

I thank my parents, Robert and Ann Yamulla, for supporting me throughout my life and PhD. They have been encouraged my love of science throughout my life and provide support in all that I do.

I also thank Huckleberry (the Pitbull), Sydney (the Samoyed), Finn (the cat), and Didji (the Degu) for mental support. Despite their disregard for personal space, love of mud, and affinity for rolling in odd scents, my pets greatly enhance my life by providing friendship and mental wellbeing.

Finally, this dissertation wouldn't have been possible without my girlfriend, Eileen Shu. Eileen has been a constant source of encouragement and companionship. She is my best friend and the person I rely on most. My life and career wouldn't be nearly as fulfilling without her.

This work was supported by grants from the Ovarian Cancer Research Fund (#327516) and NYSTEM (C029155) to JCS and AYN, from the US National Institutes of Health (NIH) and National Cancer Institute (NCI) (CA182413) to AYN, and a predoctoral fellowship to RJY (NYSTEM C30293GG).

TABLE OF CONTENTS

ABSTRACT.....III - IV

BIOGRAPHICAL SKETCH.....V - VI

ACKNOWLEDGEMENTS.....VII - VIII

CHAPTER 1: Introduction.....1

1.1 High Grade Serous Ovarian Carcinoma: the most lethal gynecological malignancy.....1 - 2

1.2 HGSOC screening methodologies are insufficient for early detection and mortality reduction.....2 - 3

1.3 HGSOC may arise from either the ovarian surface epithelium (OSE) or distal fallopian tubal epithelium (TE) .....3 - 4

1.4 Genetic factors influence HGSOC incidence and prognosis.....4 - 5

1.5 Genetic screening has revealed HGSOC-associated mutations.....5 - 6

1.6 Genomic characterization of advanced HGSOC tumors cannot differentiate driver and passenger mutations.....6 - 7

1.7 CRISPR/Cas9-driven library screening methodologies can differentiate driver and passenger mutations in a high throughput manner.....7 - 8

1.8 Dissertation goals and accomplishments.....8 - 9

1.9 References.....10 - 16

CHAPTER 2: Most commonly mutated genes in High Grade Serous Ovarian Carcinoma are nonessential for ovarian surface epithelial stem cell transformation.....17

2.1 Abstract.....18

2.2 Introduction.....19 - 24

2.3. Results.....25

2.4 Strategy for screening candidate HGSOC suppressors and construction of a validated CRISPR-based lentiviral mini-library. .....25 - 28

2.5 Random combinatorial mutagenesis of candidate HGSOC driver genes in OSE-SC and OSE-NS.....29 - 32

2.6 Enrichment of mutated gene combinations in transformed OSE-SC samples.....33

2.7 *Trp53* loss alone is necessary but insufficient for OSE-SC transformation.....33 - 34

2.8 LentiCRISPRs targeting *Trp53*, *Rb1*, *Cdkn2a*, and *Pten* are overrepresented in OSE-SC transformants.....34 - 36

2.9 Mutations in *Trp53*, *Rb1*, *Pten*, and *Cdkn2a* function synergistically to promote transformation.....37

2.10 Disruption of *Ankrd11* or *Wwox* can further enhance transformation of *Trp53*-/*Cdkn2a*-/*Pten*- OSE-SC.....37 - 38

2.11 *Brca2* disruption deters transformation of *Trp53*-/*Rb1*- OSE-SC, but enhances transformation when co-mutated with *Trp53*, *Rb1*, and *Fancd2*.....39 - 40

2.12 *Rad51c* synergizes with *Fat3* and *Gabra6* to promote transformation.....40 - 42

2.13 LentiCRISPR integration patterns in OSE-NS transformants.....42

2.14 Discussion.....43 - 50

2.15 Acknowledgements.....50

2.16 Methods.....51 - 63

2.17 References.....64 - 70

CHAPTER 3: OSE-SC transformants grown *in vitro* do not recapitulate transcriptomic characteristics of human disease.....71

3.1 Abstract.....72

3.2 Introduction.....73

3.3. Minilibrary screening of putative HGSOC driver genes reveals distinct groups of putative transformation drivers in OSE-SC...73 - 74

3.4 Overrepresented target genes are associated with ovarian carcinoma subtypes.....74 - 75

3.5 Some cultured HGOSC models resemble human tumors.....75

3.6 *In vitro* HGSOC models with common HGSOC-associated mutations resemble human disease.....76 - 77

3.7 OSE-SC transformants with specific mutation profiles may resemble human disease.....78 - 79

3.7 Results.....80

3.8 Culturing approach to preserve OSE-SC stem cell characteristics..80

3.9 Samples with identical LentiCRISPRs display transcriptomic variability.....80 - 83

3.10 Few differentially expressed genes exist between OSE-SC transformants with *Brca2*-targeting LentiCRISPRs.....84

3.11 *Brca2*- transformants differ from *Trp53*-/*Rb1*-/*Pten*-, but not from *Trp53*-/*Rb1*-/*Pten*-/*Crebbp*-/*Csmd3*- transformants.....84 - 85

3.12 *Trp53*- transformants are similar to *Brca2*- transformants.....85 - 87

3.13 Few HGSOC hallmark pathways reported by TCGA are enriched in OSE-SC transformants.....88 - 92

3.14 *Trp53*- OSE-SC transformants share downregulated genes with the TCGA-defined differentiated HGSOC subtype.....93

3.15 *Trp53*-/*Rb1*-/*Pten*- OSE-SC share downregulated genes with low malignancy potential and grades I and II ovarian cancer.....93 - 96

3.16 Gene sets shared between mouse and human HGSOC do not differentiate transformant clusters and most are not enriched among all groups.....97 - 99

3.17 Pathways involved in cell growth, adhesion, and motility differentiate *Trp53*- and *Trp53*-/*Rb1*-/*Brca2*-/*Wwox*-/*Fancd2*- from *Trp53*-/*Rb1*-/*Pten*- transformants.....100 - 101

3.18 Discussion.....101

3.19 Initiation mutations consistently influence colony growth characteristics in vitro but incompletely direct global gene expression.....102 - 103

3.20 Completely in vitro modeling may be insufficient to recapitulate human disease characteristics.....103

3.21 Culturing conditions or inherent genomic instability may influence gene expression.....103 - 105

3.22 Non-HGSOC related pathways potentially suggest differential cancerous growth characteristics of different colonies.....105

3.23 Proper comparisons with human disease likely require in vivo methodologies.....105 - 106

3.24 Methods.....106 - 108

3.25 References.....109 - 112

CHAPTER 4: Significance, Impact, and Future Directions.....113

4.1 Summary of findings.....114 - 115

4.2 Limitations.....116 - 117

4.3 Methodological implications.....117 - 118

4.4 Future directions.....118

4.5 Implications for modeling of HGSOC development.....118
4.6 *In vitro* screening of putative HGSOC driver genes in the fallopian tubal epithelium.....118 - 119
4.7 Transcriptomic characterization of tumors initiated via unique combinations of driver gene mutations.....119 - 121
4.8 CRISPRa implementation into minilibrary screening methodology.....121 - 122
4.9 Implementation of genome-wide CRISPR screening to identify genes associated with synthetic lethality in distinct transformant types.....122 - 123
4.10 Significance in cancer biology.....123 - 126
4.11 References.....127 - 129

APPENDIX 1: *In Vitro* Transformation of Fallopian Tubal Epithelial Cells.....130
A1.1 Introduction.....131 - 136
A1.2 Results.....136
A1.3 *Trp53*$^{+/-}$ TE cells inefficiently form colonies in soft agar following minilibrary transduction.....136 - 139
A1.4 Lentiviral transduction of cultured TE is inefficient relative to transduction of OSE.....139 - 140
A1.5 Discussion.....140 - 143
A1.6 Methods.....143 - 144
A1.7 References.....145 - 148

APPENDIX 2: *In Vivo* Characterization of OSE Transformant Tumorigenesis.....149
A2.1 Introduction.....150 - 151
A2.2 Results.....151
A2.3 *Trp53* and *Rb1* mutations are minimal requirements to cause tumorigenesis *in vivo*.....152 - 153
A2.4 Transformants with LentiCRISPRs targeting *Trp53*, *Rb1* and *Cdkn2a* frequently form tumors *in vivo*.....153 - 154
A2.5 Discussion.....154
A2.6 *Trp53* and *Rb1* disruption are minimal requirements for *in vivo* OSE-SC tumorigenesis.....154 - 155
A2.7 *Brca2* and/or *Fancd2* disruption neither promote nor inhibit OSE-SC transformant tumorigenesis.....155 - 156

A2.8 *Trp53*, *Rb1*, and *Cdkn2a*, but not *Pten*, *Lrp1b*, *Wwox*, *Crebbp*, or *Gabra6*, are associated with frequent tumorigenesis.....156 - 158

A2.9 Significance and conclusions.....158

A2.10 Methods.....159 - 160

A2.11 References.....161 - 162

APPENDIX 3: Chapter 2 Supplemental Figures.....163 - 186

APPENDIX 4: Chapter 2 Supplemental Tables.....187 - 193

APPENDIX 5: Chapter 3 Supplemental Tables.....194 - 199

LIST OF FIGURES

Figure 2.1 Strategy for identifying HGSOC tumor suppressor combinations.....24

Figure 2.2 OSE-SC ($ALDH^+$) transform more frequently than OSE-NS ($ALDH^-$) despite similar viral transduction rates.....27 - 28

Figure 2.3 Identification of genome-integrated LentiCRISPRs and overrepresented target gene combinations in OSE-SC.....31 - 32

Figure 2.4 Targeted OSE-SC-transformation assay and validation of overrepresented LentiCRISPR combinations.....35 - 36

Figure 2.5 Identification of genome-integrated LentiCRISPRs overrepresented target gene combinations in OSE-NS.....41

Figure 2.6 Model of mutations necessary for efficient in vitro OSE-SC transformation.....43

Figure 3.1 Strategy for transcriptomic analysis of OSE-SC transformants.....77

Figure 3.2 Principal component analyses cannot differentiate most OSE-SC transformants with different genome-integrated LentiCRISPRs.....79

Figure 3.3 Few differentially expressed genes exists between most transformant groups except for *Trp53*-/*Rb1*-/*Pten*- transformants.....82 - 83

Figure 3.4 All transformant groups exhibit similar p53 pathway component expression.....87

Figure 3.5 All transformant groups exhibit gene set enrichment for homologous recombination DNA repair genes.....89 - 90

Figure 3.6 Few HGSOC subtype-associated gene sets are enriched among transformant groups.....92

Figure 3.7 A minority of HGSOC-associated gene sets are enriched in any OSE-SC transformant groups.....95 - 96

Figure 3.8 RTK signaling pathways differential expression occurs in both *Trp53*-/*Rb1*-/*Brca2*-/*Wwox*-/*Fancd2*- and *Trp53*- transformants.....98 - 99

Figure A1.1 Strategy for identifying HGSOC tumor suppressor combinations.....134

Figure A1.2 Minilibrary transduction, but not FUGW (GFP-expressing lentivirus) transduction, causes transformation of *Trp53*$^{+/-}$ TE.....137

Figure A2.1 Combined LentiCRISPR targeting of *Trp53*, *Rb1*, and *Cdkn2a* is associated with rapid tumorigenesis.....152

Figure S1.1 Generation of a *Trp53* null mouse line congenic in strain FVB/NJ by genome editing and validation.....164 - 165

Figure S1.2 Next generation sequencing of minilibrary LentiCRISPRv2 target sites suggests that most constructs cause indels at target sites.....166 - 167

Figure S1.3 Redesigned LentiCRISPRs and LentiCRISPRs targeting *Trp53* cause mutations in target sites.....168 - 169

Figure S1.4 OSE contains a small population of ALDH^{+} cells and express the CK8 epithelial marker in culture.....170 - 171

Figure S1.5 Assessment of minilibrary viral titer and FUGW (GFP-expressing lentiviral construct) transduction efficiency.....172 - 173

Figure S1.6 *Trp53* mutations and lentiviral transduction are not sufficient for adhesion independent growth of OSE.....174

Figure S1.7 Minilibrary transduction, but not FUGW (GFP-expressing lentivirus) transduction, causes transformation of *Trp53*$^{+/-}$ unsorted OSE, OSE-SC, and OSE-NS.....175

Figure S1.8 Calculation of MOI (multiplicity of infection), SIP (single infection percentage) and random gene targeting frequency.....176

Figure S1.9 Frequently gene “hits” in OSE-SC transformants were targeted by three unique LentiCRISPRv2 constructs.....177 - 178

Figure S1.10 *Trp53, Rb1, Cdkn2a, and Pten* function synergistically in OSE-SC transformation initiation.....179

Figure S1.11 Colony size resulting from OSE-SC transformation with targeted sets of LentiCRISPRv2 constructs.....180 - 181

Figure S1.12 LentiCRISPRv2 targeting of *Ankrd11* or *Wwox* alongside *Trp53*, *Cdkn2a*, and *Pten* causes significant increases in adhesion independent growth vs combined mutagenesis of *Trp53*, *Cdkn2a*, and *Pten*.....182 - 183

Figure S1.13 Underrepresented minilibrary target genes are frequently found in colonies with greater overall quantities of targeted genes in OSE-SC.....184

Figure S1.14 *Fancd2* and *Brca2* function synergistically to promote OSE-SC adhesion independent growth.....185

Figure S1.15 Combinatorial mutagenesis of *Trp53*, *Cdkn2a*, *Pten*, *Rad51c* and either *Fat3* or *Gabra6* causes significantly greater colony growth vs disruption of *Trp53*, *Cdkn2a*, *Pten*, and *Rad51c*.....186

LIST OF TABLES

Table 2.1 Alteration frequency of minilibrary target genes in HGSOC.....22

Table S2.1 Primers for next generation sequencing used for minilibrary validation.....188 - 190

Table S2.2 Primers for surveyor assay.....191

Table S2.3 Minilibrary sgRNA sequences and exon targeted.....192 - 193

Table S3.1 HGSOC-associated gene sets published by Maniati et al.....195 - 198

Table S3.2 Low grade carcinoma gene sets.....199

CHAPTER 1: Introduction

High Grade Serous Ovarian Carcinoma: the most lethal gynecological malignancy

Ovarian cancer is a collection of malignancies that initiates in the female reproductive tract and cumulatively accounts for 14,000 deaths in the United States and 150,000 deaths worldwide each year [1–3]. It is the 5th leading cause of cancer mortality and is the most lethal gynecological malignancy [1,2,4]. Although all ovarian cancer subtypes share an anatomical location and often receive similar clinical treatment, they have divergent histologic characteristics, genetic abnormalities, progression, and putative cells of origin [2,5–8]. These differences substantially influence factors like disease prognosis and response to therapy [6,8].

Distinct ovarian cancer subtypes can be separated into two general categories: Type I and Type II disease. Type I ovarian cancers carry a wild type (WT) *TP53* allele and are generally less aggressive diseases. They present at Federation of Gynecology and Obstetrics (FIGO) stage I, or other early FIGO stages, meaning that they are typically confined to the ovary and/or fallopian tubes [2,3,9]. Accordingly, ovarian localization of Type I tumors allows for effective treatment and relatively high survival [1]. Low grade serous, mucinous, clear cell, and endometrioid carcinomas are forms of Type I disease [2]. Type II ovarian cancers, in comparison, almost universally harbor mutant *TP53* alleles and include more aggressive diseases responsible for 85-90% of ovarian cancer deaths [2,10,11]. These highly proliferative tumors exploit the lack of anatomical barrier between the ovary and female reproductive system, leading to uninhibited, frequent metastases [6].

High Grade Serous Ovarian Carcinoma (HGSOC) is the most common form of Type II ovarian cancer and is almost always detected at an advanced FIGO stage (III-IV) with both ovarian localization and substantial quantities of extraovarian disease [2]. Unfortunately, most patients diagnosed with HGSOC (~75%) survive less than five years after diagnosis and only 3% survive after ten years [12–14]. Despite decades of research into functional mechanisms underlying HGSOC, treatment and overall survival have remained relatively unchanged while survival of other non-ovarian cancers like breast and colorectal cancers has improved [15–19]. This disparity has been largely attributed to infrequent early clinical detection of HGSOC compared to other cancers [2,6,20–23]. Several screening methods have been proposed, however, with conflicting reports regarding efficacy and utility.

HGSOC screening methodologies are insufficient for early detection and mortality reduction

Carbohydrate antigen 125 (CA125) is the best characterized serum biomarker of HGSOC that has been utilized for early screening. Initial observations of elevated CA125 levels in patients with advanced stage tumors led to substantial research into its viability as an early stage HGSOC marker [24–27]. Several studies reported success using serial CA125 measurements to predict early disease [28–30]. However, use of CA125 as an early stage HGSOC marker is controversial due to only 40-62% sensitivity to early disease detection, little association with decreased HGSOC mortality, and relatively low specificity [31–33]. Several normal physiological conditions or benign conditions also cause fluctuations in CA125 serum levels, complicating interpretation of results and

leading to possible false positives [31,34,35]. Other common noninvasive methods to detect HGSOC, such as transvaginal sonograms or HE4 serum biomarker detection, were found to have little effect on disease mortality [33,36–41]. Current early HGSOC detection methodologies are therefore largely insufficient for disease identification or prevention.

HGSOC may arise from either the ovarian surface epithelium (OSE) or distal fallopian tubal epithelium (TE)

Efforts to develop viable HGSOC screening methodologies have been complicated by longstanding uncertainty regarding the initiating stages of HGSOC development [42]. One such unknown is the HGSOC initiating location, or "cell of origin". It is the subject of significant debate due to historical difficulty in locating precursor HGSOC lesions before extraovarian dissemination. Despite these difficulties however, candidate populations have been identified within the ovarian surface epithelium (OSE), distal fallopian tubal epithelium (TE), and stem cell subpopulations of either tissue [43–49].

The number of ovulatory cycles a women experiences throughout her lifetime represents a major risk factor for both OSE and TE transformation. This relationship, known as the "incessant ovulation hypothesis", posits that repeated cycles of ovulation and consequential follicular rupture physically damage the OSE, thereby necessitating cell proliferation, mobility, and repair. Follicular rupture also exposes both the OSE and distal TE to follicular fluid which contains growth factors, steroid hormones, and inflammatory factors that may predispose either tissue to carcinogenesis [45,50,51]. In support of the incessant ovulation hypothesis, factors associated with more lifetime

ovulatory cycles like early menarche or late menopause, correlate with higher rates of HGSOC incidence [2,3,52–54]. Similarly, increased parity and use of oral contraceptives result in less lifetime ovulatory cycles and correlate with lower HGSOC incidence [2,3,55–59].

Details regarding the merits of each tissue as a putative HGSOC "cell of origin" are discussed in detail in later chapters. In short however, both the OSE and TE have been demonstrated to form HGSOC-like lesions in genetically engineered mouse models [47,60–63]. Global gene expression analyses of HGSOC tumors, OSE, and TE have also demonstrated similarity between HGSOC and either TE or OSE, depending on the particular tumor [64,65]. Therefore, it's possible that some HGSOC cases may arise from either tissue [44].

Genetic factors influence HGSOC incidence and prognosis

Uncertainty regarding HGSOC initiating mutations represents another major unknown in efforts to model early disease progression. Despite these uncertainties, several clues regarding HGSOC genetic etiologies have been gathered from studies of familial or early onset HGSOC. In general, HGSOC is rare in pre-menopausal women and arises at a median age of 63 years [1,2,66]. However, 20% of HGSOC cases arise before the age of 50 and have been largely attributed to germline mutations in either *BRCA1* or *BRCA2* [67–70]. Even in the absence of a direct *BRCA1* or *BRCA2* mutation, up to 50% of HGSOC tumors exhibit inactivation of these genes, further supporting their roles in HGSOC development [6,14].

Both *BRCA1* and *BRCA2* are genes involved in homologous recombination repair of DNA. They play an important role in maintenance of chromosomal stability, detection of damage, and effective DNA repair [71–74]. Other genes involved in DNA damage such as *BRIP1*, *PALB2*, *RAD51C*, *RAD51D*, and *BARD1* are not as prevalent as *BRCA1* or *BRCA2* in HGSOC, but likewise convey a 5-15% risk of ovarian cancer [75,76]. Accordingly, previous studies have suggested that largescale genomic instability is a hallmark of HGSOC and that about 50% of HGSOC tumors exhibit defects in homologous recombination repair mechanisms [14,77]. The high degree of genomic instability in HGSOC promotes tumor heterogeneity and chemotherapy relapse due to rapid tumor evolution and production of drug-resistant subclones. Rapid tumor evolution also causes cells to acquire favorable amplifications or deletions to enhance growth characteristics, mobility, and angiogenesis [78–81].

Although *BRCA1* and *BRCA2* mutations are important risk factors for HGSOC development, mutations in these genes are rare in sporadic cases and cannot explain 70-80% of HGSOC incidence [14,68]. Previous research in mouse models has also found that null mutations in either gene are insufficient to drive tumor initiation in the OSE or TE [61,82]. Other genes, therefore, must be involved in both HGSOC initiation and tumor development. Ascertainment of these HGSOC-associated mutations may play an important role in future efforts to detect and diagnose the disease.

Genetic screening has revealed HGSOC-associated mutations

Next generation genomic and transcriptomic sequencing has been recently implemented by the Cancer Genome Atlas Research Network (TCGA) to elucidate the genomic landscape of HGSOC and better understand genetic bases of the disease. 489 epithelial ovarian carcinomas were sequenced by TCGA in the largest effort to sequence HGSOC to date. Through both genomic and transcriptomic analyses, TCGA identified common pathway alterations in retinoblastoma (RB) (67% of cases), PI3K/Ras (45%), and Notch (22%) signaling pathways, along with genes involved in homologous recombination DNA repair (51%) [14]. TCGA analyses also identified genes that are commonly mutated or deleted among all sequenced tumors. An average of 46 mutations were found per tumor with nearly ubiquitous null mutations in *TP53* (96% of tumors). However other than *TP53*, no other gene was mutated or deleted in more than 12% of HGSOC tumors. These results suggest the fundamental importance of TP53 in HGSOC tumorigenesis but are complicated by reports that *TP53* (*Trp53* in mice) is insufficient to transform putative HGSOC cells of origin alone in mouse models. Rather, additional mutations or gene activations (alongside *Trp53*) may be necessary for tumorigenesis to occur [47,60,82]. Given the heterogeneity of mutations present among human HGSOC tumors [14], it's possible that multiple mutation combinations can initiate HGSOC, and that necessary combinations depend upon the cell type in which they occur [83,84].

<u>Genomic characterization of advanced HGSOC tumors cannot differentiate driver and passenger mutations</u>

Mutations in any given tumor can be generally labeled as either driver mutations or passenger mutations. Driver mutations are mutations that convey advantageous changes onto an individual cell, usually leading to its clonal expansion and a survival advantage over other cells [84,85]. For instance, of the average 46 mutations found per HGSOC tumor by TCGA, 5 to 8 are estimated to be necessary to initiate carcinogenesis [14,84,86]. These necessary initiating mutations are known as driver mutations because they convey initiating, cancer-promoting changes onto a cell. Additional driver mutations may also be acquired following tumor initiation to promote acquisition of cancer hallmarks [84,87].

In contrast, passenger mutations are mutations that do not cause an immediate growth advantage but are detected alongside driver mutations in all cancers [84,86,88]. These mutations arise as a consequence, not a cause, of transformation [14,83,84]. The accumulation of passenger mutations among tumor cell subpopulations has been shown to increase tumor heterogeneity and enhance the evolutionary fitness of tumors [89]. While these mutations may not immediately promote transformation or the acquisition of cancer hallmarks, changes to the tumor microenvironment due to new factors like chemotherapy may favor survival of specific cell genotypes [87]. Passenger mutations may therefore become drivers under certain conditions [89–92]. HGSOC tumors are thought to be especially prone to accumulation of passenger mutations because genomic instability is a hallmark characteristic of the disease [14]. Passenger mutations also generally outnumber drivers in a given tumor, so many of the mutations found in HGSOC tumors may play no role in tumor initiation.

CRISPR/Cas9-driven library screening methodologies can differentiate driver and passenger mutations in a high throughput manner

Differentiation of driver and passenger mutations in TCGA data is difficult using traditional genetic approaches. If one set of driver mutations were to be assessed in a mouse model, for example, knockouts would be made in a mouse tissue, phenotypes would be observed, and conclusions would be made regarding whether the mutations function as driver mutations. While this methodology may be viable for a limited number of mutations, it cannot be successfully applied to the myriad of driver mutations possible in HGSOC. Given a list of 20 candidate HGSOC driver genes and assuming that 5 driver mutations are necessary to initiate HGSOC, then over 15,000 mutation combinations must be tested in order to assess all possible combinations of driver mutations. Considering the cost and time prohibitive nature of generating over 15,000 mouse models, a high throughput approach is clearly necessary to differentiate driver mutations from passenger mutations in HGSOC.

CRISPR/Cas9 knockout screening methodologies have been widely implemented in recent years as a high throughout method to screen thousands of gene mutation combinations at once and as an alternative to traditional knockout modeling [93]. Because CRISPR/Cas9 systems are programmable to induce knockouts in almost any gene, they also can be applied to gene candidate screens of any size ranging from small, targeted gene sets [94] to genome-wide functional screens [95]. CRISPR-driven screening methodologies may therefore provide a cost and time-effective opportunity to differentiate driver genes from passengers by assessing a myriad of combined

functional knockouts in putative HGSOC driver genes and identifying specific combinations associated with transformation.

Dissertation goals and accomplishments

In this dissertation, I address two fundamental questions regarding HGSOC development: “What putative HGSOC cells of origin are prone to transformation?”, and “What mutation combinations are necessary to transform each putative cell of origin?”. I employed CRISPR/Cas9 screening methodologies to approach both questions in an unbiased manner *in vitro*, and validated all results using targeted mutagenesis approaches. I also described transcriptomic characteristics of transformants produced during CRISPR/Cas9 screening and preliminary *in vivo* characterization of putative HGSOC drivers. These results led to a model of HGSOC initiation in which core transformation requirements occur in the context of specific cellular paradigms. The methodology described in this thesis may also serve as a pipeline for differentiation of driver and passenger mutations in any cancer for which a cell of origin and viable culturing methodology exists. Finally, I propose several applications for the HGSOC initiation model described here and suggest future project directions.

REFERENCES

1. Siegel, R. L., Miller, K. D. & Jemal, A. Cancer statistics, 2020. *CA Cancer J Clin* **70**, 7–30 (2020).

2. Seidman, J. D., Ronnett, B. M., Shih, I.-M., Cho, K. R. & Kurman, R. J. in *Blaustein's pathology of the female genital tract* (eds. Kurman, R. J., Hedrick Ellenson, L. & Ronnett, B. M.) 841–966 (Springer International Publishing, 2019). doi:10.1007/978-3-319-46334-6_14

3. Seidman, J. D., Cho, K. R., Ronnett, B. M. & Kurman, R. J. in *Blaustein's pathology of the female genital tract* (eds. Kurman, R. J., Ellenson, L. H. & Ronnett, B. M.) 679–784 (Springer US, 2011). doi:10.1007/978-1-4419-0489-8_14

4. Siegel, R. L., Miller, K. D. & Jemal, A. Cancer statistics, 2019. *CA Cancer J Clin* **69,** 7–34 (2019).

5. Bowtell, D. D. L. The genesis and evolution of high-grade serous ovarian cancer. *Nat. Rev. Cancer* **10,** 803–808 (2010).

6. Vaughan, S. *et al.* Rethinking ovarian cancer: recommendations for improving outcomes. *Nat. Rev. Cancer* **11,** 719–725 (2011).

7. Jelovac, D. & Armstrong, D. K. Recent progress in the diagnosis and treatment of ovarian cancer. *CA Cancer J Clin* **61,** 183–203 (2011).

8. Gadducci, A. *et al.* Current strategies for the targeted treatment of high-grade serous epithelial ovarian cancer and relevance of BRCA mutational status. *J Ovarian Res* **12,** 9 (2019).

9. Bhatla, N. & Denny, L. FIGO cancer report 2018. *Int. J. Gynaecol. Obstet.* **143,** 2–3 (2018).

10. Temkin, S. M., Bergstrom, J., Samimi, G. & Minasian, L. Ovarian Cancer Prevention in High-risk Women. *Clin Obstet Gynecol* **60,** 738–757 (2017).

11. Kohler, M. F. *et al.* Spectrum of mutation and frequency of allelic deletion of the p53 gene in ovarian cancer. *J. Natl. Cancer Inst.* **85,** 1513–1519 (1993).

12. Gao, J. *et al.* Integrative analysis of complex cancer genomics and clinical profiles using the cBioPortal. *Sci. Signal.* **6,** pl1 (2013).

13. Cerami, E. *et al.* The cBio cancer genomics portal: an open platform for exploring multidimensional cancer genomics data. *Cancer Discov.* **2,** 401–404 (2012).

14. Cancer Genome Atlas Research Network. Integrated genomic analyses of ovarian carcinoma. *Nature* **474,** 609–615 (2011).

15. Bobbs, A. S., Cole, J. M. & Cowden Dahl, K. D. Emerging and evolving ovarian cancer animal models. *Cancer Growth Metastasis* **8,** 29–36 (2015).

16. Li, X. *et al.* The impact of screening on the survival of colorectal cancer in Shanghai, China: a population based study. *BMC Public Health* **19,** 1016 (2019).

17. Morris, E. J. A. *et al.* A retrospective observational study examining the characteristics and outcomes of tumours diagnosed within and without of the English NHS Bowel Cancer Screening Programme. *Br. J. Cancer* **107,** 757–764 (2012).

18. Shapiro, S., Venet, W., Strax, P., Venet, L. & Roeser, R. Ten- to fourteen-year effect of screening on breast cancer mortality. *J. Natl. Cancer Inst.* **69,** 349–355 (1982).

19. Tabár, L. *et al.* Swedish two-county trial: impact of mammographic screening on breast cancer mortality during 3 decades. *Radiology* **260,** 658–663 (2011).

20. Kim, J. *et al.* Cell Origins of High-Grade Serous Ovarian Cancer. *Cancers (Basel)* **10,** (2018).

21. Gurung, A., Hung, T., Morin, J. & Gilks, C. B. Molecular abnormalities in ovarian carcinoma: clinical, morphological and therapeutic correlates. *Histopathology* **62,** 59–70 (2013).

22. Bowtell, D. D. *et al.* Rethinking ovarian cancer II: reducing mortality from high-grade serous ovarian cancer. *Nat. Rev. Cancer* **15,** 668–679 (2015).

23. Peres, L. C. *et al.* Invasive epithelial ovarian cancer survival by histotype and disease stage. *J. Natl. Cancer Inst.* **111,** 60–68 (2019).

24. Bast, R. C. *et al.* Reactivity of a monoclonal antibody with human ovarian carcinoma. *J. Clin. Invest.* **68,** 1331–1337 (1981).

25. Nustad, K. *et al.* Specificity and Affinity of 26 Monoclonal Antibodies against the CA 125 Antigen: First Report from the ISOBM TD-1 Workshop. *Tumor Biol.* **17,** 196–219 (1996).

26. Høgdall, E. V. S. *et al.* CA125 expression pattern, prognosis and correlation with serum CA125 in ovarian tumor patients. From The Danish “MALOVA” Ovarian Cancer Study. *Gynecol. Oncol.* **104,** 508–515 (2007).

27. Jacobs, I. & Bast, R. C. The CA 125 tumour-associated antigen: a review of the literature. *Hum. Reprod.* **4,** 1–12 (1989).

28. Lu, K. H. *et al.* A 2-stage ovarian cancer screening strategy using the Risk of Ovarian Cancer Algorithm (ROCA) identifies early-stage incident cancers and demonstrates high positive predictive value. *Cancer* **119,** 3454–3461 (2013).

29. Skates, S. J., Pauler, D. K. & Jacobs, I. J. Screening based on the risk of cancer calculation from bayesian hierarchical changepoint and mixture models of longitudinal markers. *J. Am. Stat. Assoc.* **96,** 429–439 (2001).

30. Skates, S. J. *et al.* Toward an optimal algorithm for ovarian cancer screening with longitudinal tumor markers. *Cancer* **76,** 2004–2010 (1995).

31. Nossov, V. *et al.* The early detection of ovarian cancer: from traditional methods to proteomics. Can we really do better than serum CA-125? *Am. J. Obstet. Gynecol.* **199,** 215–223 (2008).

32. Skates, S. J. *et al.* Calculation of the risk of ovarian cancer from serial CA-125 values for preclinical detection in postmenopausal women. *J. Clin. Oncol.* **21,** 206s–210s (2003).

33. Buys, S. S. *et al.* Effect of screening on ovarian cancer mortality: the Prostate, Lung, Colorectal and Ovarian (PLCO) Cancer Screening Randomized Controlled Trial. *JAMA* **305,** 2295–2303 (2011).

34. Lehtovirta, P., Apter, D. & Stenman, U. H. Serum CA 125 levels during the menstrual cycle. *Br J Obstet Gynaecol* **97,** 930–933 (1990).

35. Grover, S., Koh, H., Weideman, P. & Quinn, M. A. The effect of the menstrual cycle on serum CA 125 levels: a population study. *Am. J. Obstet. Gynecol.* **167,** 1379–1381 (1992).

36. Botesteanu, D.-A., Lee, J.-M. & Levy, D. Modeling the Dynamics of High-Grade Serous Ovarian Cancer Progression for Transvaginal Ultrasound-Based Screening and Early Detection. *PLoS One* **11,** e0156661 (2016).

37. van der Velde, N. M. *et al.* Time to stop ovarian cancer screening in BRCA1/2 mutation carriers? *Int. J. Cancer* **124,** 919–923 (2009).

38. Bhatt, R. S. *et al.* A phase 2 pilot trial of low-dose, continuous infusion, or “metronomic” paclitaxel and oral celecoxib in patients with metastatic melanoma. *Cancer* **116,** 1751–1756 (2010).

39. Van Gorp, T. *et al.* HE4 and CA125 as a diagnostic test in ovarian cancer: prospective validation of the Risk of Ovarian Malignancy Algorithm. *Br. J. Cancer* **104,** 863–870 (2011).

40. Moore, R. G. *et al.* The use of multiple novel tumor biomarkers for the detection of ovarian carcinoma in patients with a pelvic mass. *Gynecol. Oncol.* **108,** 402–408 (2008).

41. Schummer, M. *et al.* Comparative hybridization of an array of 21,500 ovarian cDNAs for the discovery of genes overexpressed in ovarian carcinomas. *Gene* **238,** 375–385 (1999).

42. Auersperg, N. The origin of ovarian cancers--hypotheses and controversies. *Front. Biosci. (Schol. Ed)* **5,** 709–719 (2013).

43. Neel, B. G. *et al.* Both Fallopian Tube and Ovarian Surface Epithelium Can Act as Cell-of-Origin for High Grade Serous Ovarian Carcinoma. *BioRxiv* (2018). doi:10.1101/481200

44. Zhang, S. *et al.* Both fallopian tube and ovarian surface epithelium are cells-of-origin for high-grade serous ovarian carcinoma. *Nat. Commun.* **10,** 5367 (2019).

45. Fathalla, M. F. Incessant ovulation--a factor in ovarian neoplasia? *Lancet* **2,** 163 (1971).

46. Piek, J. M. *et al.* Dysplastic changes in prophylactically removed Fallopian tubes of women predisposed to developing ovarian cancer. *J. Pathol.* **195,** 451–456 (2001).

47. Flesken-Nikitin, A. *et al.* Ovarian surface epithelium at the junction area contains a cancer-prone stem cell niche. *Nature* **495,** 241–245 (2013).

48. Rose, I. *et al.* WNT and inflammatory signaling distinguish human Fallopian tube epithelial cell populations. *BioRxiv* (2020). doi:10.1101/2020.01.15.908293

49. Schmoeckel, E. *et al.* LEF1 is preferentially expressed in the tubal-peritoneal junctions and is a reliable marker of tubal intraepithelial lesions. *Mod. Pathol.* **30,** 1241–1250 (2017).

50. Fathalla, M. F. Incessant ovulation and ovarian cancer - a hypothesis re-visited. *Facts Views Vis Obgyn* **5,** 292–297 (2013).

51. Espey, L. L. Current status of the hypothesis that mammalian ovulation is comparable to an inflammatory reaction. *Biol. Reprod.* **50,** 233–238 (1994).

52. Gong, T.-T., Wu, Q.-J., Vogtmann, E., Lin, B. & Wang, Y.-L. Age at menarche and risk of ovarian cancer: a meta-analysis of epidemiological studies. *Int. J. Cancer* **132,** 2894–2900 (2013).

53. Parazzini, F., La Vecchia, C., Negri, E. & Gentile, A. Menstrual factors and the risk of epithelial ovarian cancer. *J. Clin. Epidemiol.* **42,** 443–448 (1989).

54. Reid, B. M., Permuth, J. B. & Sellers, T. A. Epidemiology of ovarian cancer: a review. *Cancer Biol. Med.* **14,** 9–32 (2017).

55. Havrilesky, L. J. *et al.* Oral contraceptive pills as primary prevention for ovarian cancer: a systematic review and meta-analysis. *Obstet. Gynecol.* **122,** 139–147 (2013).

56. Lurie, G. *et al.* Combined oral contraceptive use and epithelial ovarian cancer risk: time-related effects. *Epidemiology* **19,** 237–243 (2008).

57. Fraumeni, J. F., Lloyd, J. W., Smith, E. M. & Wagoner, J. K. Cancer mortality among nuns: role of marital status in etiology of neoplastic disease in women. *J. Natl. Cancer Inst.* **42,** 455–468 (1969).

58. Adami, H. O. *et al.* Parity, age at first childbirth, and risk of ovarian cancer. *Lancet* **344,** 1250–1254 (1994).

59. Vachon, C. M. *et al.* Association of parity and ovarian cancer risk by family history of breast or ovarian cancer in a population-based study of postmenopausal women. *Epidemiology* **13,** 66–71 (2002).

60. Flesken-Nikitin, A., Choi, K.-C., Eng, J. P., Shmidt, E. N. & Nikitin, A. Y. Induction of carcinogenesis by concurrent inactivation of p53 and Rb1 in the mouse ovarian surface epithelium. *Cancer Res.* **63,** 3459–3463 (2003).

61. Perets, R. *et al.* Transformation of the fallopian tube secretory epithelium leads to high-grade serous ovarian cancer in Brca;Tp53;Pten models. *Cancer Cell* **24,** 751–765 (2013).

62. Maniati, E. *et al.* Mouse ovarian cancer models recapitulate the human tumor microenvironment and patient response to treatment. *Cell Rep.* **30,** 525–540.e7 (2020).

63. Sherman-Baust, C. A. *et al.* A genetically engineered ovarian cancer mouse model based on fallopian tube transformation mimics human high-grade serous carcinoma development. *J. Pathol.* **233,** 228–237 (2014).

64. Lawrenson, K. *et al.* A Study of High-Grade Serous Ovarian Cancer Origins Implicates the SOX18 Transcription Factor in Tumor Development. *Cell Rep.* **29,** 3726–3735.e4 (2019).

65. Hao, D. *et al.* Integrated Analysis Reveals Tubal- and Ovarian-Originated Serous Ovarian Cancer and Predicts Differential Therapeutic Responses. *Clin. Cancer Res.* **23,** 7400–7411 (2017).

66. Webb, P. M. & Jordan, S. J. Epidemiology of epithelial ovarian cancer. *Best Pract Res Clin Obstet Gynaecol* **41,** 3–14 (2017).

67. Risch, H. A. *et al.* Population BRCA1 and BRCA2 mutation frequencies and cancer penetrances: a kin-cohort study in Ontario, Canada. *J. Natl. Cancer Inst.* **98,** 1694–1706 (2006).

68. Risch, H. A. *et al.* Prevalence and penetrance of germline BRCA1 and BRCA2 mutations in a population series of 649 women with ovarian cancer. *Am. J. Hum. Genet.* **68,** 700–710 (2001).

69. Chen, S. & Parmigiani, G. Meta-analysis of BRCA1 and BRCA2 penetrance. *J. Clin. Oncol.* **25,** 1329–1333 (2007).

70. Antoniou, A. *et al.* Average risks of breast and ovarian cancer associated with BRCA1 or BRCA2 mutations detected in case Series unselected for family history: a combined analysis of 22 studies. *Am. J. Hum. Genet.* **72,** 1117–1130 (2003).

71. Stoppa-Lyonnet, D. The biological effects and clinical implications of BRCA mutations: where do we go from here? *Eur. J. Hum. Genet.* **24 Suppl 1,** S3–9 (2016).

72. Venkitaraman, A. R. Functions of BRCA1 and BRCA2 in the biological response to DNA damage. *J. Cell Sci.* **114,** 3591–3598 (2001).

73. Feng, W. & Jasin, M. BRCA2 suppresses replication stress-induced mitotic and G1 abnormalities through homologous recombination. *Nat. Commun.* **8,** 525 (2017).

74. Petrucelli, N., Daly, M. B. & Pal, T. in *GeneReviews(®)* (eds. Pagon, R. A. *et al.*) (University of Washington, Seattle, 1993).

75. Norquist, B. M. *et al.* Inherited mutations in women with ovarian carcinoma. *JAMA Oncol.* **2,** 482–490 (2016).

76. Neff, R. T., Senter, L. & Salani, R. BRCA mutation in ovarian cancer: testing, implications and treatment considerations. *Ther Adv Med Oncol* **9,** 519–531 (2017).

77. Chien, J. *et al.* TP53 mutations, tetraploidy and homologous recombination repair defects in early stage high-grade serous ovarian cancer. *Nucleic Acids Res.* **43,** 6945–6958 (2015).

78. Wang, Z. C. *et al.* Profiles of genomic instability in high-grade serous ovarian cancer predict treatment outcome. *Clin. Cancer Res.* **18,** 5806–5815 (2012).

79. Stanta, G. & Bonin, S. Overview on Clinical Relevance of Intra-Tumor Heterogeneity. *Front Med (Lausanne)* **5,** 85 (2018).

80. Caswell, D. R. & Swanton, C. The role of tumour heterogeneity and clonal cooperativity in metastasis, immune evasion and clinical outcome. *BMC Med.* **15,** 133 (2017).

81. Bakhoum, S. F. & Landau, D. A. Chromosomal instability as a driver of tumor heterogeneity and evolution. *Cold Spring Harb. Perspect. Med.* **7,** (2017).

82. Szabova, L. *et al.* Perturbation of Rb, p53, and Brca1 or Brca2 cooperate in inducing metastatic serous epithelial ovarian cancer. *Cancer Res.* **72,** 4141–4153 (2012).

83. Kandoth, C. *et al.* Mutational landscape and significance across 12 major cancer types. *Nature* **502,** 333–339 (2013).

84. Pon, J. R. & Marra, M. A. Driver and passenger mutations in cancer. *Annu. Rev. Pathol.* **10,** 25–50 (2015).

85. Pepper, J. W., Scott Findlay, C., Kassen, R., Spencer, S. L. & Maley, C. C. Cancer research meets evolutionary biology. *Evol. Appl.* **2,** 62–70 (2009).

86. Stratton, M. R., Campbell, P. J. & Futreal, P. A. The cancer genome. *Nature* **458,** 719–724 (2009).

87. Hanahan, D. & Weinberg, R. A. Hallmarks of cancer: the next generation. *Cell* **144,** 646–674 (2011).

88. Hess, J. M. *et al.* Passenger hotspot mutations in cancer. *Cancer Cell* **36,** 288–301.e14 (2019).

89. Dagogo-Jack, I. & Shaw, A. T. Tumour heterogeneity and resistance to cancer therapies. *Nat. Rev. Clin. Oncol.* **15,** 81–94 (2018).

90. Merid, S. K., Goranskaya, D. & Alexeyenko, A. Distinguishing between driver and passenger mutations in individual cancer genomes by network enrichment analysis. *BMC Bioinformatics* **15,** 308 (2014).

91. McFarland, C. D., Korolev, K. S., Kryukov, G. V., Sunyaev, S. R. & Mirny, L. A. Impact of deleterious passenger mutations on cancer progression. *Proc. Natl. Acad. Sci. USA* **110,** 2910–2915 (2013).

92. Bozic, I., Gerold, J. M. & Nowak, M. A. Quantifying clonal and subclonal passenger mutations in cancer evolution. *PLoS Comput. Biol.* **12,** e1004731 (2016).

93. Doench, J. G. *et al.* Rational design of highly active sgRNAs for CRISPR-Cas9-mediated gene inactivation. *Nat. Biotechnol.* **32,** 1262–1267 (2014).

94. Wang, G. *et al.* Mapping a functional cancer genome atlas of tumor suppressors in mouse liver using AAV-CRISPR-mediated direct in vivo screening. *Sci. Adv.* **4,** eaao5508 (2018).

95. Shalem, O. *et al.* Genome-scale CRISPR-Cas9 knockout screening in human cells. *Science* **343,** 84–87 (2014).

Chapter 2: Most commonly mutated genes in High Grade Serous Ovarian Carcinoma are nonessential for ovarian surface epithelial stem cell transformation

The following chapter is adapted from a manuscript submitted to Cell Reports (manuscript number CELL-REPORTS-D-20-00575). The paper was written by RJY and edited by AFN, AYN, and JCS. All experiments were completed by RJY. SN provided experimental assistance.

See Appendices 3 and 4 for supplemental figures and tables, respectively.

Authors: Robert J. Yamulla, Shreya Nalubola, Andrea Flesken-Nikitin, Alexander Yu. Nikitin, John C. Schimenti

ABSTRACT

High grade serous ovarian carcinoma (HGSOC) is the most lethal gynecological cancer and the 5th leading cause of cancer-related deaths of women in the USA. Disease-associated mutations have been identified by the Cancer Genome Atlas Research Network. However, aside from mutations in *TP53* or alterations in the *RB1* pathway that are extremely common in HGSOC, the contributions of other mutation combinations have been difficult to assess experimentally or with genomic data alone. Previous research identified ALDH^{+} stem cells of the ovarian surface epithelium (OSE) as one of the putative cells of HGSOC origin. Here, we performed combinatorial CRISPR mutagenesis of 20 putative HGSOC driver genes to identify mutation combinations that transformed OSE stem cells (OSE-SC) and non-stem cells (OSE-NS). Overrepresented mutations and mutation combinations were identified in all transformants and were investigated directly in targeted assays. Our results support the OSE stem cell theory of HGSOC initiation and suggest that most commonly mutated genes in HGSOC have no effect on OSE-SC transformation initiation. We suggest a model in which combined disruption of *RB1* and *PTEN*, in addition to *TP53* deficiency, constitutes a core set of mutations required for efficient transformation *in vitro.* A few previously uncharacterized mutation combinations further enhanced transformation but may have done so via TP53-related mechanisms. Together, our results identify mutation combinations that are critical for OSE-SC transformation and may contribute to more accurate modeling of HGSOC development. Our cancer driver screening methodology may also serve as a model for high throughput functional assessment of commonly mutated genes uncovered in other cancers by large scale sequencing.

INTRODUCTION

Ovarian cancer is a complex disease consisting of several distinct subtypes that differ in progression, prognosis, cell of origin, and genetic alterations [1]. It is the fifth leading cause of cancer-related female deaths in the western world [2]. High grade serous ovarian carcinoma (HGSOC) is the most common (about 70%) and lethal subtype of ovarian cancer, in part due to its propensity to metastasize, and to relapse following chemotherapy [3]. Additionally, HGSOC screening methodologies are inefficient, typically resulting in late stage diagnosis. The rarity of early stage HGSOC detection has complicated ascertainment of the cell of origin, initiating mutations, and the identification of precursor lesions [3,4].

Much progress has been made regarding the genetic etiologies of HGSOC. The Cancer Genome Atlas (TCGA) completed a comprehensive genomic analysis of patient tumor samples and commonly dysregulated genes and pathways (Table 1) [5]. Common mutations and deletions of genes are of particular interest, as they may drive HGSOC initiation and development. Several of the putative TCGA driver genes have been thoroughly investigated. For instance, *TP53 (Trp53* in mice*)* is mutated or inactivated in nearly all tumors [5], and has been validated as a crucial driver of carcinogenesis in mouse models [6–8]. However, most of the recurrently altered HGSOC driver genes are mutated or deleted in a smaller subset of tumors and have not been validated experimentally in animal models or cell transformation paradigms. Several, including *WWOX*, *LRP1B*, *CDKN2A*, and *PTEN*, exist near fragile sites in the genome, and therefore may be mutated simply as a consequence of genome instability rather than cancer initiation [9].

Although *TP53* is mutated in nearly all HGSOC cases, experiments with mouse models indicate that *Trp53* mutagenesis is insufficient for HGSOC initiation; rather, multiple mutations appear to be required, consistent with the multi-hit hypothesis of cancer [10,11]. For example concurrent inactivation of *Trp53* and *Brca1*, both commonly mutated in HGSOC, could not drive transformation in mice [12]. However, activation of *Myc* along with disruption of both *Trp53* and *Brca1* did initiate HGSOC. It was also reported that disruption of *Trp53* or *Rb1* alone in the ovarian surface epithelium (OSE) caused neoplasms in only 4/31 and 1/21 mice, respectively, but simultaneous mutations in both caused 100% cancer incidence after a median 227 days [11]. Given the substantial numbers of commonly mutated genes identified by TCGA, there are a myriad of possible TCGA driver gene combinations, but very little data regarding how these different combinations could affect transformation efficiency of putative HGSOC "cells of origin."

There is a growing consensus that HGSOC may have several places of origin, such as OSE, tubal epithelium and peritoneal serosa [6,8,13–15]. The OSE is a flat to cuboidal cell monolayer that overlies the ovary and was originally proposed as the HGSOC putative cell type-of-origin due to correlation with tumor localization and the observation that a greater number of ovulatory cycles correlates with increased cancer incidence [3,16–18]. Research has suggested that repeated cycles of follicular rupture, OSE damage, inflammation, and repair may trigger oncogenic transformation of OSE [19]. Inclusion cysts, or entrapment of OSE within the ovarian stroma, may also facilitate OSE transformation by exposing it to high concentrations of hormones, growth factors, and inflammatory cytokines that are not present at the ovarian surface. OSE within

inclusion cysts has been previously shown to express HGSOC markers like PAX8 [3]. Importantly, the OSE has been experimentally shown to transform into HGSOC-like neoplasms [8,11,13].

Table 1: Alteration frequency of minilibrary target genes in HGSOC

Gene Name	Mutations	Amplifications	Deletions	Total	% Disrupted
Trp53	303	2	1	306	96.20%
Brca1	37	1	1	39	12.03%
Brca2	34	3	2	39	11.39%
Csmd3	19	47	1	67	6.33%
Nf1	12	1	24	37	11.39%
Fat3	18	8	1	27	6.01%
Gabra6	6	3	1	10	2.22%
Rb1	6	1	25	32	9.81%
Apc	7	2	3	12	3.16%
Lrp1b	13	6	13	32	8.23%
Prim2	0	6	2	8	0.63%
Cdkn2a	0	1	7	8	2.22%
Crebbp	7	3	10	20	5.38%
Wwox	0	2	14	16	4.43%
Ankrd11	4	1	10	15	4.43%
Map2k4	1	0	11	12	3.80%
Fancm	2	3	0	5	0.63%
Fancd2	1	3	0	4	0.32%
Rad51c	0	2	0	2	0.00%
Pten	2	2	21	25	7.28%

Legend: Putative HGSOC driver genes were derived primarily from the Cancer Genome Atlas Research Network. Most genes, except for *FANCM* and *APC,* were found to be significantly mutated or deleted in HGSOC tumors by TCGA.

In mice, HGSOC can initiate from OSE stem cells (OSE-SC) [20]. Such cells have high levels of Aldehyde dehydrogenase (ALDH) activity and transform more readily than OSE cells with low ALDH activity ($ALDH^-$, non-stem). OSE-SC were found to have increased colony-forming potential in primary culture, greater sphere formation capacity *in vitro*, and an increased ability to proliferate in culture before undergoing senescence [20]. The cells also express multipotency markers and readily transform following combined knockout of *Trp53* and *Rb1* in mice. Thus, the $ALDH^+$ OSE stem cell subpopulation is a candidate originating source of HGSOC.

Here, we sought to identify and functionally validate combinations of putative driver genes in HGSOC, and the transformation susceptibility of different ovarian epithelial cell types to combinations of mutations. The 20 candidate genes tested were primarily those that are most commonly mutated in HGSOC (Table 1). Random sets of mutations were induced by infection of mouse OSE stem cells (OSE-SC) and non-stem cells (OSE-NS) with a minilibrary of lentiviruses encoding Cas9 and CRISPR guide RNAs directed against the candidate driver genes. We found that OSE-SC transform more efficiently than OSE-NS, and that only a fraction of commonly mutated HGSOC genes contribute to transformation *in vitro*. In addition to *Trp53* and *Rb1*, mutation of *Pten* was found to be centrally important for transformation of mouse OSE *in vitro*. We also report novel transformation-enhancing mutation combinations and propose a model of core OSE-SC transformation requirements.

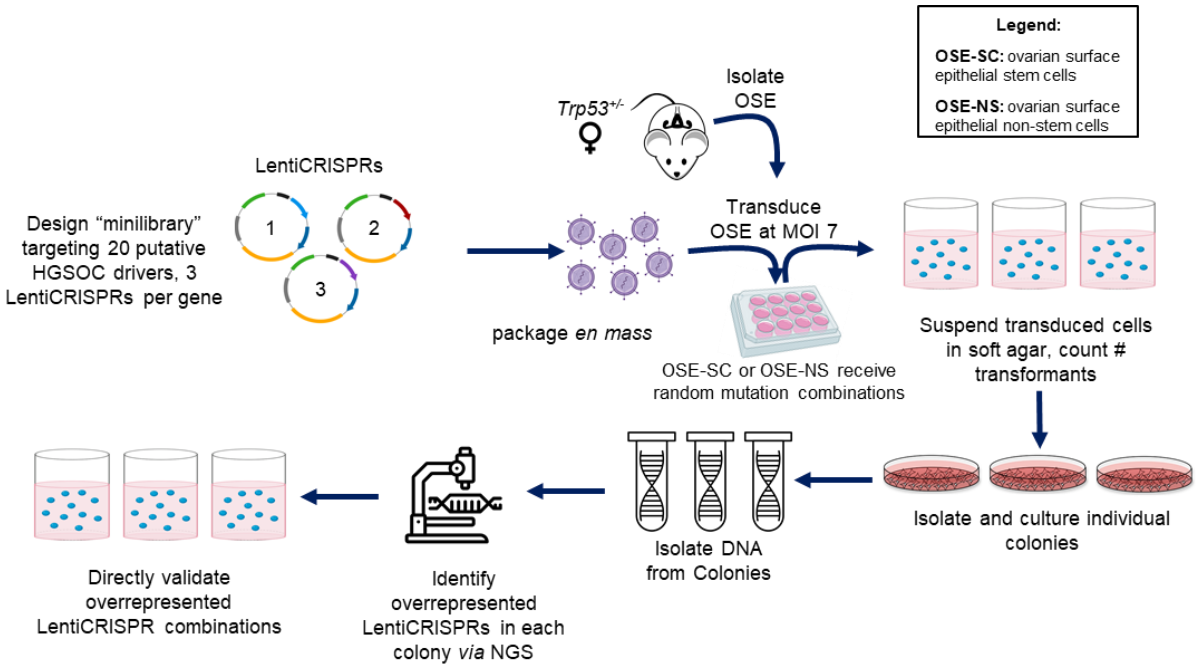

Figure 1. Strategy for identifying HGSOC tumor suppressor combinations. A total of 60 constructs were made in the vector LentiCRISPRv2, constituting the "minilibrary". OSE-NS or OSE-SC were transduced with functionally-validated LentiCRISPRs and then plated in soft agar. Individual transformants/colonies were isolated and individually cultured. Genome-integrated LentiCRISPRs from each transformant were identified by sequencing, and overrepresented combinations later validated in directed soft agar transformation assays. OSE-SC, ovarian surface epithelium stem cells; OSE-NS, ovarian surface epithelium non-stem cells; NGS, next-generation sequencing.

RESULTS

Strategy for screening candidate HGSOC suppressors and construction of a validated CRISPR-based lentiviral mini-library.

We adapted a strategy (Figure 1), analogous to that described by Zender and colleagues [21,22], to validate candidate tumor suppressors in a sensitized cell type. Sensitized cells do not undergo transformation in culture or *in vivo* upon transfer to a mouse host but can do so when an additional gene or combination of genes are disrupted. Since *TP53* is mutated in nearly all HGSOCs but *Trp53* mutagenesis alone does not cause spontaneous ovarian tumors in mice [11,23,24], we decided to use *Trp53*$^{+/-}$ cells in an inbred mouse strain background as the sensitized platform. Accordingly, we created and validated a new null *Trp53* allele in strain FVB/NJ as a source of ovarian surface epithelial cells (Figure S1A-D) for all screening experiments. Strain FVB/NJ was chosen because it is neither susceptible nor resistant to spontaneous ovarian lesions [25,26].

We generated a list of 20 potential HGSOC driver genes, largely corresponding to the most commonly mutated or deleted genes according to TCGA. We also included *FANCM* due to the putative role of Fanconi anemia-related genes in HGSOC development and *APC* because of to its critical role in canonical Wnt signaling and association with Type I ovarian carcinoma [1,3,5,27] (Table 1). We hypothesized that if these genes were true tumor suppressors, then mutating them alone or in combination with *Trp53* and/or other gene mutations would drive transformation in the relevant cell type. We next constructed a lentiviral CRISPR (version 2; hereafter called "LentiCRISPR") [28,29] "minilibrary" targeting the 20 putative HGSOC tumor drivers, infected the potential cells-

of-origin at a high multiplicity of infection (MOI), and assessed which vectors were overrepresented in transformed cells (See Methods, Figure 1). The library contained 3 constructs per gene, with the sgRNAs in each vector targeting the earliest possible exon of each gene to increase the likelihood of causing loss-of-function indel mutations via error-prone non-homologous end-joining (NHEJ) repair. We tested the minilibrary for gene editing efficiency in pilot assays prior to its use in HGSOC driver screening (Figure S2, Table S1), and designed new guides to replace vectors that did not efficiently mutate targets (Figure S3, Table S2).

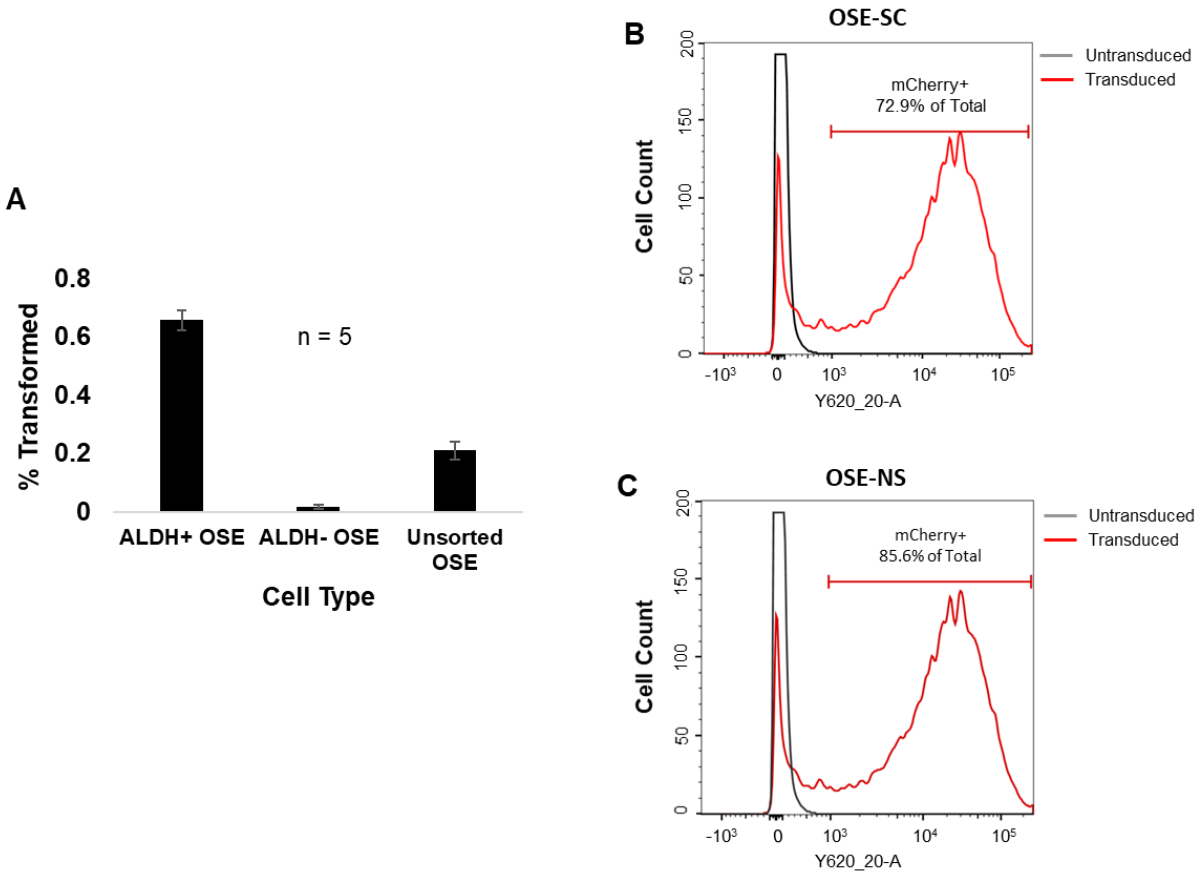

Figure 2. OSE-SC (ALDH$^+$) transform more frequently than OSE-NS (ALDH$^-$) despite similar viral transduction rates. (A) Percent transformation of OSE-SC, OSE-NS and unsorted OSE following LentiCRISPRv2 minilibrary transduction. OSE-SC transformed more frequently than OSE-NS and unsorted OSE. Unsorted OSE transformed more frequently than OSE-NS (5 replicates. SEM error bars). (**B,C)** FUGW-mCherry (mCherry-expressing lentivirus) transduction efficiency in OSE-SC and OSE-NS detected via flow cytometry. Flow cytometry was used to count mCherry$^+$ cells following transduction with equal concentrations of FUGW-mCherry lentivirus. Percentages indicate the percentage of total cells that are mCherry$^+$. The dark grey lines represent cell counts of untransduced cells. The red line represents cell counts of

FUGW-mCherry transduced cells. OSE-SC and OSE-NS gained mCherry fluorescence at similar rates following lentiviral transduction.

Random combinatorial mutagenesis of candidate HGSOC driver genes in OSE-SC and OSE-NS

To assess transformation frequency *in vitro*, we infected FACS-sorted *Trp53*$^{+/-}$ OSE-SC and OSE-NS (Figure S4) with either the lentiCRISPR minilibrary or a GFP-containing lentivirus, both at a MOI of ~ 7 (Figures S5, S6). The cells were then plated in soft agar to allow for assessment of adhesion-independent growth, a hallmark of carcinogenesis and transformation (hereafter, formation of adhesion independent colonies will be referred to as "transformation", and individual colonies will be referred to as "transformants") [30–35]. No colonies were observed in either non-transduced cells or cells infected with the GFP-containing vector (Figures S1E,F; S6; S7). Thus, heterozygosity for *Trp53* alone, or the process of infection, did not enable transformation of either cell type. However, transformants were observed in cells transfected with the entire library, albeit at low frequency despite an efficient infection frequency as judged by control infections with GFP lentivirus and LentiCRISPRv2 serial dilution assays (Figures 2A; S5, S7). OSE-SC were transformed (formed colonies) 41-fold more frequently than OSE-NS or unsorted OSE (0.66%, 0.02% and 0.21% of total plated cells, respectively) (Figure 2A, S7). The low transformation frequency suggests that only a few mutation combinations can initiate colony growth. That unsorted OSE produced 10.5-fold more colonies than OSE-NS is likely due to its OSE-SC subpopulation (Figures 2A; S4A, S7). To rule out the possibility that OSE-SC are simply infected by lentiviruses more efficiently than OSE-NS, we transduced each cell type with equal concentrations of mCherry lentivirus and scored for mCherry expression in each population. OSE-SC and OSE-NS were transduced at similar rates (72.9% and

85.6% mCherry expression, respectively), suggesting that transformation efficiency differences were indeed cell-type specific (Figure 2B,C).

Given a MOI of 7, and 3 LentiCRISPRs per gene, each gene represented in the minilibrary should be present in 30.2% of transduced cells (Figure S8). Control experiments supported this estimate and lack of technical biases, including the appearance of a control GFP LentiCRISPR at an expected random frequency of 12% (Methods; Figures 3A,B; S8).

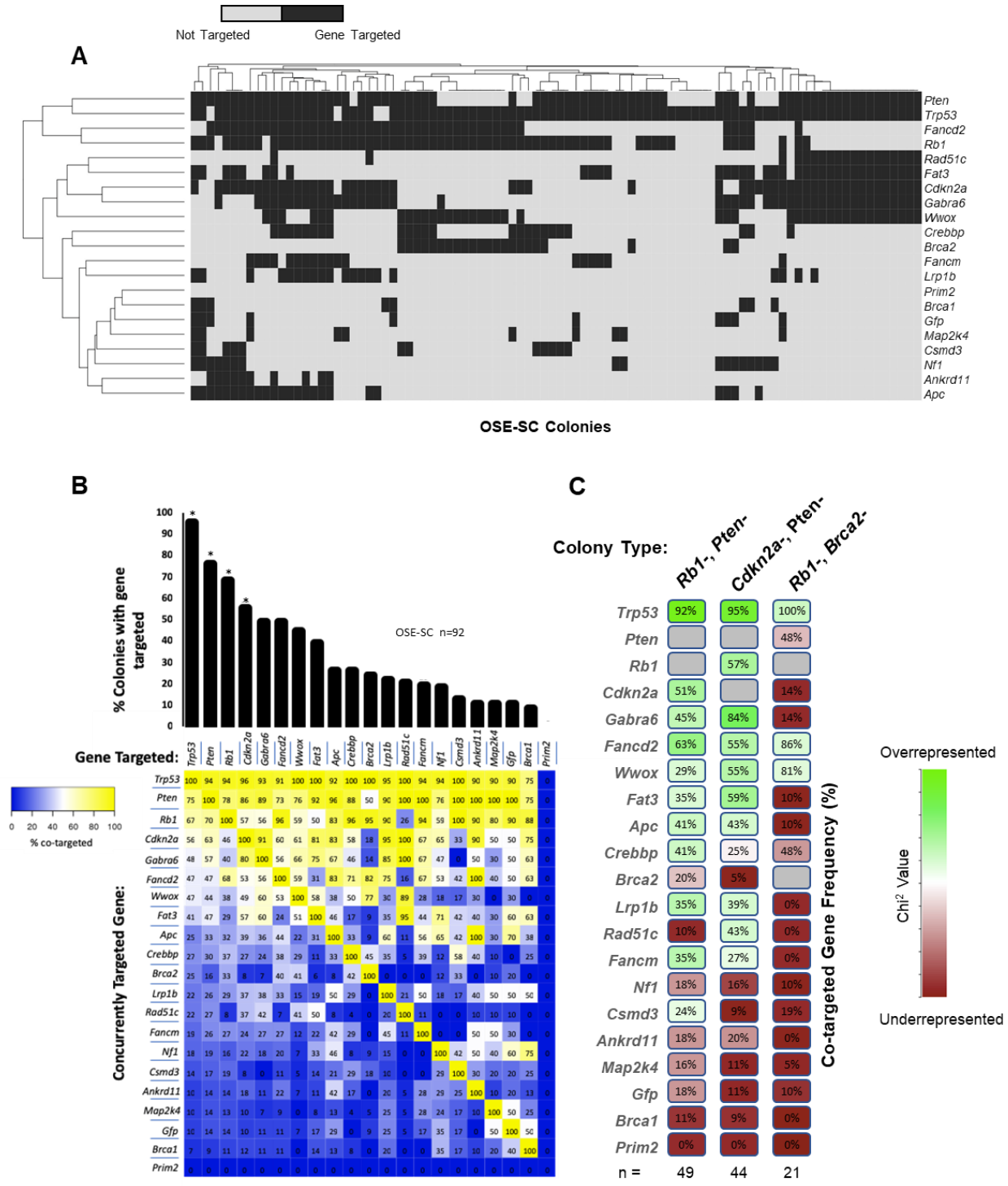

Figure 3. Identification of genome-integrated LentiCRISPRs and overrepresented target gene combinations in OSE-SC. (A) Genome-integration and hierarchical

clustering of LentiCRISPRv2 constructs in OSE-SC samples. Hierarchical clustering was performed on both sample similarity and gene targeting. **(B)** Overall percent gene targeting and co-targeting frequency. Significance ($p < 0.05$) for single integration overall was assessed using Chi^2 (df=19) and is indicated with an asterisk. The heat map displays co-integration frequency of each gene present on the x axis with a gene shown on the y axis. **(C)** Overrepresentation of co-targeted genes in sample subgroups. Over or underrepresentation was determined using Chi^2 analyses. Chi^2 values corresponding to $p \leq 0.05$ (df = 19) are colored in green. Red coloration indicates that co-integration may have occurred by chance, and that the p value is ≥ 0.05.

Enrichment of mutated gene combinations in transformed OSE-SC samples

Next, we determined whether particular minilibrary constructs and combinations thereof were over-represented in the transformants. To do this, we isolated all individual colonies and cultured them as transformed, adherent, clonal cell lines. The LentiCRISPR vectors were identical save for a unique 20bp Cas9 guide sequence which provided a unique molecular barcode (Table S3). We therefore identified all genome-integrated LentiCRISPRs from genomic DNA isolated from each transformant line using a next-generation sequencing-based approach (Figure 1). Three LentiCRISPRs per target gene were included in our minilibrary to control for unintended effects of any single construct. Overrepresented integration of only one of three gene targeting constructs would indicate potential spurious technical errors such as excessively high titer or off-target effects. Our sequencing dataset revealed genome integration of all three LentiCRISPRs corresponding to target genes found in more than 30% of colonies, suggesting that gene targeting was not a consequence of technical issues (Figure S9A).

Trp53 loss alone is necessary but insufficient for OSE-SC transformation

Nearly all (96%) OSE-SC colonies contained LentiCRISPRs targeting *Trp53*, consistent with human tumor samples which almost universally harbor *TP53* mutations (Figure 3A,B) (X^2 (19); $p < 0.05$). As expected given the high MOI, most OSE-SC transformants (88 of 92) also harbored lentiCRIPSRs targeting other genes. The most common genome-integrated vectors corresponded to *Pten* (76%), *Rb1* (68%), *Cdkn2a* (55%), *Fancd2* (49%), *Wwox* (45%), *Gabra6* (49%), *Fat3* (39%), *Apc* (26%), *Crebbp*

(26%), and *Brca2* (24%) (Figures 3A,B; S9B). The rarity of transformants lacking *Trp53* LentiCRISPRs (4%) suggests that heterozygosity of *Trp53* is insufficient for transformation, even in the context of other mutations that can synergize with partial *Trp53* loss (Figure 3A,B). Frequent co-targeting of *Trp53* also supports previous assertions that inactivating mutations in *Trp53* are crucial transformation precursors but are alone insufficient for OSE transformation [11].

LentiCRISPRs targeting *Trp53*, *Rb1*, *Cdkn2a*, and *Pten* are overrepresented in OSE-SC transformants

In addition to *Trp53,* most colonies (74%) had LentiCRISPRs targeting either *Rb1* or *Pten*, and nearly half (45%) had LentiCRISPRs targeting both (Figure 3 A,B). Most *Pten*- colonies (hereafter, we will refer to transformants bearing particular LentiCRISPRs by the corresponding gene symbol followed by "-"; e.g. *Pten1*-, with the caveat that the actual target gene may not have been mutated to a null state) were also *Rb1*- (70%), suggesting that concurrent inactivation of these two genes facilitates transformation (Figure 3B). This observation supports significant co-occurrence of *RB1* and *PTEN* mutations in HGSOC, and also in many other cancers, such as metastatic prostate cancer, lipomas, and astrocytomas [5,36–40]. Although *Rb1* was not targeted in all *Pten*- colonies, 88% of *Pten*- colonies lacking a *Rb1* LentiCRISPR had at least one LentiCRISPR targeting *Cdkn2a* (Figure 3A), which encodes p14ARF and p16INK4a. These are important regulators of TRP53 and RB1, respectively [41–43]. Only 3% of *Pten*- colonies in our dataset had no *Rb1* or *Cdkn2a* LentiCRISPRs, suggesting that either direct or indirect disruption of *Rb1* is important in *Pten*- colonies (Figure 3A).

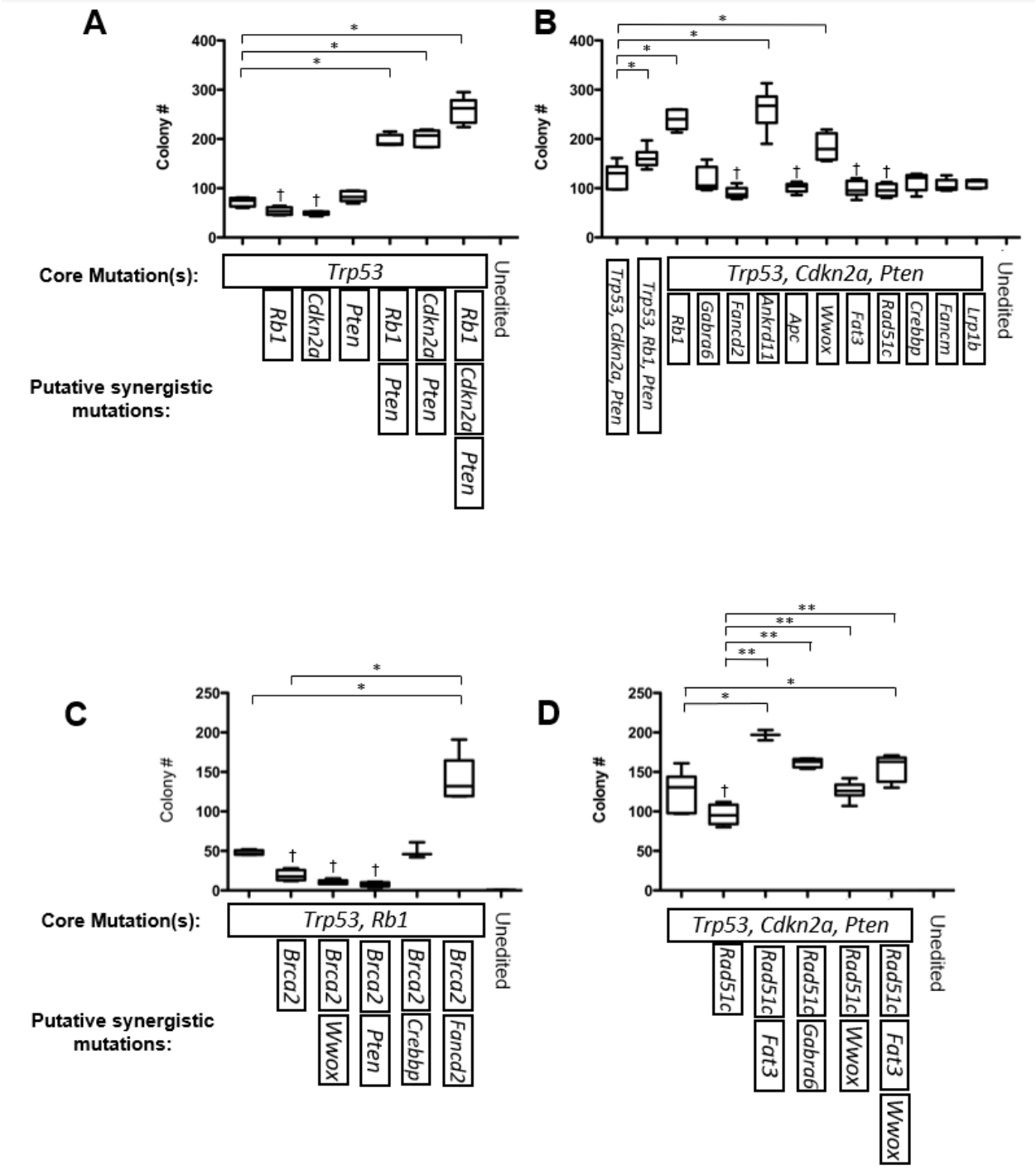

Figure 4. Targeted OSE-SC-transformation assay and validation of overrepresented LentiCRISPR combinations. A baseline level of adhesion independent growth was first assessed via induction of specific “core mutations” via LentiCRISPRv2 targeting. Additional minilibrary target genes were then mutated (using

LentiCRISPRv2) alongside core mutations to assess whether they act synergistically to promote adhesion independent growth. Colony counts that are significantly greater than baseline rates (core mutations alone) are labeled with an asterisk (*) (Students' two-tailed t-test $p<0.05$). Colony counts that are significantly lower than baseline rates are labeled with an obelisk (†). Standard error of the mean (SEM) error bars. **(A)** Targeted transduction of *Trp53*, *Rb1*, *Pten* and *Cdkn2a* LentiCRISPRs in OSE-SC. Significantly greater rates of OSE-SC transformation vs OSE-SC transduced with *Trp53* LentiCRISPRs alone occurred when all four genes were targeted together, or via mutagenesis of *Trp53*, *Rb1* (or *Cdkn2a*) and *Pten* (Students' two-tailed t-test $p \leq 0.05$, n=6). **(B)** Targeted transduction of *Trp53*, *Cdkn2a* and *Pten* LentiCRISPRs plus putative transformation enhancers. Only the addition of *Ankrd11* or *Wwox* LentiCRISPRs to *Trp53*, *Cdkn2a* and *Pten* LentiCRISPRs significantly enhanced colony formation vs *Trp53-/Cdkn2a-/Pten-* OSE-SC (Students' two-tailed t-test $p<0.05$, n=6). The addition of *Fancd2*, *Apc*, *Fat3*, and *Rad51c* significantly decreased colony count (Students' two-tailed t-test $p<0.05$). **(C)** Targeted transduction of *Brca2* LentiCRISPRs and *Brca2*-associated LentiCRISPRs. *Fancd2* mutations functioned synergistically with *Brca2, Trp53 and Rb1* mutations to significantly enhance colony formation vs *Trp53-*/*Rb1-*/*Brca2-* or *Trp53-*/*Rb1-* OSE-SC (Students' two-tailed t-test $p \leq 0.05$, n=6). **(D)** Targeted mutagenesis of *Rad51c* LentiCRISPRs and *Rad51c*-associated LentiCRISPRs. *Fat3* and *Gabra6* mutagenesis alongside *Trp53*, *Cdkn2a*, *Pten* and *Rad51c* significantly increased colony count compared to *Trp53-/Rb1-/Pten-/Rad51c-* OSE-SC (Students' two-tailed t-test $p \leq 0.05$, n=6).

Mutations in *Trp53*, *Rb1*, *Pten*, and *Cdkn2a* function synergistically to promote transformation

To validate and dissect the apparent major contributions of *Trp53*, *Pten*, *Rb1* and *Cdkn2a* in suppressing OSE-SC transformation, we performed additional infections with vectors corresponding to combinations of just these four genes. Confirming our observations from the whole library screen (see above), mutating the second allele of *Trp53* alone in *Trp53*$^{+/-}$ OSE-SC was inefficient in transformation (Figures 4A; S10, S11A). However, co-mutagenesis with combinations of *Rb1*, *Cdkn2a*, and *Pten* significantly enhanced transformation efficiency (colony number) and colony size (Figures 4A; S10; S11A). Specifically, we observed that targeting *Trp53* alongside *Pten* and *Rb1*, *Pten* and *Cdkn2a*, or *Pten*, *Rb1* and *Cdkn2a* led to greater transformation efficiencies and larger colonies (Figures 4A; S10; S11A). The most efficient transformation and largest colony sizes occurred when *Trp53, Rb1, Cdkn2a*, and *Pten* were targeted simultaneously (Figure 4A; S10; S11A). There was no significant increase in transformation efficiency when *Trp53* was co-targeted with only one of the other 3 genes, although there was a significant increase in the size of *Trp53-/Rb1-* and *Trp53-/Cdkn2a-* colonies (Figure S11A). These results indicate that deficiency of *Trp53, Rb1* and *Pten* constitute a core state for efficient transformation of OSE-SC *in vitro*.

Disruption of *Ankrd11* or *Wwox* can further enhance transformation of *Trp53-/Cdkn2a-/Pten-* OSE-SC

Interestingly, certain cohorts of genes were co-targeted at significant frequencies in *Trp53-/Rb1-/Pten-* (*Cdkn2a*, *Gabra6*, *Fancd2, Wwox*, *Fat3*, *Apc*, *Crebbp*, *Lrp1b*,

Fancm, and *Csmd3*; $X^2 = 19$, $p < 0.05$) or *Trp53-/Cdkn2a-/Pten-* colonies (*Rb1*, *Gabra6*, *Fancd2*, *Wwox*, *Fat3*, *Apc*, *Lrp1b*, *Rad51c*, and *Fancm*; $X^2 = 19$, $p < 0.05$), despite vectors for each being underrepresented overall (Figure 3B,C). To explore whether mutations in these genes influenced transformation, we performed additional OSE-SC infections in which individual genes were mutated along with the core combinations of *Trp53*, *Cdkn2a* (or *Rb1*) and *Pten*. Most (*Lrp1b*, *Fancm*, *Crebbp*, *Rad51c*, *Fat3*, *Apc*, *Fancd2*, and *Gabra6*) did not enhance transformation rates, and several (*Fancd2*, *Apc*, *Fat3*, and *Rad51c*) actually decreased transformation rates (Figures 4B; S12). However, significant increases in transformation frequency were observed when LentiCRISPRs targeting *Ankrd11* or *Wwox* were added to the core of *Trp53, Cdkn2a* and *Pten* (Figure 4B). No significant increase in colony size was noted following mutagenesis of any TCGA driver genes other than *Trp53*, *Rb1*, *Cdkn2a*, and *Pten* (Figure S11B). We surmised that the overall underrepresented target genes that had no (or a negative) effect on OSE-SC transformation in targeted experiments, but which were often present in cells with high numbers of other vectors, was a technical artifact. Indeed, an association between underrepresented target genes and the number of genes targeted per colony was observed (Figure S13). For instance, most samples with LentiCRISPRs targeting *Ankrd11*, *Apc*, *Lrp1b*, *Brca1*, *Nf1*, *Fancm, Fancd2*, and *Map2k4* occurred in colonies with 8 or more targeted genes (Figure S13). Such clones also generally contained common LentiCRISPRs for *Trp53*, *Rb1*, *Pten*, and *Cdkn2a* (Figure 3A,B), suggesting that many or all of these lower-frequency “hits” are unrelated to transformation, but perhaps the parental cell was particularly susceptible to viral infection.

Brca2 disruption deters transformation of *Trp53*-/*Rb1*- OSE-SC, but enhances transformation when co-mutated with *Trp53*, *Rb1*, and *Fancd2*.

Notably, LentiCRISPRs for *Brca2* were underrepresented overall in OSE-SC colonies, despite the association of mutations in this gene with familial HGSOC (Figure 3 A,B) [5,44,45]. *Brca2* deficiency is cell lethal in the absence of other mutations, causing replication stress, mitotic abnormalities, 53BP1 activation, and G1 arrest [46,47]. However, most cancer cells develop mechanisms to overcome this G1 arrest through rescuing mutations in other genes like *Trp53* [46]. In our screen, 95% of *Brca2*- colonies were also *Trp53*-/*Rb1*- (Figure 3A,B). Many *Brca2*- colonies also contained LentiCRISPRs targeting *Fancd2* (82%), *Wwox* (77%), and *Crebbp* (45%) (Figure 3B). Constructs targeting *Trp53*, *Fancd2* and *Wwox*, in particular, were overrepresented alongside *Brca2* and *Rb1* (X^2 (19); $p < 0.05$). We hypothesized, therefore, that many of these co-targeted genes are necessary for efficient *Brca2*- colony growth. Targeted LentiCRISPR co-infections revealed that *Brca2* mutation significantly reduced transformation rates of cells also targeted for *Trp53* and *Rb1*, in agreement with previous reports (Figure 4C; S14) [46,47]. However, we found that the addition of *Fancd2* LentiCRISPRs to constructs targeting *Trp53*, *Rb1* and *Brca2* rescued the detrimental effects of single mutations in either *Brca2* or *Fancd2* on transformation rate, and significantly increased colony size (Figure 4C; S11C, S14). *Trp53*-/*Rb1*-/*Fancd2*-/*Brca2*- cells had three-fold more colonies than *Trp53*-/*Rb1*- OSE-SC (Figure 4C; S14). Despite co-targeting with *Brca2* in 48% of cases, neither *Pten* nor *Wwox* LentiCRISPR transductions significantly increased number or size relative to *Trp53*-/*Rb1*- or *Trp53*-

/*Rb1*-/*Brca2*- colonies (Figure 4C; S11C, S14). We did, however, find that *Crebbp* targeting restored *Trp53*-/*Rb1*-/*Brca2*- colony formation to the level observed for *Trp53*-/*Rb1*- colonies, and significantly increased colony size (Figure 4C; S11C). These results suggest that multiple concurrent driver mutations are necessary to overcome growth-deterring effects of *Brca2* mutagenesis.

Rad51c synergizes with *Fat3* and *Gabra6* to promote transformation

Like *Brca2*, *Rad51c* is involved in DNA double strand break repair [48]. Loss of *Rad51c* has also been shown to be detrimental to cell growth, so synergistic mutations may be required for efficient adhesion independent growth of *Rad51c*- OSE-SC [49]. Although *Rad51c* mutagenesis was detrimental to the transformation of *Trp53*-/*Cdkn2a*-/*Pten*- OSE-SC (Figure 4B), we observed that *Rad51c* was frequently co-mutated with *Gabra6* (100%), *Wwox* (89%) and *Fat3* (95%) in our screen (Figures 3B). We therefore performed targeted infections of LentiCRISPRs targeting *Gabra6*, *Wwox*, and *Fat3* alongside *Rad51c* and core mutations in *Trp53*, *Cdkn2a*, and *Pten*. We observed significantly increased transformation rates following concurrent mutagenesis of *Rad51c* and *Fat3* or *Gabra6*, but not *Wwox*, in *Trp53*-/*Cdkn2a*-/*Pten*- colonies (Figure 4D; S15). Only *Trp53-/Cdkn2a-/Pten-/Rad51c-/Gabra6*- colonies were significantly larger than *Trp53-/Cdkn2a-/Pten*- or *Trp53-/Cdkn2a-/Pten-/Rad51c*- colonies (Figure S11D). These results suggest that some HGSOC-associated mutations, like those in *Rad51c*, can promote transformation only with additional synergistic mutations to overcome synthetic lethality.

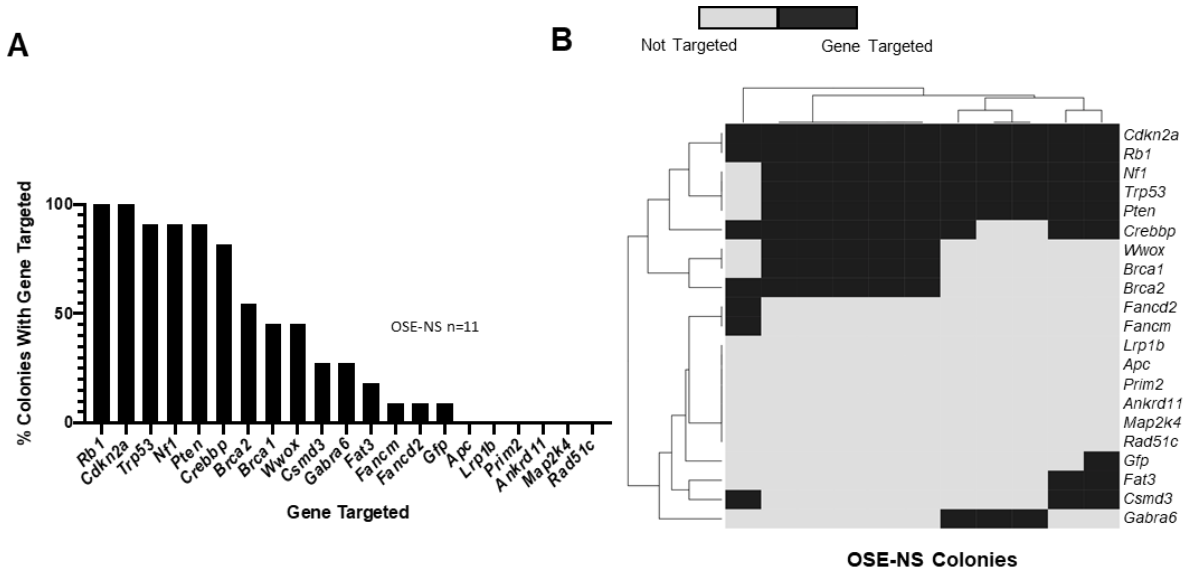

Figure 5. Identification of genome-integrated LentiCRISPRs overrepresented target gene combinations in OSE-NS. (A) Percent gene targeting frequency in OSE-NS colonies. **(B)** Genome-integration and hierarchical clustering of LentiCRISPRv2 constructs in OSE-SC samples. The binary color scale shows whether a gene is targeted by at least one LentiCRISPR in each individual sample. Light grey indicates that a given gene was not targeted, while dark grey indicates that a gene was targeted by at least one LentiCRISPRv2 construct. Hierarchical clustering was performed on both sample similarity and gene targeting, resulting in several clusters of co-targeted genes and similar transformants.

LentiCRISPR integration patterns in OSE-NS transformants

OSE-NS transformed much less efficiently than OSE-SC, yielding only 11 colonies for analyses (Figure 5). This small sample size preempted meaningful statistical analyses of target gene overrepresentation. Nevertheless, like OSE-SC, most (10/11) clones contained LentiCRISPRs targeting *Trp53*, *Rb1*, *Pten*, and *Cdkn2a*. Other overall commonly targeted genes include *Nf1* (91%), *Crebbp* (82%), *Brca2* (55%), *Brca1* (46%), and *Wwox* (46%).

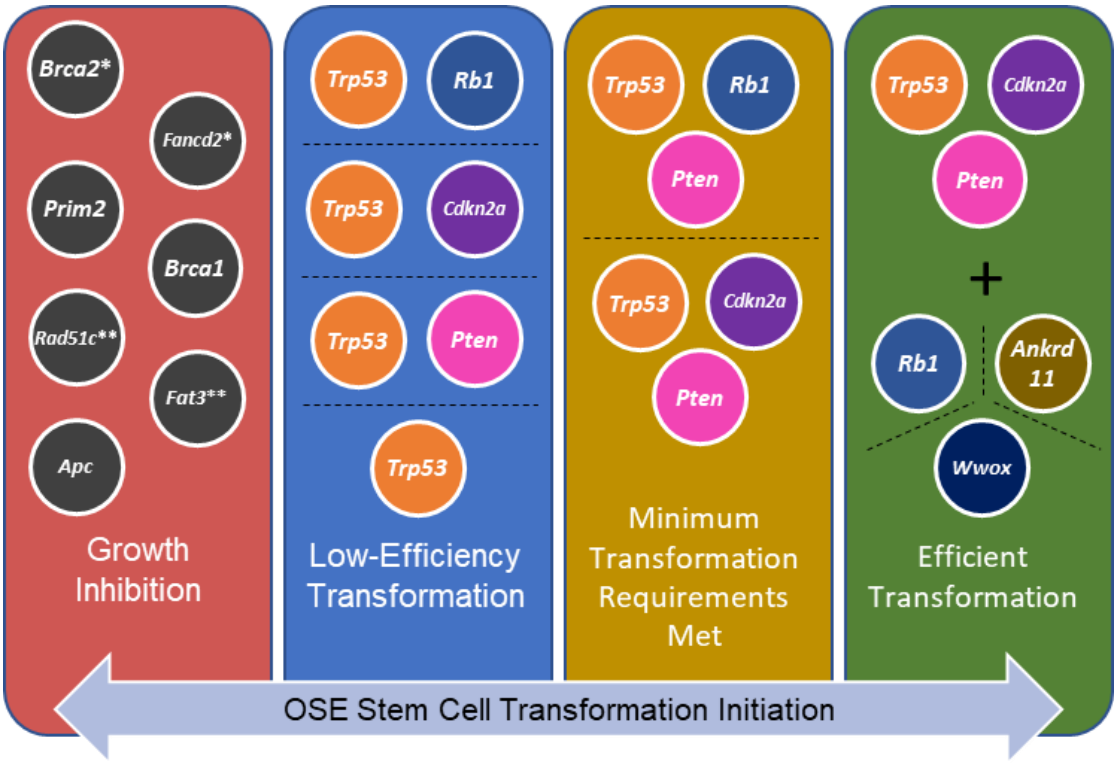

Figure 6. Model of mutations necessary for efficient *in vitro* OSE-SC transformation. Random mutagenesis assays and targeted experiments revealed minimal requirements for adhesion independent growth and mutations that enhance transformation. The blue box contains genes that are ”minimal requirements” for transformation, or cause transformation at low efficiency. The addition of mutations shown in the yellow box cause significant degrees of transformation. Addition of further mutations in genes shown in the green box allow for the highest rates of transformation. Genes listed in the red box inhibit transformation. However, two exceptions exist. *Brca2* and *Fancd2* (marked with a single asterisk) co-mutagenesis alongside *Trp53* and *Rb1* result in efficient OSE-SC transformation. Similarly, *Rad51c* and *Fat3* (or *Gabra6*) (marked with two asterisks) plus *Trp53*, *Cdkn2a* and *Pten* caused efficient transformation.

DISCUSSION

It has long been recognized that carcinogenesis typically requires multiple genetic events, and tumor sequencing, as exemplified by the TCGA, has not only supported this tenet, but also informed the constellations of mutations that are commonly present and thus likely contributing to cancer formation and progression. However, the requirements for tumor initiation can be complex in terms of gene combinations and susceptible cells; for HGSOC, precursor lesions have not been conclusively identified, and patient tumor samples have an average of 46 mutations [5]. Mathematical modeling of cancer driver events suggest that only 5 to 8 driver mutations may be necessary for initiation [50,51], so most of the mutations present in late stage tumors are irrelevant to initiating events. Whereas contributions of some putative initiating driver genes have been assessed using *in vitro* and *in vivo* systems [6–8,13,52], these directed approaches cannot experimentally assess the thousands of mutation combinations in the many commonly altered genes in HGSOC. Our screen represents the first effort to experimentally define the combinations of mutations that drive transformation of ovarian epithelial cells in a random, unbiased manner.

The issue of HGSOC initiation is further complicated by several potential sources of the HGSOC cell of origin. We focused on OSE as a source of putative HGSOC cells of origin, but there are others, such as the distal fallopian tubal epithelium (TE), which can be transformed [53–58]. The presence of serous tubal intraepithelial carcinomas (STICs) in patients with HGSOC, and frequent presence therein of identical *TP53* mutations with those in concurrent HGSOC tumors, led to the proposal that HGSOC

can initiate at the TE [53,59]. The TE also shares several well-characterized markers of HGSOC that have not been observed in the OSE [60]. For example, secretory cells in the TE express PAX8, which is present in HGSOC but not in untransformed OSE [61–63]. Monolayers of PAX8-positive TE cells can also form lesions that express “p53 signatures” that are often associated with mutant *TP53*, but generally have a low proliferative index and lack cellular atypia [64,65]. Correlative links between the TE and HGSOC have been supported by recent algorithmic comparison of HGSOC and distal TE global gene expression landscapes in which similarities were found between HGSOC and the distal TE, but also with OSE-SC in many cases [14,15]. It is possible therefore that all three cell types (OSE-SC, OSE-NS, and TE) have the ability to transform into HGSOC, as has been suggested by others [8,13,66]. These data are supported by direct clinical evidence in which about half of HGSOCs can be reliably explained by STIC origin [53,59,67].

We focused on the OSE here because it consists of a single cell type (unlike the heterogeneous TE) for which well-established isolation and culturing methodology exists [11,68]. It is also been shown to transform in animal models such as rat and mouse, and is where HGSOC localizes in patients [8,11,67,69–72]. Similarities between OSE-sourced tumors and HGSOC have been demonstrated both genomically and histopathologically [11,13,15,20,73,74]. However, recent evidence has suggested that only a small subpopulation of the OSE (OSE-SC) is particularly cancer-prone [20]. Such cells have been shown to possess stem cell-like characteristics such as the ability to replace OSE lost during ovulation and expression of stem cell markers including LGR5, ALDH1, LEF1, CK6B, and CD133 [20]. That study also found that *Trp53* and *Rb1* knockouts in

OSE-SC result in significantly more tumors and much lower latency compared to *Trp53* and *Rb1* knockouts in non-stem cells.

Our screening results and targeted mutagenesis assays support the theory that the ovarian hilum, which is the putative location of OSE-SC and a transition zone between the OSE, TE, and mesothelium, is particularly prone to transformation. Following random mutagenesis of 20 putative HGSOC driver genes, we found that OSE-SC transformed 41-fold more frequently than OSE-NS. These data support longstanding suspicion that adult stem cells within transition zones are especially prone to carcinogenesis [75–77]. Interestingly, the stem cell theory of cancer initiation may be a unifying concept between OSE- and TE-sourced tumors. Seidman and colleagues (2015) recently demonstrated that most STICs occur in close proximity to the tubal-peritoneal junction [78]. Other studies have demonstrated that the tubal-peritoneal junction, like the ovarian hilum region, contains LEF1-expressing cells, and that patients with higher LEF1 expression had poorer five year survival [79]. It is possible, therefore, that HGSOC lesions arise in either OSE-SC or TE stem cells located in transitional zones.

Based on the most common mutation combinations we observed in colonies produced by infection of OSE-SC with the LentiCRISPR minilibrary, and in follow-up validation experiments with specific LentiCRIPSR combinations, we developed a model of events for OSE-SC transformation initiation (Figure 6). We propose that functional loss of only 3 of the 20 genes assessed in this study, *Trp53*, *Rb1*, and *Pten,* are necessary for efficient OSE-SC transformation (Figures 3A,C. 4A; S11A). Knockout of these three genes in the OSE has been previously shown to cause development of both

low grade and high grade serous carcinoma in mouse models [80]. Mutation of *Cdkn2a* could partially compensate for *Rb1* disruption because *Cdkn2a* encodes p16(INK4a) and p14(ARF), known regulators of *Rb1* and *Trp53*, respectively [43]. Our model also suggests that *Trp53* and/or *Rb1* disruption can cause low efficiency transformation without *Pten* mutations, but colony size was much smaller. The greatest colony size and quantity was observed in *Trp53*-/*Rb1*-/*Cdkn2a*-/*Pten*- colonies, suggesting additive effects of mutations in each gene.

Our proposition that *Trp53* and *Rb1* mutations are core minimal OSE transformation requirements is supported by previous evidence in genetically engineered mouse models (GEMMs). Flesken-Nikitin and colleagues (2003) showed that combined knockout of *Trp53* and *Rb1* in the OSE causes higher rates of carcinogenesis and lower latency compared to single knockout of *Trp53* or *Rb1* alone [11]. These results were backed by mouse modeling of *Trp53* and *Rb1* knockouts in the OSE. For example, *Brca1*/*2* or *Trp53* mutations alone failed to cause significant pathologic changes to the OSE, but *Trp53*$^{-/-}$ *Rb1*$^{-/-}$, *Trp53*$^{-/-}$ *Rb1*$^{-/-}$ *Brca1*$^{-/-}$, and *Trp53*$^{-/-}$ *Rb1*$^{-/-}$ *Brca2*$^{-/-}$ genotypes resulted in tumors histopathologically similar to HGSOC [81]. These and other models support findings that *TP53* mutations are nearly ubiquitous in ovarian carcinoma and that the *RB1* pathway is dysregulated in 67% of HGSOC tumors [5,11,56,82].

Our observation that *Pten* disruption significantly increases transformation frequency and colony size is also consistent with data from GEMMs. HGSOC-like tumor development in mouse models without *Pten* mutations have longer latencies than mice with *Pten* mutations [57,83]. Tumors with *PTEN* mutations are more aggressive and

have a worse prognoses [84]. *PTEN* and *RB1* mutations also significantly co-occur in HGSOC, suggesting that they may act synergistically in carcinogenesis [5,36,37].

In addition to identifying a core set of transformation-enhancing mutations, our data suggest that mutating two other TCGA driver genes can further enhance OSE-SC transformation susceptibility (Figure 6). Given a core set of mutations in *Trp53*, *Cdkn2a* and *Pten*, additional disruption of *Ankrd11* or *Wwox* significantly promoted adhesion-independent growth. Interestingly, genomic analyses of tumors from a mouse model deficient for *Trp53*, *Brca1*, *Brca2*, and *Pten* revealed deletions in both *Ankrd11* and *Wwox*, suggesting that they may play a role in tumor initiation or progression [57]. Both *Ankrd11* and *Wwox* have also been implicated in *Trp53*-related pathways. ANKRD11 is a putative tumor suppressor that interacts with TP53 and promotes its transcription factor activity [85–87]. The protein has also been shown to bind mutant TP53 and partially restore its DNA binding capacity to the *CDKN1A* promoter [85,87]. WWOX greatly influences the response of TP53 to genotoxic stress, and *Wwox* mRNA inhibition abolishes TRP53-dependent apoptosis [88,89]. Mutations in *Wwox* and *Ankrd11* in our project may therefore contribute to further dysregulation of *Trp53* or may promote transformation in the presence of non-null mutations in *Trp53* induced by LentiCRISPR mutagenesis.

Several genes assessed in our study, namely *Brca2*, *Fancd2*, *Prim2*, *Brca1*, *Rad51c*, *Fat3*, and *Apc*, appeared to deter OSE-SC adhesion-independent growth when singly mutated alongside core disruption of *Trp53*, *Rb1* and/or *Pten*. However, we found that combined disruptions of subsets of these genes actually function synergistically to enhance OSE-SC transformation. Namely, co-mutation of *Brca2* and

Fancd2, *Rad51c* and *Fat3*, or *Rad51c* and *Gabra6,* in addition to the core mutations, caused significant increases in colony growth. The growth-deterring effects of *Brca2*, *Fancd2* or *Rad51c* single mutagenesis observed in our assays have also been documented by others. Cells lacking *Brca2* accumulate spontaneous DNA damage during G2/S phase and often senesce following the G1 checkpoint [46]. Similarly, cells deficient in either *Rad51c* or *Fancd2* display reduced cell proliferation, especially after further induction of DNA Damage [49,90–93]. We speculate that concurrent mutagenesis of these potentially growth-deterring genes may be necessary to rescue proliferation. It remains to be investigated whether the potential synthetic lethality or growth deterrence observed here may be relevant for targeted drug development.

A fundamental aspect of our project was not only to identify and validate combinations of transformation-associated genes, but also to assess whether commonly-mutated HGSOC genes are simply passengers or unnecessary for transformation initiation. For many genes in our study, there was no evidence for involvement in OSE transformation. They include *Apc*, *Crebbp*, *Fancm*, *Nf1*, *Csmd3*, *Map2k4*, *Brca1*, and *Prim2.* Although mutations in these genes are associated with developed tumors, sequencing data alone is unable to distinguish whether mutations occurred during cancer initiation or were later events. Our study only assessed transformation initiation, so it's possible that these genes facilitate later stages of carcinogenesis. Alternatively, many genes that are not involved in transformation initiation may be passenger mutations or a consequence of the genomic instability associated with HGSOC tumor cells.

Our study has elucidated core mutations necessary for cell autonomous transformation and has addressed fundamental questions surrounding ovarian carcinoma initiation mechanisms. However, it will be important to model the various mutation combinations *in vivo* for their abilities to induce clinically relevant cancers. Such efforts are now under way using information obtained from these studies *in vitro*. To date, TCGA has generated comprehensive genomic and transcriptomic data for 33 cancer types using over 20,000 primary tumor samples [94]. These comprehensive datasets report genes that are significantly mutated or commonly deleted in different diseases, but the roles of many of these genes in cancer initiation or downstream biology is unclear. Unbiased combinatorial screening efforts, such as that we've applied here, in the proper cellular paradigms, may help disentangle steps of neoplastic transformation in multiple types of cancer.

ACKNOWLEDGEMENTS

We thank Q. Sun and P. Schweitzer for providing assistance with processing and analysis of sequence data; L. Johnson for help with statistical analyses, and the staff (R. Munroe and C. Abratte) of Cornell's transgenic facility for producing *Trp53* mutant mice. We also acknowledge technical support and advice from the following individuals: A. McNairn, L. Wang, A. Kolarzyk and M. Baccas. This work was supported by grant from the Ovarian Cancer Research Fund (#327516) and NYSTEM (C029155) to JCS and AYN, from the US National Institutes of Health (NIH) and National Cancer Institute (NCI) (CA182413) to AYN, and a predoctoral fellowship to RJY (NYSTEM C30293GG).

METHODS

Generation of *Trp53*$^{+/-}$ FVB/NJ Mice

CRISPR/Cas9 gene editing was used to generate a *Trp53*$^{+/-}$ co-isogenic mouse line in strain FVB/NJ. A cloning-free overlap PCR method was used to generate the DNA template for making sgRNA [95]. The following guide RNA sequence corresponding to exon 4 of *Trp53* was used: AGTGAAGCCCTCCGAGTGTC [28,29]. The DNA template was reverse transcribed into RNA using the MEGAshortscript T7 Transcription kit (Ambion), then purified using MinElute Columns (Qiagen; Cat#: 28004). The sgRNA (50ng/uL) and Cas9 mRNA (25ng/uL, TriLink) was microinjected into the pronuclei of FVB/NJ zygotes, then transferred injected zygotes into oviducts of pseudopregnant females. A male founder carrying a 1bp insertion in exon 4 and a predicted STOP codon before the DNA binding domain of TRP53 was selected to establish a line (Figure S1 A,B). Initial phenotyping was done after three generations, all of which were crossed to FVB/NJ animals (Figure S1 C,D).

Mouse Embryonic Fibroblast Isolation

Mouse Embryonic Fibroblasts (MEFs) were generated using previously described methodology [96]. Briefly, embryos were isolated from pregnant mice at 13 dpc (day post-coitum) and washed in PBS. Working with one embryo at a time, each embryo was placed in a clean petri dish with 0.25% trypsin EDTA solution. A small biopsy was collected for later genotyping. Sterile scalpel blades were used to mince tissue until it was able to be maneuvered with a pipette. Minced tissue incubated for 15 minutes at 37˚C in trypsin solution. DMEM with 10% FBS was then used to inactivate

trypsin. MEFs were plated on 10cm plates in DMEM with 10% FBS and expanded until passage 2.

Western blotting

Trp53$^{+/+}$, *Trp53*$^{+/-}$, and *Trp53*$^{-/-}$ MEFs were treated with 10Gy irradiation to activate the p53 pathway. Equal quantities of cells from each group were pelleted, lysed with RIPA buffer, and utilized for immunoblotting experiments. Protein samples were collected from cell pellets lysed with RIPA buffer. Protein concentrations were normalized via both cell number and BCA assay. Samples were run through 4-15% gradient polyacrylamide gels (BioRad; Cat#: 4561083EDU) and transferred onto nitrocellulose membranes (Thermo Fisher; Cat#: 88018). We used the Rabbit anti *TRP53* primary antibody (Cell Signaling; Cat#: 9282) for detection of *TRP53*, along with goat anti-rabbit HRP-linked secondary antibody (Cell Signaling; Cat#: 7074S). Rabbit primary antibody was used for detection of *ACTB* (β-actin) (Abcam: Cat#: ab8227), along with goat anti-rabbit HRP-linked secondary antibody (Cell Signaling; Cat#: 7074S) (Figure S1C).

LentiCRISPRv2 construct design and cloning

LentiCRISPR v2 was obtained from Addgene (plasmid # 52961; http://n2t.net/addgene:52961; RRID:Addgene 52961). We designed sgRNA guides targeting the earliest possible exon of 20 TCGA driver genes (Table 1) with the intent of inducing a gene-inactivating nonsense mutation in targets. Guides were designed using parameters described previously [97]. With few exceptions, guide sequences were

chosen with an optimal off target score (>75). If no guides with a score of 75 or greater were found, we chose a guide with the highest possible score (Supplemental Table 3). Synthetic sense and antisense oligonucleotides for each guide were produced as in 25nmol quantities by Integrated DNA Technologies, such that each strand has overhangs necessary for cloning using the BSMBI restriction enzyme (New England Biolabs; Cat#: R0580S).

Target guide sequences were cloned into LentiCRISPRv2 plasmids using previously published methodology [28,29]. Briefly, sense and antisense oligonucleotides corresponding to each sgRNA were annealed to one another in a thermocycler (BioRad MyCycler). LentiCRISPRv2 plasmid was cut using BSMB1 restriction enzyme (New England Biolabs; Cat#: R0580S), and T4 DNA ligase (NEB; Cat#: M0202S) was used to ligate oligos into LentiCRISPRv2 plasmid. LentiCRISRv2 plasmids were transformed into One Shot Stbl3 chemically competent *E. coli* (ThermoFisher; Cat#: C737303). Transformed bacteria were plated on LB agar plates with ampicillin (Sigma-Aldrich; Cat#: A0166) for selection, and single colonies were picked and cultured in LB broth (Sigma-Aldrich; Cat#: L3147). Plasmid was isolated from bacteria using the GeneJet Plasmid Miniprep kit (ThermoFisher; Cat#: K0502) or the GeneJet Plasmid Midiprep kit (ThermoFisher; Cat#: K0481).

We validated that each LentiCRISPRv2 construct contained the correct guide via Sanger sequencing (Cornell Biotechnology Resource Center) primed with the following oligonucleotide: 5'-GAGGGCCTATTTCCCATGATT-3'.

Tissue culture of the OSN2 cell line and primary OSE

We cultured OSE, OSE-SC and OSE-NS following previously described methodology [20]. Briefly, ovaries were isolated from *Trp53* heterozygous FVB/NJ adult females and placed into phosphate-buffered saline (PBS) without Ca^{2+} or Mg^{2+} on ice. Ovaries were washed three times with PBS under a laminar flow hood, and a sterile scalpel blade was used to separate ovaries from the bursa. OSE was separated from the ovary via treatment with a digestion buffer consisting of collagenase (Sigma-Aldrich; Cat#: 10269638001), dispase (Sigma-Aldrich; Cat#: 10269638001), DNaseI (Sigma-Aldrich; Cat#: 11284932001) and Bovine Serum Albumin (BSA) (Sigma-Aldrich; Cat#: A9418). We finally added the pellet from each ovary to 2mL OSE medium on gelatin-coated 24 well culture plates (Corning Costar; Cat#: CLS3527-100EA. Epithelial lineage of isolated cells was determined via detection of CK8 expression using immunofluorescent microscopy (Figure S4B-D).

Primary OSE cultures and the OSN2 cell line[11] were maintained in culture in media containing DMEM (VWR; Cat#: 10-017-CM), Hams F12 (Thermo Fisher, Cat#: 11320033), 5% FBS (Atlanta Biologicals; Cat#: S11050H), hydrocortisone (Sigma-Aldrich; Cat#: H4001), insulin-transferrin-sodium selenite (Sigma Aldrich), non essential amino acids (NEAA) (Thermo Fisher; Cat#: 11140050), glutamate (Thermo Fisher; Cat#: 25030081), sodium pyruvate (Thermo Fisher; Cat#: 11360070), and penicillin-streptomycin (Thermo Fisher; Cat#: 15140122) on 0.2% gelatin-coated culture plates (Corning Costar; Cat#: 07-200-83). Cells were passaged up to two times using 0.25% Trypsin-EDTA with Phenol Red (Thermo Fisher; Cat#: 25200072) to remove adherent cells from plates.

Immunofluorescent Microscopy

OSE, OSE-SC, OSE-NS, MEFs from FVB/N mice and OSN2 cells were grown on gelatin-coated glass cover slips for 24 hours and then fixed using methanol. Fixed cells were washed with PBS, and then blocked using goat serum (Sigma Aldrich; Cat#: NS02L). Primary Rat anti CK8 (TROMA1) antibody (University of Iowa Developmental Hybridoma Bank; Cat#: AB_531826) was added to coverslips overnight at 4˚C, followed by PBS washes. Alexa Fluor 488 goat anti rat antibody (ThermoFisher; Cat#: A-11006) was added for one hour using the manufacturer-recommended concentration. One drop of mounting media (Vector Laboratories; Cat#: H-1000) was used to adhere cover slips to slides, and cells were imaged using an Olympus BX51 microscope and Olympus XM10 camera at 10x magnification. GFP expression conveyed by FUGW viral transductions was detected using a BioRad ZOE Fluorescent Cell Imager at 20x.

Tissue Culture of HEK293T, HELA and MEF cells

HEK293T (ATCC CRL-3216) and HELA (ATCC CCL-2) cells were cultured in DMEM with 10% FBS, NEAA, and sodium pyruvate on gelatin-coated plates, and HELA cells were cultured in DMEM containing 10% FBS on plates coated with 0.2% gelatin. MEFs were isolated from female E13.5 embryos isolated from a breeding of two *Trp53* heterozygous parents. They were cultured on uncoated plates and were grown in DMEM containing 10% FBS. Cells were passaged onto 10cm plates using 0.25% Trypsin-EDTA with phenol Red to remove adherent cells from plates.

Isolation and characterization of OSE subpopulations

We used the ALDEFLUOR detection kit (Stemcell Technologies; Cat#: 01700) to detect ALDH enzymatic activity in primary OSE cells. ALDEFLUOR reagent contains bodipy-aminoacetaldehyde (BAAA), which is a substrate for ALDH and can be acted upon by the enzyme. The molecule is water soluble and can pass freely into cells. ALDH converts BAAA into bodipy-aminoacetate, which is negatively charged and consequently becomes trapped within cells with ALDH activity. Intracellular BAA accumulation leads to fluorescence. In a mixed population of cells, those with the highest levels of ALDH enzyme will convert larger quantities of BAAA to BAA, making them more fluorescent than cells with lower ALDH activity. 4-diethylamino benzaldehyde (DEAB) is an inhibitor of the ALDH enzyme and can be added to a portion of ALDEFLUOR-treated cells to act as a negative control. Inhibition of ALDH prevents high levels of BAAA conversion to BAA, resulting in lower levels of fluorescence.

Cells ($4x10^6$) were placed in ALDEFLUOR buffer and active reagent according to the manufacturer's protocol. A subpopulation of ALDEFLUOR-treated cells was also treated with DEAB as a negative control. Fluorescence activated cell sorting (FACS) of ALDEFLUOR-treated cells was performed on an Aria II sorter using FACS DiVa software (BD Biosciences). The brightest 2–5% of ALDEFLUOR-treated cells were identified and gated electronically based on their characteristic light-scatter properties on the fluorescein isothiocyanate (FITC)-channel emission pattern after excitation with a 13–20 mW, 488-nm ellipse-shaped laser (elliptical) BD FACSAria II. The ALDH fluorescence emissions were captured simultaneously through a 515/20-nm band-pass and 505-nm long-pass filter. $ALDH^+$ (OSE-SC) and $ALDH^-$ (OSE-NS) OSE cells were

collected in 5ml falcon tubes, cultured, and were subjected to lentiviral transduction and colony formation assays (Figure S4A).

Viral Packaging

The following vectors were used for lentivirus packaging: PsPax2 (Addgene plasmid #12260); VSV-G (Addgene plasmid #8454); LentiCRISPRv2 (Addgene plasmid #52961). HEK293T cells were transfected with 10ug LentiCRISPRv2, 7.5ug PsPax2 and 2.5ug VSV-G using TransIT-LT1 transfection reagent via manufacturer instructions (Mirus; Cat#: MIR 2305). FUGW (Addgene; Cat#: 14883), a GFP-expression lentiviral construct, was also packaged separately to perform control viral transduction experiments (Figure S5, S6, S7).

Following transfection of HEK293T cells, cell media was collected after 48 hours and 72 hours. Media was concentrated via centrifugation in Amicon Ultra-15 columns (Millipore; Cat#: UFC903024) such that final volume was 500uL. Concentrated virus was filtered using 0.45um syringe filters (ThermoFisher; Cat#: 725-2545) and immediately added to cultured OSE in 24-well plates. Cells were transduced with lentivirus for 48 hours. After transduction, viral media was replaced with OSE media.

Viral Titer Calculation

LentiCRISPRv2 constructs have a puromycin resistance gene, which allows any cell transduced with a LentiCRISPRv2 virus to survive puromycin treatment. Puromycin survival amongst a population of transduced cells is therefore a function of higher viral MOI. Higher survival due to high MOI is also negatively correlated with single infection

percentage, since a higher number of viral particles in solution increases the probability that a given cell will receive more than one transduction. The mathematical relationship between puromycin survival and MOI/SIP has been described by Sanjana et al. 2014 [29] (Figure S8A). If no minilibrary genes influence cell growth, then any gene could be expected to be targeted at a random rate. The random rate of gene targeting is equal to the number of ways a cell could receive at least one of three LentiCRISPRs targeting a specific gene from 60 total, divided by the total number of possibilities. Because there are 7 functional viral particles per cell, the total number of ways to get one of 3 LentiCRISPRs is 60^7. The number of ways that a different gene can be targeted is 57^7. The total number of possibilities is 60^7. We therefore determined that the rate of random gene targeting given a library with MOI of 7 is 30.2% (Figure S8B).

Minilibrary functional validation using next-generation sequencing

OSN2 cells (*Trp53*$^{+/-}$) were transduced with all 60 minilibrary constructs at a MOI of 7 for 48 hours, and all transduced cells were collected following brief culture. Cells were spun down, then genomic DNA was isolated from cells using the Agencourt DNAdvance DNA isolation kit (Beckman Coulter; Cat#: A48705). All LentiCRISPR target sites (except for those targeting *Trp53*) were amplified using PCR, and amplicons were barcoded (Supplementary Table 1). Successful amplification of all LentiCRISPRv2 target sites was verified via agarose gel electrophoresis to assess amplicon size. We also performed Sanger sequencing on all PCR products to confirm that all intended regions were amplified. Following verification, all reactions were pooled into a single tube and purified using the QiAquick PCR purification kit (Qiagen; Cat#: 28104) (Figure

S2A). LentiCRISPRs targeting *Trp53* were excluded from initial verification experiments because OSN2 cells lack *Trp53* alleles but were later assessed using a Surveyor mutagenesis assay (Integrated DNA Technologies; Cat#: 706020).

300bp paired end sequencing was performed using Illumina MiSeq to detect indels in minilibrary target site amplicons at a read depth of 25 million reads. BWA MEM software was used for genome alignment (arXiv:1303.3997). Insertions or deletions greater than 4 base pairs in all minilibrary target sites were then tallied in transduced and untransduced control cells. Individual minilibrary constructs were considered "functional" if two-fold more indels were present in transduced cells compared to untransduced cells. We found that most constructs were functional (Figure S2B). Non-functional LentiCRISPRs (less than two-fold difference in number of indels) or those targeting *Trp53* were redesigned and functionally validated using a Surveyor mutagenesis assay (Figure S3).

Surveyor Mutagenesis Assay

The Surveyor mutagenesis assay was used to validate activity of some vectors (Figure S3). OSE cells were transduced with *Trp53*-targeting LentiCRISPRs because OSN2 cells lack *Trp53* alleles. OSN2 cells were transduced with redesigned LentiCRISPRs intended to replace non-functional constructs. Briefly, LentiCRISPR target sites were PCR-amplified in transduced (edited) and untransduced (control) OSE cells (Supplemental Table 2). Amplicons from control and edited cells were mixed in equal concentrations, heated to cause separation of complementary strands, then cooled to cause re-annealing of complementary strands. If a mutation is present in the

transduced cell amplicons, then heteroduplexes containing several unmatched basepairs will form as amplicons from LentiCRISPR-transduced cells try to anneal with amplicons from untransduced cells. As a control, amplicons from untransduced cells were mixed with amplicons from other untransduced cells. Heating and re-annealing of amplicons from untransduced cells are not expected to cause mismatches in re-annealed DNA, since amplicons do not contain LentiCRISPR-induced mutations and should all be identical. Surveyor nuclease recognizes mismatches in annealed amplicons and cleaves DNA at that site. Therefore, if a LentiCRISPR-induced mutation(s) is present in amplicons from transduced cells, and DNA from those amplicons are annealed to non-mutated amplicons from the same genomic region, a mismatch would occur and the site would be cut by Surveyor nuclease. Surveyor nuclease was added to both experimental and control groups, and all samples were run through a 2% agarose gel. Bands unique to transduced samples indicate that mutagenesis of transduced cell target sites has occurred. Numbers displayed below gene names refers to minilibrary construct ID number. We observed unique bands in all transduced DNA samples, suggesting that all replacement LentiCRISPRs and *Trp53*-targeting LentiCRISPRs possess editing ability.

Efforts to functionally assess all minilibrary constructs resulted in a validated minilibrary of 60 constructs, including one construct targeting *Gfp* as a negative control (Figure S2, S3). *Rad51c* was only targeted by two LentiCRISPRs in the finalized library due to failed validation of a third construct.

Soft Agar Culture, Colony Isolation, and Imaging

Adhesion independent growth was assessed using Cell Biolabs Inc 96 Well Cell Transformation Assay (Cell Biolabs; Cat#: CBA-135). Cells were plated at a density of 3000 cells per well in a 48 well dish and were suspended in 150ul agar/media solution. Transformation was monitored for one week, and colonies were collected following the manufacturer's instructions. In short, Cell Biolabs Inc matrix solubilization solution was added to each well of cells (Cell Biolabs; Cat#: CBA-135). Colonies were resuspended in OSE media and plated at very low density on 15cm plates. Individual, distinct colonies growing on 15cm plates were picked and cultured independently. Sterile filter paper was soaked in trypsin and was used to pick individual colonies from plates. Picked colonies were added to 24-well plates and were passaged using OSE culturing methodology. Brightfield images of culture wells were taken using a Nikon SMZ1500 microscope and Nikon Digital Sight DS-Fi1 camera system at 2x magnification. 10x and 20x images were taken using a Nikon TMS-F microscope and Moticam 2300 3.0MP Live Resolution camera system.

LentiCRISPRv2 identification via Next Generation Sequencing

Individual transformants from soft agar assays were isolated and expanded in culture as adherent cell lines. 500,000 cells per transformant were grown, spun down, and lysed for DNA extraction using the Agencourt DNAdvance DNA isolation kit. We designed a single pair of primers flanking unique LentiCRISPR guide sequences to amplify all genome-integrated constructs in each sample. We used the following primers: CTTGGCTTTATATATCTTGTGGAAAGG and CGACTCGGTGCCACTTT. Illumina overhangs were also added to each primer. PCR reactions were performed on

genomic DNA isolates from each individual colony, resulting in amplification of any genome-integrated LentiCRISPRv2 construct. Amplicons corresponding to individual transformants were uniquely barcoded and library prep was completed using the Miseq Reagent Kit v2 (illumina; Cat#: MS-102-2001) according to the manufacturer's instructions. 2 x 251bp paired end sequencing was performed on pooled, uniquely barcoded amplicons.

We created a custom "genome" of guide sequences and used BWA MEM to align reads from uniquely barcoded transformants to guide sequences. Each alignment to a particular guide represents a "hit", meaning that a particular genome-integrated guide was PCR-amplified in transformant DNA isolates, and was detected via sequencing. We calculated the average number of reads per construct and determined the average background read count. We designated any individual construct as genome-integrated if it had more aligned reads than twice the background read count. We finally performed hierarchical clustering of integration data to best visualize patterns of LentiCRISPR integration.

Mice and Genotyping

All animal use was conducted under protocol (2004-0038) to J.C.S. and approved by Cornell University's Institutional Animal Use and Care Committee.

We followed previously described methodology to generate crude tissue lysates for PCR [98]. The following forward and reverse primers were used for PCR and genotyping: TTGTTTTCCAGACTTCCTCCA and GCATTGAAAGGTCACACGAA. PCR

success was confirmed on an agarose gel, and the forward primer was re-used for Sanger sequencing.

Materials Availability

All LentiCRISPRv2 plasmids, *Trp53*$^{+/-}$ FVB/NJ mice, and all transformed cell lines, generated in this study are available upon request.

REFERENCES

1. Bowtell, D. D. L. The genesis and evolution of high-grade serous ovarian cancer. *Nat. Rev. Cancer* **10,** 803–808 (2010).
2. Siegel, R. L., Miller, K. D. & Jemal, A. Cancer statistics, 2020. *CA Cancer J Clin* **70,** 7–30 (2020).
3. Auersperg, N. Ovarian surface epithelium as a source of ovarian cancers: unwarranted speculation or evidence-based hypothesis? *Gynecol. Oncol.* **130,** 246–251 (2013).
4. Feeley, K. M. & Wells, M. Precursor lesions of ovarian epithelial malignancy. *Histopathology* **38,** 87–95 (2001).
5. Cancer Genome Atlas Research Network. Integrated genomic analyses of ovarian carcinoma. *Nature* **474,** 609–615 (2011).
6. Harlan, B. A. & Nikitin, A. Y. A quest for better mouse models of breast and ovarian cancers. *EBioMedicine* **2,** 1268–1269 (2015).
7. Bobbs, A. S., Cole, J. M. & Cowden Dahl, K. D. Emerging and evolving ovarian cancer animal models. *Cancer Growth Metastasis* **8,** 29–36 (2015).
8. Kim, J. *et al.* Cell Origins of High-Grade Serous Ovarian Cancer. *Cancers (Basel)* **10,** (2018).
9. Hess, J. M. *et al.* Passenger hotspot mutations in cancer. *Cancer Cell* **36,** 288–301.e14 (2019).
10. Knudson, A. G. Mutation and cancer: statistical study of retinoblastoma. *Proc. Natl. Acad. Sci. USA* **68,** 820–823 (1971).
11. Flesken-Nikitin, A., Choi, K.-C., Eng, J. P., Shmidt, E. N. & Nikitin, A. Y. Induction of carcinogenesis by concurrent inactivation of p53 and Rb1 in the mouse ovarian surface epithelium. *Cancer Res.* **63,** 3459–3463 (2003).
12. Xing, D. & Orsulic, S. A mouse model for the molecular characterization of brca1-associated ovarian carcinoma. *Cancer Res.* **66,** 8949–8953 (2006).
13. Zhang, S. *et al.* Both fallopian tube and ovarian surface epithelium are cells-of-origin for high-grade serous ovarian carcinoma. *Nat. Commun.* **10,** 5367 (2019).
14. Lawrenson, K. *et al.* A Study of High-Grade Serous Ovarian Cancer Origins Implicates the SOX18 Transcription Factor in Tumor Development. *Cell Rep.* **29,** 3726–3735.e4 (2019).
15. Hao, D. *et al.* Integrated Analysis Reveals Tubal- and Ovarian-Originated Serous Ovarian Cancer and Predicts Differential Therapeutic Responses. *Clin. Cancer Res.* **23,** 7400–7411 (2017).

16. Fathalla, M. F. Incessant ovulation--a factor in ovarian neoplasia? *Lancet* **2,** 163 (1971).

17. Fathalla, M. F. Incessant ovulation and ovarian cancer - a hypothesis re-visited. *Facts Views Vis Obgyn* **5,** 292–297 (2013).

18. Okamura, H., Katabuchi, H., Nitta, M. & Ohtake, H. Structural changes and cell properties of human ovarian surface epithelium in ovarian pathophysiology. *Microsc. Res. Tech.* **69,** 469–481 (2006).

19. Katabuchi, H. & Okamura, H. Cell biology of human ovarian surface epithelial cells and ovarian carcinogenesis. *Med. Electron Microsc.* **36,** 74–86 (2003).

20. Flesken-Nikitin, A. *et al.* Ovarian surface epithelium at the junction area contains a cancer-prone stem cell niche. *Nature* **495,** 241–245 (2013).

21. Zender, L. *et al.* Identification and validation of oncogenes in liver cancer using an integrative oncogenomic approach. *Cell* **125,** 1253–1267 (2006).

22. Zender, L. *et al.* Cancer gene discovery in hepatocellular carcinoma. *J. Hepatol.* **52,** 921–929 (2010).

23. Donehower, L. A. The p53-deficient mouse: a model for basic and applied cancer studies. *Semin. Cancer Biol.* **7,** 269–278 (1996).

24. Donehower, L. A. Insights into wild-type and mutant p53 functions provided by genetically engineered mice. *Hum. Mutat.* **35,** 715–727 (2014).

25. Huang, P., Duda, D. G., Jain, R. K. & Fukumura, D. Histopathologic findings and establishment of novel tumor lines from spontaneous tumors in FVB/N mice. *Comp Med* **58,** 253–263 (2008).

26. Mahler, J. F., Stokes, W., Mann, P. C., Takaoka, M. & Maronpot, R. R. Spontaneous lesions in aging FVB/N mice. *Toxicol. Pathol.* **24,** 710–716 (1996).

27. Yamulla, R. J. *et al.* Testing models of the APC tumor suppressor/β-catenin interaction reshapes our view of the destruction complex in Wnt signaling. *Genetics* **197,** 1285–1302 (2014).

28. Shalem, O. *et al.* Genome-scale CRISPR-Cas9 knockout screening in human cells. *Science* **343,** 84–87 (2014).

29. Sanjana, N. E., Shalem, O. & Zhang, F. Improved vectors and genome-wide libraries for CRISPR screening. *Nat. Methods* **11,** 783–784 (2014).

30. Horibata, S., Vo, T. V., Subramanian, V., Thompson, P. R. & Coonrod, S. A. Utilization of the soft agar colony formation assay to identify inhibitors of tumorigenicity in breast cancer cells. *J. Vis. Exp.* e52727 (2015). doi:10.3791/52727

31. Borowicz, S. *et al.* The soft agar colony formation assay. *J. Vis. Exp.* e51998

(2014). doi:10.3791/51998

32. Puck, T. T., Marcus, P. I. & Cieciura, S. J. Clonal growth of mammalian cells in vitro; growth characteristics of colonies from single HeLa cells with and without a feeder layer. *J. Exp. Med.* **103,** 273–283 (1956).

33. Roberts, A. B. *et al.* Type beta transforming growth factor: a bifunctional regulator of cellular growth. *Proc. Natl. Acad. Sci. USA* **82,** 119–123 (1985).

34. de Larco, J. E. & Todaro, G. J. Growth factors from murine sarcoma virus-transformed cells. *Proc. Natl. Acad. Sci. USA* **75,** 4001–4005 (1978).

35. Hamburger, A. W. & Salmon, S. E. Primary bioassay of human tumor stem cells. *Science* **197,** 461–463 (1977).

36. Gao, J. *et al.* Integrative analysis of complex cancer genomics and clinical profiles using the cBioPortal. *Sci. Signal.* **6,** pl1 (2013).

37. Cerami, E. *et al.* The cBio cancer genomics portal: an open platform for exploring multidimensional cancer genomics data. *Cancer Discov.* **2,** 401–404 (2012).

38. Hamid, A. A. *et al.* Compound genomic alterations of TP53, PTEN, and RB1 tumor suppressors in localized and metastatic prostate cancer. *Eur. Urol.* **76,** 89–97 (2019).

39. Filtz, E. A. *et al.* Rb1 and Pten Co-Deletion in Osteoblast Precursor Cells Causes Rapid Lipoma Formation in Mice. *PLoS One* **10,** e0136729 (2015).

40. Chow, L. M. L. *et al.* Cooperativity within and among Pten, p53, and Rb pathways induces high-grade astrocytoma in adult brain. *Cancer Cell* **19,** 305–316 (2011).

41. Zhao, R., Choi, B. Y., Lee, M.-H., Bode, A. M. & Dong, Z. Implications of genetic and epigenetic alterations of CDKN2A (p16(ink4a)) in cancer. *EBioMedicine* **8,** 30–39 (2016).

42. Li, J., Poi, M. J. & Tsai, M.-D. Regulatory mechanisms of tumor suppressor P16(INK4A) and their relevance to cancer. *Biochemistry* **50,** 5566–5582 (2011).

43. Nielsen, G. P., Burns, K. L., Rosenberg, A. E. & Louis, D. N. CDKN2A gene deletions and loss of p16 expression occur in osteosarcomas that lack RB alterations. *Am. J. Pathol.* **153,** 159–163 (1998).

44. Risch, H. A. *et al.* Population BRCA1 and BRCA2 mutation frequencies and cancer penetrances: a kin-cohort study in Ontario, Canada. *J. Natl. Cancer Inst.* **98,** 1694–1706 (2006).

45. Walsh, C. S. Two decades beyond BRCA1/2: Homologous recombination, hereditary cancer risk and a target for ovarian cancer therapy. *Gynecol. Oncol.* **137,** 343–350 (2015).

46. Feng, W. & Jasin, M. BRCA2 suppresses replication stress-induced mitotic and G1 abnormalities through homologous recombination. *Nat. Commun.* **8,** 525 (2017).

47. Zhu, J. *et al.* FANCD2 influences replication fork processes and genome stability in response to clustered DSBs. *Cell Cycle* **14,** 1809–1822 (2015).

48. Somyajit, K., Subramanya, S. & Nagaraju, G. RAD51C: a novel cancer susceptibility gene is linked to Fanconi anemia and breast cancer. *Carcinogenesis* **31,** 2031–2038 (2010).

49. Kuznetsov, S. G., Haines, D. C., Martin, B. K. & Sharan, S. K. Loss of Rad51c leads to embryonic lethality and modulation of Trp53-dependent tumorigenesis in mice. *Cancer Res.* **69,** 863–872 (2009).

50. Stratton, M. R., Campbell, P. J. & Futreal, P. A. The cancer genome. *Nature* **458,** 719–724 (2009).

51. Pon, J. R. & Marra, M. A. Driver and passenger mutations in cancer. *Annu. Rev. Pathol.* **10,** 25–50 (2015).

52. Hasan, N., Ohman, A. W. & Dinulescu, D. M. The promise and challenge of ovarian cancer models. *Transl. Cancer Res.* **4,** 14–28 (2015).

53. Piek, J. M. *et al.* Dysplastic changes in prophylactically removed Fallopian tubes of women predisposed to developing ovarian cancer. *J. Pathol.* **195,** 451–456 (2001).

54. Sherman-Baust, C. A. *et al.* A genetically engineered ovarian cancer mouse model based on fallopian tube transformation mimics human high-grade serous carcinoma development. *J. Pathol.* **233,** 228–237 (2014).

55. Corzo, C., Iniesta, M. D., Patrono, M. G., Lu, K. H. & Ramirez, P. T. Role of fallopian tubes in the development of ovarian cancer. *J Minim Invasive Gynecol* **24,** 230–234 (2017).

56. Karst, A. M., Levanon, K. & Drapkin, R. Modeling high-grade serous ovarian carcinogenesis from the fallopian tube. *Proc. Natl. Acad. Sci. USA* **108,** 7547–7552 (2011).

57. Perets, R. *et al.* Transformation of the fallopian tube secretory epithelium leads to high-grade serous ovarian cancer in Brca;Tp53;Pten models. *Cancer Cell* **24,** 751–765 (2013).

58. Labidi-Galy, S. I. *et al.* High grade serous ovarian carcinomas originate in the fallopian tube. *Nat. Commun.* **8,** 1093 (2017).

59. Kindelberger, D. W. *et al.* Intraepithelial carcinoma of the fimbria and pelvic serous carcinoma: Evidence for a causal relationship. *Am. J. Surg. Pathol.* **31,** 161–169 (2007).

60. Perets, R. & Drapkin, R. It's totally tubular....riding the new wave of ovarian cancer

research. *Cancer Res.* **76,** 10–17 (2016).

61. Adler, E., Mhawech-Fauceglia, P., Gayther, S. A. & Lawrenson, K. PAX8 expression in ovarian surface epithelial cells. *Hum. Pathol.* **46,** 948–956 (2015).

62. Tacha, D., Zhou, D. & Cheng, L. Expression of PAX8 in normal and neoplastic tissues: a comprehensive immunohistochemical study. *Appl Immunohistochem Mol Morphol* **19,** 293–299 (2011).

63. Ozcan, A., Liles, N., Coffey, D., Shen, S. S. & Truong, L. D. PAX2 and PAX8 expression in primary and metastatic müllerian epithelial tumors: a comprehensive comparison. *Am. J. Surg. Pathol.* **35,** 1837–1847 (2011).

64. Lee, Y. *et al.* A candidate precursor to serous carcinoma that originates in the distal fallopian tube. *J. Pathol.* **211,** 26–35 (2007).

65. Leonhardt, K., Einenkel, J., Sohr, S., Engeland, K. & Horn, L.-C. p53 signature and serous tubal in-situ carcinoma in cases of primary tubal and peritoneal carcinomas and serous borderline tumors of the ovary. *Int J Gynecol Pathol* **30,** 417–424 (2011).

66. Neel, B. G. *et al.* Both Fallopian Tube and Ovarian Surface Epithelium Can Act as Cell-of-Origin for High Grade Serous Ovarian Carcinoma. *BioRxiv* (2018). doi:10.1101/481200

67. Auersperg, N., Woo, M. M. M. & Gilks, C. B. The origin of ovarian carcinomas: A developmental view. *Gynecol. Oncol.* **110,** 452–454 (2008).

68. Auersperg, N., Wong, A. S., Choi, K. C., Kang, S. K. & Leung, P. C. Ovarian surface epithelium: biology, endocrinology, and pathology. *Endocr. Rev.* **22,** 255–288 (2001).

69. Godwin, A. K. *et al.* Spontaneous transformation of rat ovarian surface epithelial cells: association with cytogenetic changes and implications of repeated ovulation in the etiology of ovarian cancer. *J. Natl. Cancer Inst.* **84,** 592–601 (1992).

70. Testa, J. R. *et al.* Spontaneous transformation of rat ovarian surface epithelial cells results in well to poorly differentiated tumors with a parallel range of cytogenetic complexity. *Cancer Res.* **54,** 2778–2784 (1994).

71. Orsulic, S. *et al.* Induction of ovarian cancer by defined multiple genetic changes in a mouse model system. *Cancer Cell* **1,** 53–62 (2002).

72. Scully, R. E. *Tumors Of The Ovary, Maldeveloped Gonads, Fallopian Tube, And Broad Ligament*. (Armed Forces Institute Of Pathology Available From The American Registry Of Pathology, Armed Forces Institute Of Pathology, 1999).

73. Rosen, D. G. *et al.* Ovarian cancer: pathology, biology, and disease models. *Front. Biosci. (Landmark Ed)* **14,** 2089–2102 (2009).

74. Matz, M. *et al.* The histology of ovarian cancer: worldwide distribution and implications for international survival comparisons (CONCORD-2). *Gynecol. Oncol.* **144,** 405–413 (2017).

75. Ferraro, F., Celso, C. L. & Scadden, D. Adult stem cels and their niches. *Adv. Exp. Med. Biol.* **695,** 155–168 (2010).

76. Greene, D. R., Wheeler, T. M., Egawa, S., Dunn, J. K. & Scardino, P. T. A comparison of the morphological features of cancer arising in the transition zone and in the peripheral zone of the prostate. *J. Urol.* **146,** 1069–1076 (1991).

77. Mcnairn, A. J. & Guasch, G. Epithelial transition zones: merging microenvironments, niches, and cellular transformation. *Eur J Dermatol* **21 Suppl 2,** 21–28 (2011).

78. Seidman, J. D. Serous tubal intraepithelial carcinoma localizes to the tubal-peritoneal junction: a pivotal clue to the site of origin of extrauterine high-grade serous carcinoma (ovarian cancer). *Int J Gynecol Pathol* **34,** 112–120 (2015).

79. Schmoeckel, E. *et al.* LEF1 is preferentially expressed in the tubal-peritoneal junctions and is a reliable marker of tubal intraepithelial lesions. *Mod. Pathol.* **30,** 1241–1250 (2017).

80. Shi, M. *et al.* Inactivation of TRP53, PTEN, RB1 and/or CDH1 in the ovarian surface epithelium induces ovarian cancer transformation and metastasis. *Biol. Reprod.* (2020). doi:10.1093/biolre/ioaa008

81. Szabova, L. *et al.* Perturbation of Rb, p53, and Brca1 or Brca2 cooperate in inducing metastatic serous epithelial ovarian cancer. *Cancer Res.* **72,** 4141–4153 (2012).

82. Chien, J. *et al.* TP53 mutations, tetraploidy and homologous recombination repair defects in early stage high-grade serous ovarian cancer. *Nucleic Acids Res.* **43,** 6945–6958 (2015).

83. Zhai, Y. *et al.* High-grade serous carcinomas arise in the mouse oviduct via defects linked to the human disease. *J. Pathol.* **243,** 16–25 (2017).

84. Martins, F. C. *et al.* Combined image and genomic analysis of high-grade serous ovarian cancer reveals PTEN loss as a common driver event and prognostic classifier. *Genome Biol.* **15,** 526 (2014).

85. Neilsen, P. M. *et al.* Identification of ANKRD11 as a p53 coactivator. *J. Cell Sci.* **121,** 3541–3552 (2008).

86. Lim, S. P. *et al.* Specific-site methylation of tumour suppressor ANKRD11 in breast cancer. *Eur. J. Cancer* **48,** 3300–3309 (2012).

87. Noll, J. E. *et al.* Mutant p53 drives multinucleation and invasion through a process

that is suppressed by ANKRD11. *Oncogene* **31,** 2836–2848 (2012).

88. Chang, N. S. *et al.* Hyaluronidase induction of a WW domain-containing oxidoreductase that enhances tumor necrosis factor cytotoxicity. *J. Biol. Chem.* **276,** 3361–3370 (2001).

89. Schrock, M. S. & Huebner, K. WWOX: a fragile tumor suppressor. *Exp. Biol. Med.* **240,** 296–304 (2015).

90. Hinz, J. M., Helleday, T. & Meuth, M. Reduced apoptotic response to camptothecin in CHO cells deficient in XRCC3. *Carcinogenesis* **24,** 249–253 (2003).

91. Kondrashova, O. *et al.* Secondary Somatic Mutations Restoring RAD51C and RAD51D Associated with Acquired Resistance to the PARP Inhibitor Rucaparib in High-Grade Ovarian Carcinoma. *Cancer Discov.* **7,** 984–998 (2017).

92. Thompson, E. L. *et al.* FANCI and FANCD2 have common as well as independent functions during the cellular replication stress response. *Nucleic Acids Res.* **45,** 11837–11857 (2017).

93. Tian, Y. *et al.* Constitutive role of the Fanconi anemia D2 gene in the replication stress response. *J. Biol. Chem.* **292,** 20184–20195 (2017).

94. Gao, G. F. *et al.* Before and after: comparison of legacy and harmonized TCGA genomic data commons' data. *Cell Syst.* **9,** 24–34.e10 (2019).

95. Carrington, B., Varshney, G. K., Burgess, S. M. & Sood, R. CRISPR-STAT: an easy and reliable PCR-based method to evaluate target-specific sgRNA activity. *Nucleic Acids Res.* **43,** e157 (2015).

96. Todaro, G. J. & Green, H. Quantitative studies of the growth of mouse embryo cells in culture and their development into established lines. *J. Cell Biol.* **17,** 299–313 (1963).

97. Hsu, P. D. *et al.* DNA targeting specificity of RNA-guided Cas9 nucleases. *Nat. Biotechnol.* **31,** 827–832 (2013).

98. Truett, G. E. *et al.* Preparation of PCR-quality mouse genomic DNA with hot sodium hydroxide and tris (HotSHOT). *BioTechniques* **29,** 52–54 (2000).

Chapter 3: OSE-SC transformants grown *in vitro* do not recapitulate transcriptomic characteristics of human disease

The following chapter details transcriptomic analyses of OSE-SC transformants described in Chapter 2. Global gene expression was compared among transformants and pathway analyses were completed to compare transformants to human disease. These results have not been submitted for publication.

ABSTRACT

Genes associated with increased OSE-SC transformation and growth propensity were identified via LentiCRISPRv2-based screening of putative HGSOC driver genes in Chapter 2. These phenotypic differences suggest that specific LentiCRISPR-targeted genes are important for OSE-SC transformation. However, growth and transformation assays are unable to reveal whether overrepresented LentiCRISPR constructs cause transcriptomic similarity to human HGSOC. It's also possible that LentiCRISPR constructs that are uninvolved in OSE-SC transformation are important for HGSOC-like differentiation of cells. To address these unknowns, 3' RNA sequencing was completed on OSE-SC transformants with different sets of genome-integrated LentiCRISPRs. Transformants with similar and different lentiCRISPR construct combinations were compared to one another and to human disease. These analyses revealed that LentiCRISPR-targeted genes are not the sole drivers of transformant phenotypes and that culturing conditions substantially influence global gene expression. *In vivo* cell growth is likely required for meaningful comparisons to be made between HGSOC models and HGSOC.

INTRODUCTION

Minilibrary screening of putative HGSOC driver genes reveals distinct groups of putative transformation drivers in OSE-SC

In previous chapters, I described the generation of OSE-SC and OSE-NS transformants following random, combinatorial mutagenesis of putative HGSOC driver genes via screening with a LentiCRISPR minilibrary. OSE-NS transformation was rare, preempting meaningful analyses of overrepresented LentiCRISPR constructs. However, overrepresented LentiCRISPR combinations associated with OSE-SC transformation were identified among nearly 100 colonies (transformants) and several distinct gene co-targeting patterns were observed (Chapter 2, Figure 3). Although some genes (such as *Trp53, Rb1, Pten,* or *Cdkn2a*) were targeted in most transformants, distinct clusters of samples were characterized by the presence or absence of additional LentiCRISPR constructs (Chapter 2, Figure 3). These differences in targeted gene frequency among transformants led to the question of whether specific LentiCRISPR-induced mutations caused phenotypic changes to OSE-SC.

To explore potential differences between OSE-SC transformants with different LentiCRISPR-induced initiating mutations, targeted mutagenesis assays were performed in which transformation rate and colony size were assessed given a specific set of LentiCRISPRv2 constructs. Several distinct mutation combinations were associated with elevated OSE-SC transformation and colony size (Chapter 2, Figure 4). However, colony formation-based experiments cannot reveal whether OSE-SC with different mutations transcriptomically diverge. Furthermore, mutations that do not effect

transformation initiation or colony growth may be still influence transformant gene expression.

Overrepresented target genes are associated with ovarian carcinoma subtypes

Past research into several of the genes targeted within OSE-SC transformant clusters suggests that they may drive differentiation toward distinct ovarian cancer subtypes. *Pten*, for instance, was targeted in 76% of OSE-SC transformants (Chapter 2, Figure 3) and was shown to influence transformant quantity and size (Chapter 2, Figure 4). These results complemented previous research suggesting that Pten conveys highly proliferative phenotypes, lower tumor latency, and poor prognosis in HGSOC mouse models and in human tumors [1,2]. However, direct *Pten* mutagenesis actually occurs in a minority of HGSOC tumors (7%) and is more closely associated with low grade gynecological malignancies [3–6]. The highest rates of direct *Pten* mutagenesis (67%) are observed in endometrioid carcinomas [4]. It is possible, therefore, that *Pten* mutations cause OSE-SC transformants to transcriptomically resemble low grade gynecological malignancies rather than HGSOC.

Several other commonly targeted genes in OSE-SC transformants such as *Trp53* and *Rb1* are highly associated with sporadic HGSOC and may consequently promote transcriptomic similarity to HGSOC tumors. Nearly all human HGSOC tumors harbor a mutation in *TP53*, which is why it is often used as a marker to differentiate high grade and low grade ovarian cancer [7]. Most tumors (67%) also exhibit dysregulation of *RB1*, with direct mutagenesis occurring in 10% of tumors [6,8]. Correlatively, *Trp53* and *Rb1* were targeted in 96% and 67% of OSE-SC transformants, respectively, in support of their putative role in HGSOC development and phenotypes (Chapter 2, Figure 3). Other

minilibrary screening “hits” like *Brca2* are well-documented HGSOC risk factors with 19% penetrance, suggesting contributions to HGSOC differentiation [6,7,9–12]. Besides *Trp53*, *Rb1*, and *Brca2*, however, most targeted genes within OSE-SC transformant subgroups are not mutated in over 12% of HGSOC tumors [6]. Their predicted effects on transformant transcriptomic phenotypes are therefore unknown.

Some cultured HGSOC models resemble human tumors

HGSOC driver screening descried in Chapter 2 was completed on mouse OSE, but previous research has suggested that some mouse-derived HGSOC models can recapitulate human tumor transcriptomic characteristics. Maniati and colleagues (2020) cultured primary OSE or TE with functional knockouts in several subsets of the HGSOC-associated tumor suppressors, *Trp53, Rb1, Brca1, Brca2* and *Pten,* from genetically engineered mouse models.[13] Following brief culture, cells were intraperitoneally injected into congenic mice to model the peritoneal dissemination that is characteristic of human HGSOC. Despite the consequential tumors being derived from cultured OSE or TE, the authors found that they had serous morphology and exhibited significant transcriptomic overlap with human HGSOC transcriptomic data [6]. Specifically, tumors from injected cells shared tumor microenvironment-related pathways with human HGSOC such as transforming growth factor B, hypoxia, ECM-receptor interactions, wound healing, immune and inflammatory responses, and angiogenesis [13]. It’s possible, therefore, that mouse-derived systems containing mutations uncovered via minilibrary screening in Chapter 2 (i.e. *Trp53*, *Rb1*, *Pten* and *Brca2*) can transcriptomically resemble human HGSOC.

In vitro HGSOC models with common HGSOC-associated mutations resemble human disease

Other studies have suggested that fully *in vitro* ovarian cancer model systems can recapitulate HGSOC or low-grade ovarian carcinoma transcriptomic characteristics, largely as a function of HGSOC-associated mutations. SK-OV-3 and A2780, for example, are ovarian carcinoma cell lines present in at least 60% of publications utilizing ovarian cancer cell lines. Surprisingly, they lack several HGSOC-associated mutations and high copy number. They also possess low grade ovarian carcinoma-associated mutations in *ARID1A*, *BRAF*, *PIK3CA*, and *PTEN* [14]. Accordingly, they transcriptomically diverge from average HGSOC tumors and more closely resemble low grade ovarian malignancies [14]. Ovarian carcinoma lines with HGSOC-associated mutations, including KURAMOCHI, COV362, and JHOS2, are transcriptomically similar to average HGSOC tumor samples [14]. These data and other similar analyses suggest that cultured cells can emulate a source tissue or cancer subtype, especially if the cultures possess ovarian cancer subtype-associated mutations [14–18].

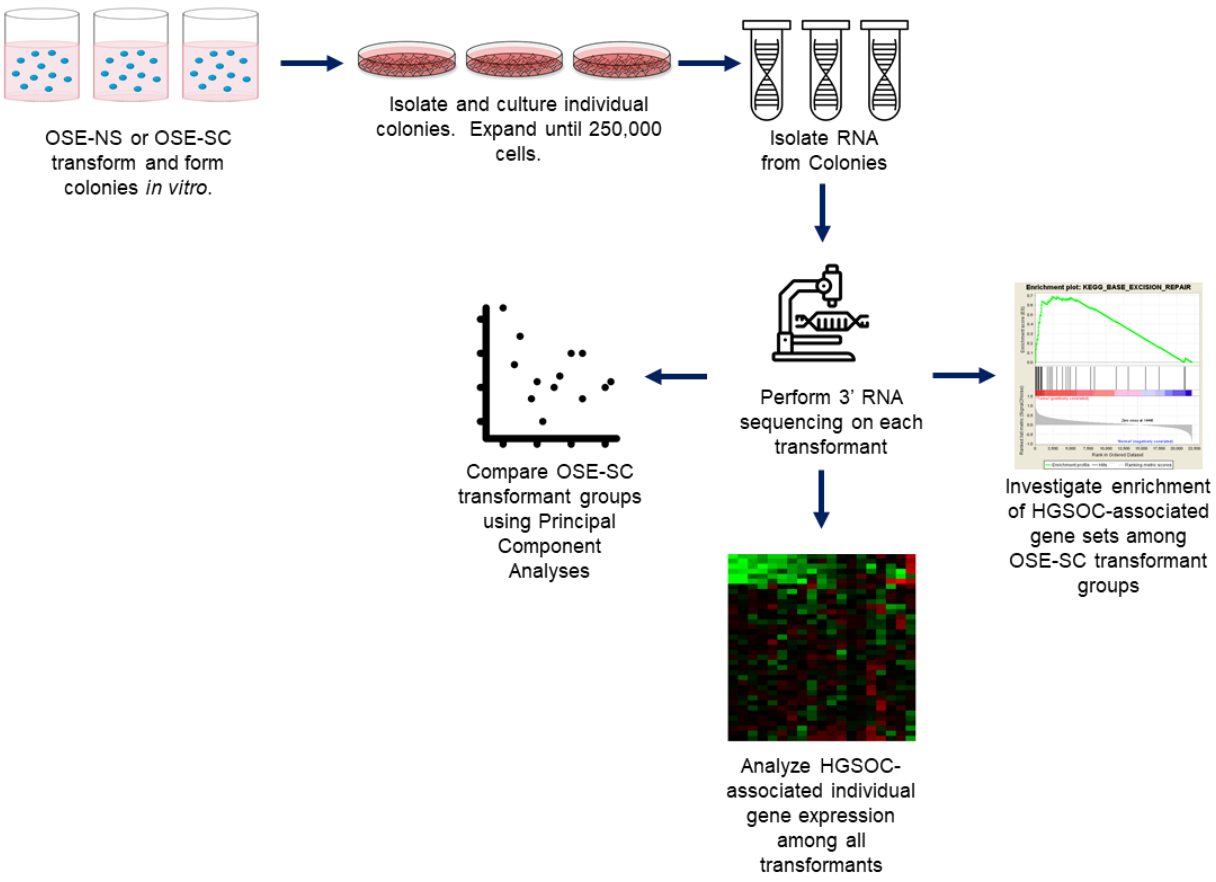

Figure 1. Strategy for transcriptomic analysis of OSE-SC transformants. 92 OSE-SC transformants were generated and individually cultured following random mutagenesis of 20 putative HGSOC driver genes using a LentiCRISPRv2 minilibrary (see chapter 1). RNA was isolated from each transformant, and 3' RNA sequencing was performed. Principal component, differential expression, and pathway enrichment analyses were completed on transcriptomic data.

OSE-SC transformants with specific mutation profiles may resemble human disease

In light of previous literature suggesting that *in vitro* models can transcriptomically resemble human HGSOC, I performed 3' RNA sequencing of OSE-SC and OSE-NS transformants with different LentiCRISPR-targeted genes (transformant clusters) to ascertain transcriptomic differences (Figure 1). Results indicate surprising overall transcriptomic similarity between most transformant types, despite differences in LentiCRISPR-targeted genes. There was significant (False Discovery Rate (FDR) = "q", $q < 0.05$) differential gene expression between *Brca2*- or *Trp53*- transformants and *Trp53-/Rb1-/Pten*- transformants (hereafter LentiCRISPR targeting of a gene in a transformant will be called "gene-" and a lack of targeting will be called "gene+"). However, differences were not due to disparities in ovarian cancer subtype-specific gene set enrichment or gene expression. Together, 3' RNA sequencing results suggest that the transcriptomic landscape of cultured SE-SC transformants is largely influenced by culturing conditions and is not reflective of human disease.

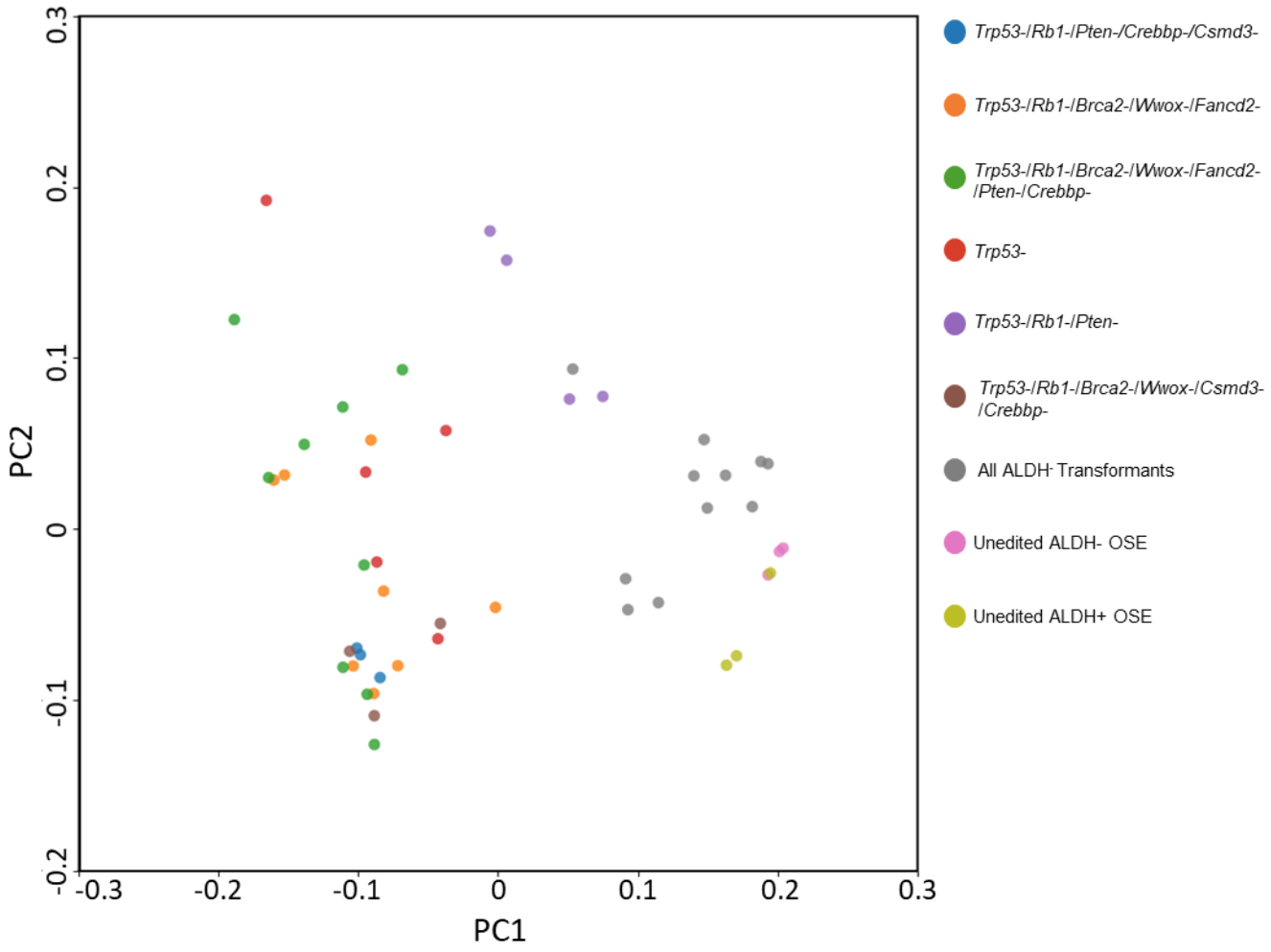

Figure 2. Principal component analyses cannot differentiate most OSE-SC transformants with different genome-integrated LentiCRISPRs. Principal component analyses were completed on normalized transcriptomic data from transformant groups with distinct sets of genome-integrated LentiCRISPRs. Each color signifies a OSE-SC transformant group with identical genes targeted by genome-integrated LentiCRISPRs.

RESULTS

Culturing approach to preserve OSE-SC stem cell characteristics

Previous research into prolonged culture of cells has suggested that *in vitro* culturing conditions alter cell characteristics and can cause loss of stem cell hallmarks over time [19,20]. Therefore, in order to preserve inherent characteristics and stemness of OSE-SC transformants, colony-derived cultures were expanded only as necessary to produce a sufficient quantity for RNA isolation (Figure 1). Sequencing was performed and differentially expressed genes were identified between OSE-SC transformant clusters with differing combinations of genome-integrated LentiCRISPRs (Figure 1).

Samples with identical LentiCRISPRs display transcriptomic variability

Principal component (PC) analysis of individual sample normalized reads (edgeR, [21,22]) suggested divergence between unedited OSE-SC and OSE-NS Cultures (Figure 2). One unedited OSE-SC culture was an exception and clustered near OSE-NS samples, suggesting potential loss of stem cell characteristics or contamination with OSE-NS cells (Figure 2). Transformed OSE-SC and OSE-NS also grouped apart from one another with no overlap, suggesting divergent transcriptomic characteristics of transformed OSE-SC and OSE-NS (Figure 2).

Among OSE-SC transformants, some clear separation between sample clusters with differing LentiCRISPR target genes was observed. *Trp53*-/*Rb1*-/*Pten*-transformants diverged from all other groups, whereas *Trp53*-, *Trp53*-/*Rb1*-/*Brca2*-/*Wwox*-/*Fancd2*-, *Trp53*-/*Rb1*-/*Pten*-/*Crebbp*-/*Csmd3*- and *Trp53*-/*Rb1*-/*Brca2*-/*Wwox*-

/*Fancd2*-/*Pten*-/*Crebbp*- transformants overlapped (Figure 2). PC analysis also demonstrated that differences may exist between individual transformants with identical LentiCRISPRv2-targeted genes. Individual sample separation was noted within *Trp53*-, *Trp53*-/*Rb1*-/*Brca2*-/*Wwox*-/*Fancd2*-, and *Trp53*-/*Rb1*-/*Brca2*-/*Wwox*-/*Fancd2*-/*Pten*-/*Crebbp*- groups (Figure 2). It's possible, therefore, that LentiCRISPR-induced mutations are not the only drivers of *in vitro* transcriptomic characteristics in transformed OSE-SC. They may rather only drive the first step of transformation. Many cellular changes occurring after transduction may not completely depend upon transformation-initiating events.

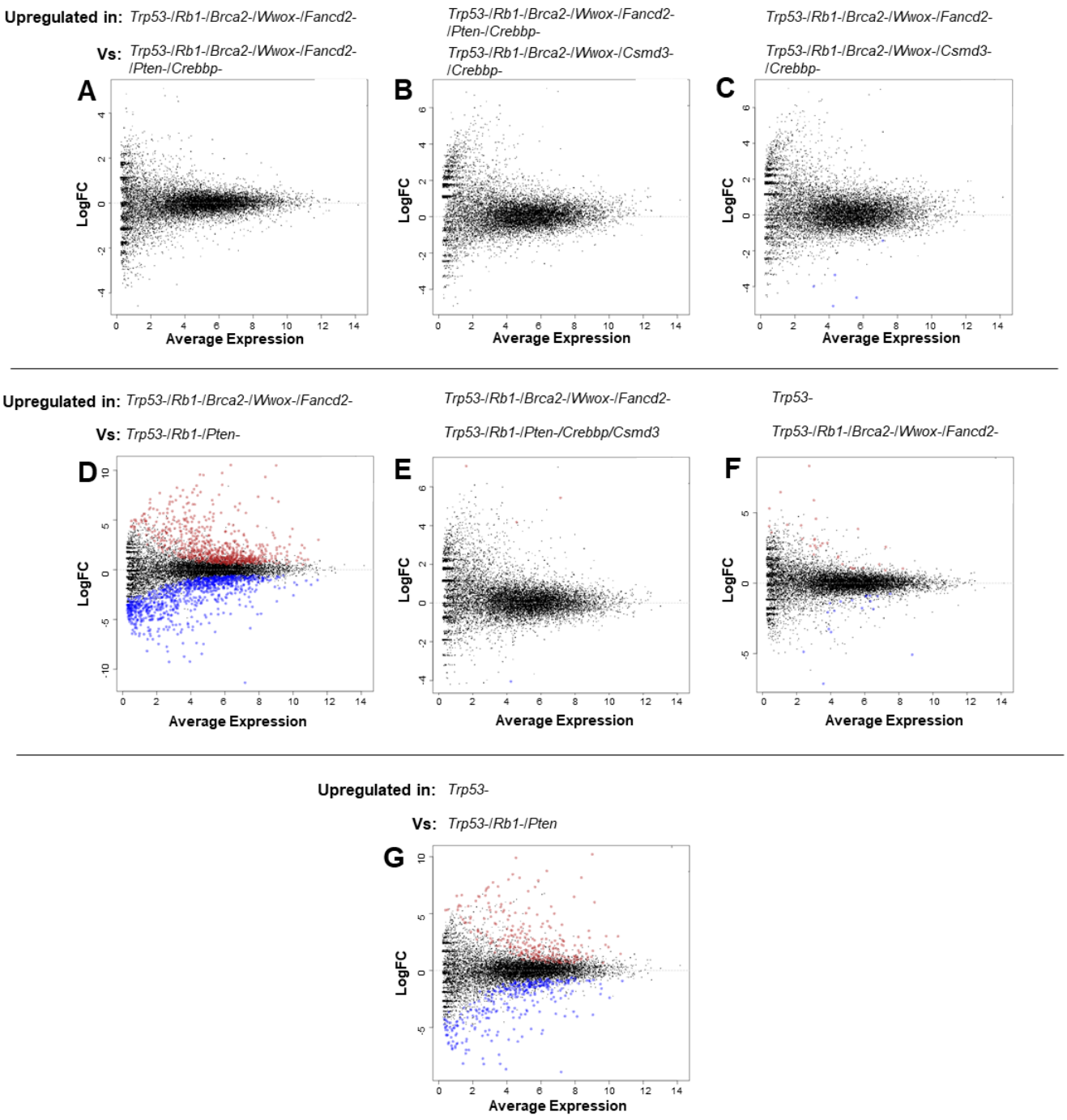

Figure 3. Few differentially expressed genes exists between most transformant groups except for *Trp53-/Rb1-/*Pten- transformants. Differentially expressed genes between transformants with different sets of genome-integrated LentiCRISPRs were identified using EdgeR and plotted on MA plots. Red dots indicate significantly (q <

0.05) upregulated genes within the indicated group. Blue dots indicate significantly ($q < 0.05$) downregulated genes within the indicated group. Black dots indicate genes that are neither significantly upregulated nor downregulated. Most groups had few or zero differentially expressed genes compared to one another. *Trp53*-/*Rb1*-/Pten-transformants were an outlier with many significantly differentially expressed genes compared to other groups.

Few differentially expressed genes exist between OSE-SC transformants with *Brca2*-targeting LentiCRISPRs

Differential expression analyses using EdgeR [21,22] was implemented to investigate differences between transformants with distinct genome-integrated LentiCRISPRs. These analyses revealed striking similarity between transformant clusters with *Brca2*-targeting LentiCRISPRs (Figure 3A,B,C). There were no significantly ($q < 0.05$) differentially expressed genes between *Trp53*-/*Rb1*-/*Brca2*-/*Wwox*-/*Fancd2*- and *Trp53*-/*Rb1*-/*Brca2*-/*Wwox*-/*Fancd2*-/*Pten*-/*Crebbp*- transformants, suggesting that the addition of *Pten* and *Crebbp* mutagenesis to *Trp53*-/*Rb1*-/*Brca2*-/*Wwox*-/*Fancd2*- cells did not greatly influence global gene expression. Similarly, there were no significantly ($q < 0.05$) differentially expressed genes between *Trp53*-/*Rb1*-/*Brca2*-/*Wwox*-/*Fancd2*-/*Pten*-/*Crebbp*- and *Trp53*-/*Rb1*-/*Brca2*-/*Wwox*-/*Csmd3*-/*Crebbp*- transformants (Figure 3B). Only 4 differentially expressed genes (*Hoxd11*, *Thbdm Uhrf1bp1l*, and *Pbx2*) were found between *Trp53*-/*Rb1*-/*Brca2*-/*Wwox*-/*Fancd2*- and *Trp53*-/*Rb1*-/*Brca2*-/*Wwox*-/*Csmd3*-/*Crebbp*- transformants (Figure 3C). The removal of *Fancd2* or *Pten* and the addition of *Csmd3* and *Crebbp* mutations therefore did not considerably influence global gene expression.

Brca2- transformants differ from *Trp53*-/*Rb1*-/*Pten*-, but not from *Trp53*-/*Rb1*-/*Pten*-/*Crebbp*-/*Csmd3*- transformants

To determine the relative contribution of *Brca2* mutagenesis on transcriptomic changes, differentially expressed genes were also identified between groups with or

without *Brca2* LentiCRISPR integration(s). *Trp53*-/*Rb1*-/*Pten*- or *Trp53*-/*Rb1*-/*Pten*-/*Crebbp*-/*Csmd3*- transformants were compared to *Trp53*-/*Rb1*-/*Brca2*-/*Wwox*-/*Fancd2*- transformants. Unlike comparisons between *Brca2*- clusters, differentially expressed genes were found between some transformant groups containing *Brca2*-targeting LentiCRISPRs and those without *Brca2*-targeting. Specifically, 1583 genes were differentially expressed between *Trp53*-/*Rb1*-/*Pten*- and *Trp53*-/*Rb1*-/*Brca2*-/*Wwox*-/*Fancd2*- transformants (Figure 3D). However, surprising similarity was observed between *Trp53*-/*Rb1*-/*Brca2*-/*Wwox*-/*Fancd2*- and *Trp53*-/*Rb1*-/*Pten*-/*Crebbp*-/*Csmd3*- transformants, as only four genes gene, *Myo1b, Hoxd11, Nid1,* and *Sall1*, were differentially expressed (Figure 3F). These results suggest transcriptomic divergence between *Trp53*-/*Rb1*-/*Pten*- and *Trp53*-/*Rb1*-/*Brca2*-/*Wwox*-/*Fancd2*- transformants. They also suggest that the addition of *Crebbp* and *Csmd3* mutations to *Trp53*-/*Rb1*-/*Pten*- cells results in transcriptomic similarity to *Brca2*- transformants. Alternatively, *Trp53*-/*Rb1*-/*Pten*- transformants could be outliers, as few differentially expressed genes exist between other groups.

<u>*Trp53*- transformants are similar to *Brca2*- transformants</u>

Trp53- colonies (lacking all non-*Trp53* lentiCRISPRs) were relative rare in in our screen, likely due to the previously documented inability of *Trp53* alone to cause frequent OSE transformation [23]. Presumably, colonies with only *Trp53*-targeting LentiCRISPRs require additional mutations following LentiCRISPRv2 library transduction to cause transformation in agreement with the multi-hit hypothesis of cancer and estimated quantity of necessary driver mutations [24,25]. It's possible that

transcriptomic similarities between *Trp53*- transformants and other transformants with additional genome-integrated LentiCRISPRs may elucidate additional disrupted pathways or genes. Therefore, to investigate the direction of *Trp53*- transformant differentiation, *Trp53*- transformant transcriptomes were compared to both *Trp53*-/*Rb1*-/*Brca2*-/*Wwox*-/*Fancd2*- and *Trp53*-/*Rb1*-/*Pten*- transformants via differential expression analyses. Interestingly, there were only 51 differentially expressed genes between *Trp53*- and *Trp53*-/*Rb1*-/*Brca2*-/*Wwox*-/*Fancd2*- transformants (Figure 3F), whereas *Trp53*- and *Trp53*-/*Rb1*-/*Pten*- transformants had 580 differentially expressed genes (Figure 3G). These results suggest that *Trp53*- transformant transcriptomes are more similar to *Brca2*- transformants than to *Trp53*-/*Rb1*-/*Pten*- transformants.

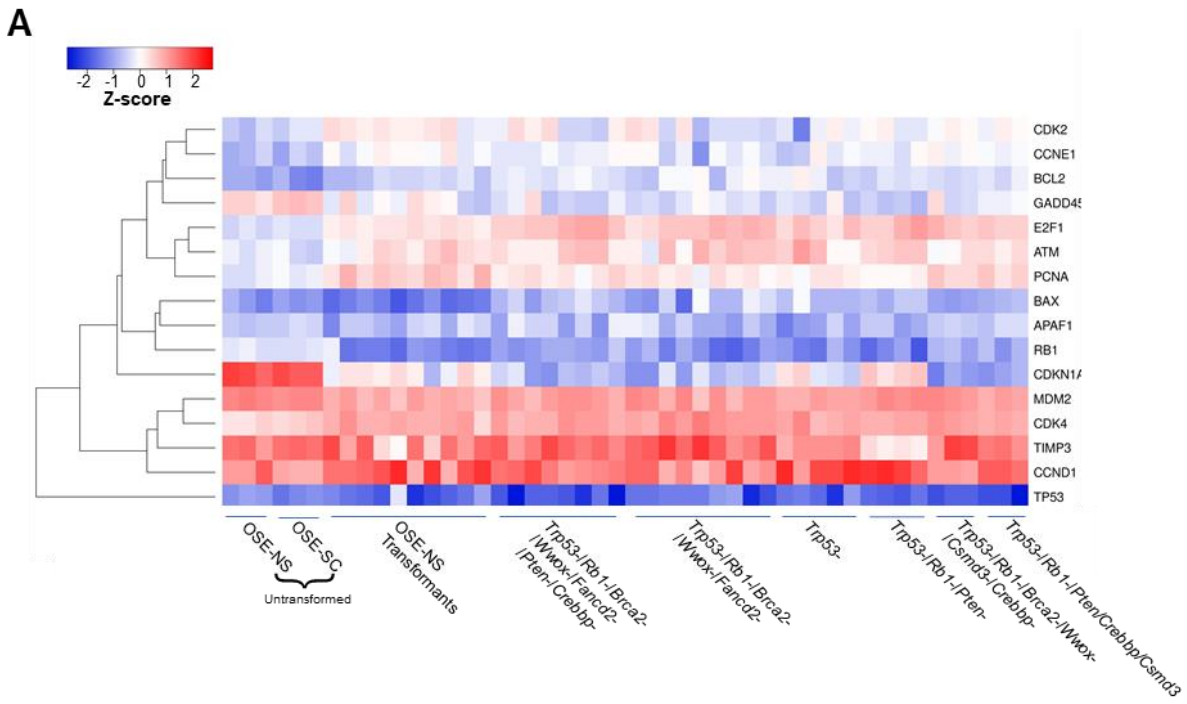

Figure 4. All transformant groups exhibit similar p53 pathway component expression. Z-scores for normalized reads were calculated for each gene and sample. Columns along the x axis represents a unique transformants. Transformants with identical LentiCRISPR-targeted genes are labeled. Rows along the y axis represent distinct genes.

Few HGSOC hallmark pathways reported by TCGA are enriched in OSE-SC transformants

Identification of differentially expressed genes between *Trp53*-/*Rb1*-/*Pten*-transformants, *Trp53*- transformants, and transformants with *Brca2*-targeting LentiCRISPRs led to the question of whether HGSOC or low-grade ovarian carcinoma-associated pathways are enriched among OSE-SC groups. Relative expression (z-scores) of genes within HGSOC-associated pathways were plotted on heat maps to visualize differences in expression among samples (Figures 4-6). I found that all OSE-SC transformant groups, regardless of LentiCRISPR-targeted genes, exhibited similar *Trp53* pathway gene expression (Figure 4). Transformants exhibited downregulation of genes like *Cdkn1a* (p21), *Rb1*, *Gadd45*, and *Bax*, which are associated with cell senescence or apoptosis (Figure 4A) [26–28]. Cell growth-associated genes such as *Pcna* and *E2f1* were also upregulated in nearly all transformants[27] (Figure 4). In comparison, untransduced cells expressed both *Gadd45* and *Cdkn1a* while downregulating *E2f1* and *Pcna* (Figure 4), suggesting potential resistance to transformation or excessive growth.

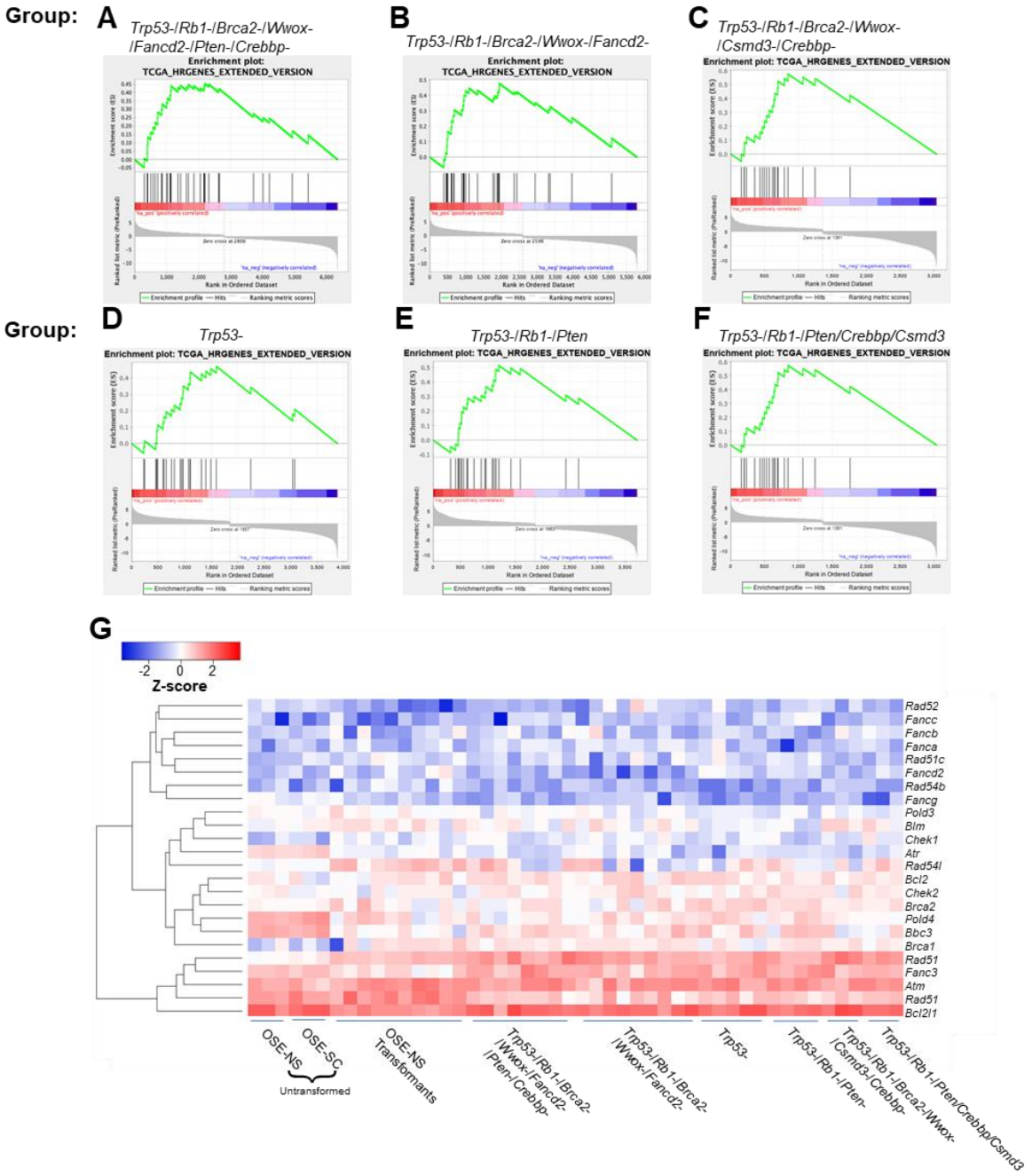

Figure 5. All transformant groups exhibit gene set enrichment for homologous recombination DNA repair genes. **(A-F)** Gene set enrichment analyses were performed for a gene set containing homologous recombination DNA repair genes reported by TCGA. All transformant groups exhibited significant enrichment. **(G)** Z-

scores for normalized reads were calculated for each gene and sample. Columns along the x axis represents a unique transformants. Transformants with identical LentiCRISPR-targeted genes are labeled. Rows along the y axis represent distinct genes.

A TCGA-defined DNA damage response gene set was also significantly enriched in all OSE-SC transformant groups (Figure 5A-F), and few differences in homologous recombination repair-related genes relative expression (z-scores) were observed among individual transformants (Figure 5G). For instance, nearly all samples exhibited upregulation of DNA damage response genes like *Atm*, *Rad50* and *Rad51* (Figure 5G). These results suggest that all transformants, regardless of whether or not they received a *Brca2*-targeting LentiCRISPR, may experience DNA damage (Figure 5). However, these results do not indicate whether DNA-damage associated gene expression is due to convergence with a HGSOC-like cell fate or is an inherent characteristic of cell culturing conditions as has been observed in other culturing systems [29,30].

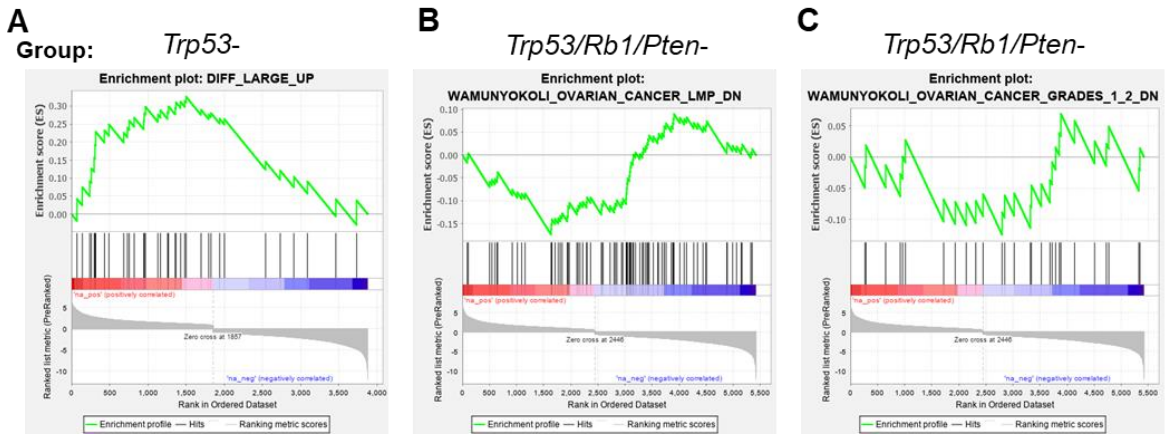

Figure 6. Few HGSOC subtype-associated gene sets are enriched among transformant groups. **(A-C)** Gene set enrichment analyses were performed for previously-published gene sets associated with HGSOC subtypes. *Trp53*-transformants were significantly enriched associated with the HGSOC differentiated subtype. *Trp53*-/*Rb1*-/*Pten*- transformants were negatively enriched for genes downregulated in low malignancy potential and grade I or II ovarian cancer.

Trp53- OSE-SC transformants share downregulated genes with the TCGA-defined differentiated HGSOC subtype

The Cancer Genome Atlas and others have also previously defined HGSOC subtypes that are linked to clinical outcome [6,31,32]. Subtypes include immunoreactive, differentiated, proliferative, and mesenchymal groups [6]. I completed gene set enrichment analyses to determine whether differentially expressed genes in any transformant subtype are enriched for HGSOC subtype-specific genes. The only significant ($q < 0.05$) enrichment occurred for *Trp53*- OSE-SC transformants, which were enriched for genes upregulated in the differentiated subtype (figure 6A). Differentiated tumors would be expected to exhibit better clinical outcomes than both the proliferative and mesenchymal groups [33].

Trp53-/*Rb1*-/*Pten*- OSE-SC share downregulated genes with low malignancy potential and grades I and II ovarian cancer

Gene set enrichment analysis was also completed on low grade and endometrioid carcinoma-associated gene sets to probe potential similarities between transformant gene expression and other ovarian cancer subtypes. Gene sets included those associated with Ras signaling (Biocarta), Wnt signaling (KEGG and Biocarta), PI3K signaling (Reactome and Hallmark), endometrial cancer (KEGG), Erbb signaling (KEGG), and low grade (grades I and II) ovarian cancer [34]. *Trp53*-/*Rb1*-/*Pten*- OSE-SC were negatively enriched for downregulated genes in grade I or II ovarian cancer and for downregulated genes associated with low malignancy potential ovarian tumors

(Figure 6B,C). However, this result was inconsistent because no positive enrichment was observed for upregulated genes associated with Grade I/II ovarian cancer or for low malignancy potential ovarian tumors. No transformant cluster had significant enrichment for any other low-grade ovarian cancer or endometrioid carcinoma-associated pathways. Similarity between *Trp53*-/*Rb1*-/*Pten*- transformants, or any other transformant group, with low grade ovarian cancer or endometrioid carcinoma is therefore unclear.

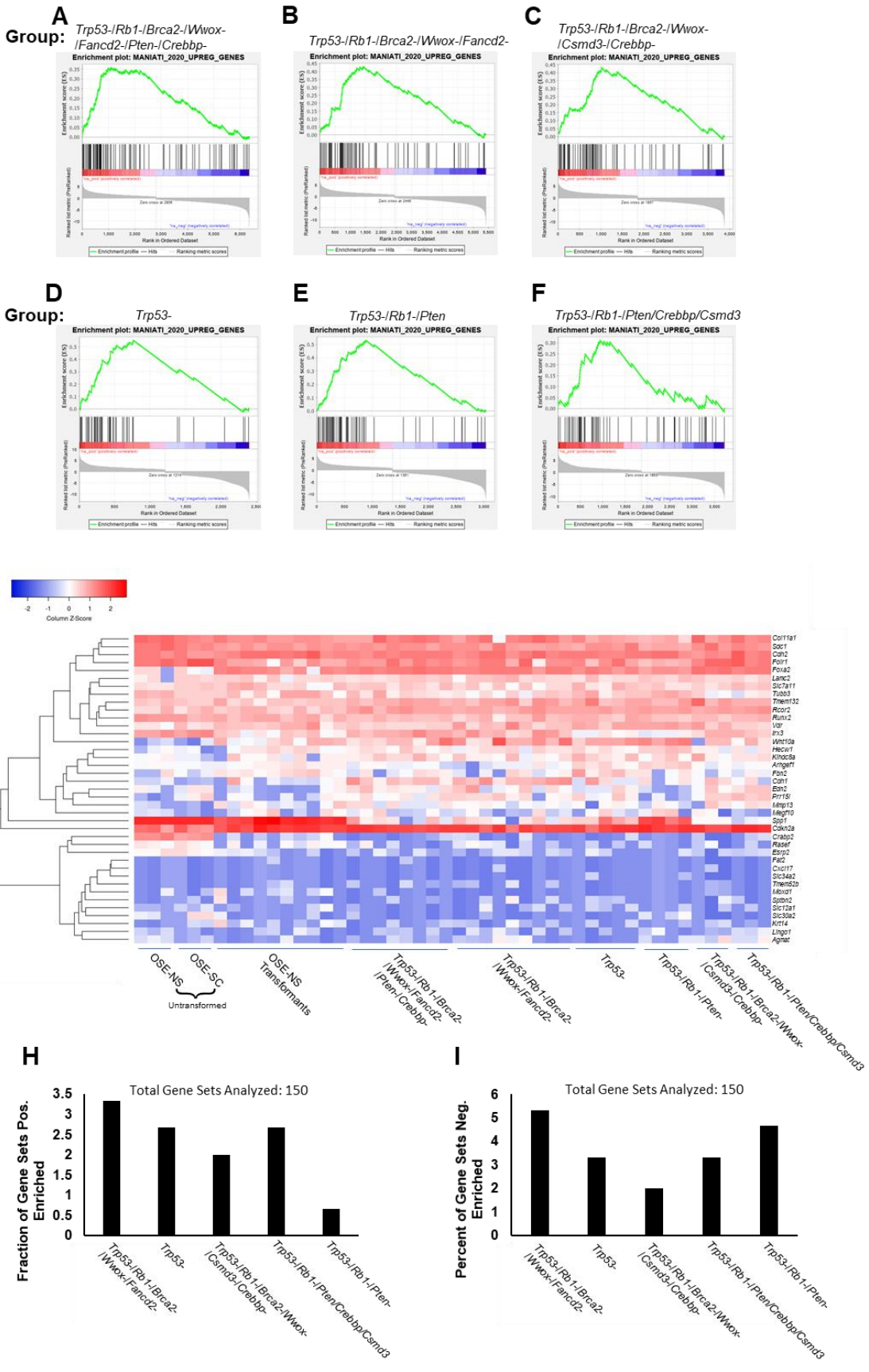
A
Group:
Trp53-/Rb1-/Brca2-/Wwox-/Fancd2-/Pten-/Crebbp-
B
Trp53-/Rb1-/Brca2-/Wwox-/Fancd2-
C
Trp53-/Rb1-/Brca2-/Wwox-/Csmd3-/Crebbp-
D
Group:
Trp53-
E
Trp53-/Rb1-/Pten
F
Trp53-/Rb1-/Pten/Crebbp/Csmd3
Enrichment plot: MANIATI_2020_UPREG_GENES
G
Column Z-Score
OSE-NS
OSE-SC
Untransformed
OSE-NS Transformants
Trp53-/Rb1-/Brca2-/Wwox-/Fancd2-/Pten-/Crebbp-
Trp53-/Rb1-/Brca2-/Wwox-/Fancd2-
Trp53-
Trp53-/Rb1-/Pten-
Trp53-/Rb1-/Brca2-/Wwox-/Csmd3-/Crebbp-
Trp53-/Rb1-/Pten/Crebbp/Csmd3
H
Total Gene Sets Analyzed: 150
Fraction of Gene Sets Pos. Enriched
I
Total Gene Sets Analyzed: 150
Percent of Gene Sets Neg. Enriched

Figure 7. A minority of HGSOC-associated gene sets are enriched in any OSE-SC transformant groups. **(A-F)** All transformant groups were significantly enriched ($q < 0.05$) for a gene set published by Maniati et al. (2020) containing genes upregulated in both mouse-derived HGSOC models and human HGSOC. **(G)** Many genes reportedly upregulated in HGSOC are not upregulated in most OSE-SC transformants. **(H-I)** Fraction of HGSOC-associated gene sets that are enriched among OSE-SC transformant groups ($n = 150$).

Gene sets shared between mouse and human HGSOC do not differentiate transformant clusters and most are not enriched among all groups

Previous work has identified gene sets and significantly upregulated genes in both mouse HGSOC models from either the OSE or TE and human HGSOC [13]. I performed GSEA on all mouse and human HGSOC shared gene sets to investigate whether OSE-SC transformant clusters share HGSOC-associated gene expression. All clusters were significantly enriched ($q < 0.05$) for a general gene set containing shared highly upregulated genes between mouse HGSOC models and human HGSOC (Figure 7 A-F) and few differences in gene set component expression were noted between groups (Figure 7G). However, Most other mouse and human HGSOC-associated gene sets[13] were not enriched in any transformant group (Figure 7H,I). These results suggest that fundamental differences may exist between transcriptomic characteristics of OSE-SC cultured transformants, previously-described mouse HGSOC models[13] and human HGSOC [6].

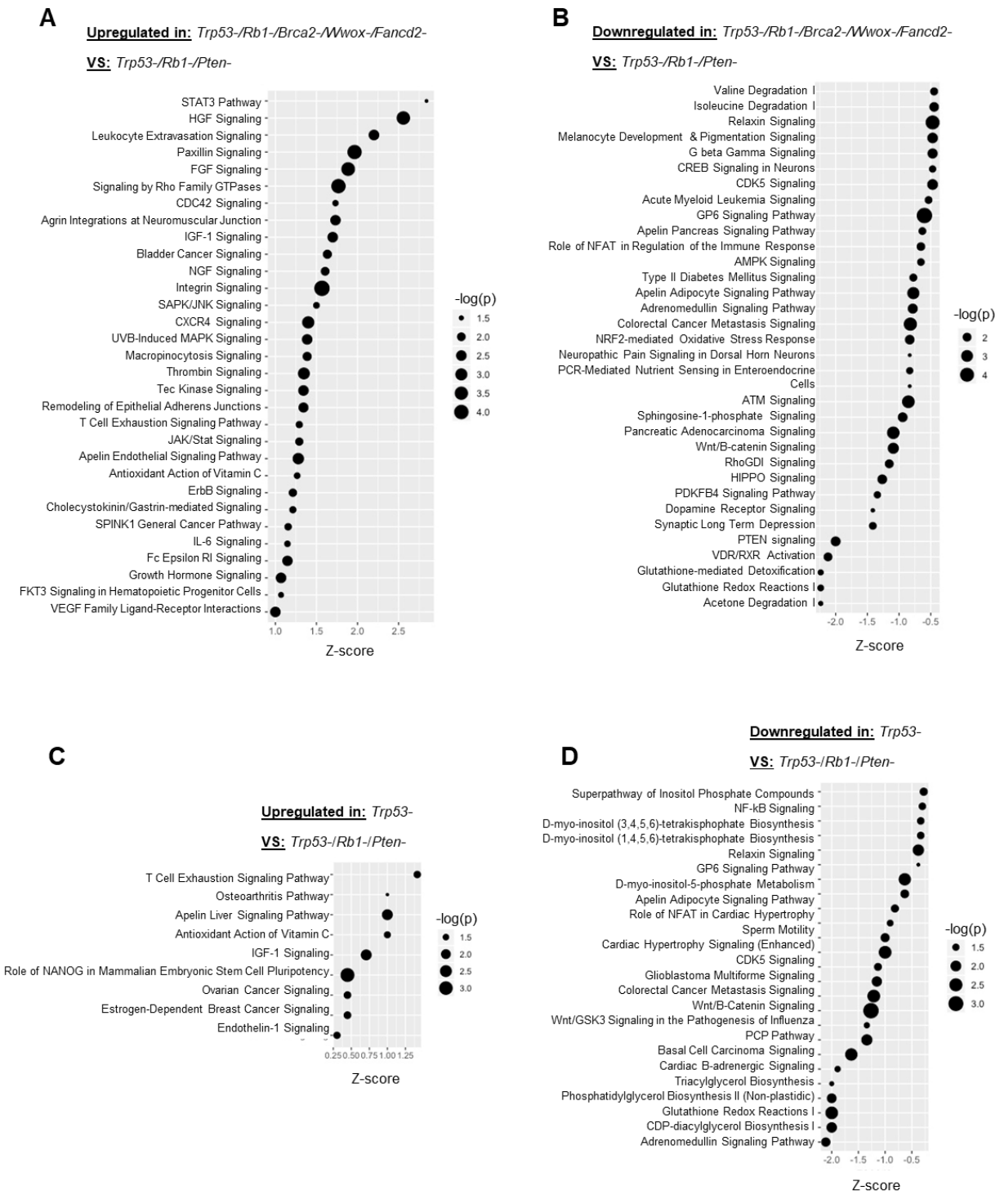

Figure 8. RTK signaling pathways differential expression occurs in both *Trp53-/Rb1-/Brca2-/Wwox-/Fancd2-* and *Trp53-* transformants. (A-D) IPA pathways analyses (Qiagen Inc) were used to identify pathways significantly enriched in

differentially expressed genes between groups. The y axes list pathways, and the x axes show the expression z-score. Bubble size corresponds to -log(p value). Only pathways with significant differential expression ($p < 0.05$) were plotted.

Pathways involved in cell growth, adhesion, and motility differentiate *Trp53*- and *Trp53*-/*Rb1*-/*Brca2*-/*Wwox*-/*Fancd2*- from *Trp53*-/*Rb1*-/*Pten*- transformants

Because few HGSOC or low grade ovarian cancer-related gene sets explained differences between transformant groups, I investigated other pathways that may explain differences between either *Trp53*- or *Trp53*-/*Rb1*-/*Brca2*-/*Wwox*-/*Fancd2*- and *Trp53*-/*Rb1*-/*Pten*- transformants. These transformant groups were chosen due to their differential gene expression. IPA pathway analyses revealed that *Trp53*-/*Rb1*-/*Brca2*-/*Wwox*-/*Fancd2*- transformants are enriched for pathways involved in cell growth, survival, adhesion, and metastases relative to *Trp53*-/*Rb1*-/*Pten*- transformants (Figure 8A). Specifically, tyrosine kinase-related signaling pathways such as STAT3 signaling, HGF signaling, Rho signaling, fibroblast growth factor signaling (FGF), IGF signaling, and NGF signaling are enriched in *Trp53*-/*Rb1*-/*Brca2*-/*Wwox*-/*Fancd2*- transformants relative to *Trp53*-/*Rb1*-/*Pten*- transformants (Figure 8A). *Trp53*-/*Rb1*-/*Brca2*-/*Wwox*-/*Fancd2*- transformants also express factors involved in extravasation, along with pathways involved with cell adhesion, angiogenesis, shape and mobility via Paxillin, VEGF and Integrin signaling (Figure 8A). *Trp53*-/*Rb1*-/*Brca2*-/*Wwox*-/*Fancd2*- cells may therefore possess a more aggressive growth phenotype and enhanced cellular mobility relative to *Trp53*-/*Rb1*-/*Pten*- transformants. In comparison to *Trp53*-/*Rb1*-/*Brca2*-/*Wwox*-/*Fancd2*- cells, *Trp53*-/*Rb1*-/*Pten*- transformants exhibited expression of stress response factors, Wnt signaling, and Hippo signaling (Figure 8B).

Like *Trp53*-/*Rb1*-/*Brca2*-/*Wwox*-/*Fancd2*- cells, *Trp53*- transformants also had increased RTK-related pathway expression relative to *Trp53*-/*Rb1*-/*Pten*- transformants. Significant enrichment for the “Ovarian Cancer Signaling (combined low and high grade)

and “Estrogen-Dependent Breast Cancer Signaling” pathways were noted (Figure 8C). These IPA pathways contain genes related to AKT, PI3K, and IGFR pathway activation, suggesting RTK-related gene expression overlap with *Trp53*-/*Rb1*-/*Brca2*-/*Wwox*-/*Fancd2*- transformants. Again, *Trp53*-/*Rb1*-/*Pten*- transformants were enriched for WNT signaling and stress response pathways relative to *Trp53*- transformants (Figure 8D). Together, these results suggest that well-established cell growth, invasion and mobility-related pathways are differentially expressed in both *Trp53*- and *Trp53*-/*Rb1*-/*Brca2*-/*Wwox*-/*Fancd2*- transformants (Figure 8).

DISCUSSION

Both *in vivo* and *in vitro* modeling systems are commonly utilized in cancer research to elucidate fundamental mechanisms of tumor initiation, growth and development. Although *in vivo* research is thoroughly pursued due to well-documented reliability advantages, *in vitro* systems are attractive due to their relatively low cost and fast data collection rates vs *in vivo* models [35,36]. Such *in vitro* systems often involve the use of established (immortalized) cell lines, primary cultures from model organisms or patients, and rely on the fundamental assumption that cultured cells share a high degree of characteristics with their original source tissue [37]. However, previous work has suggested that this assumption may depend on the particular culturing system being implemented, and the experimental context of its implementation [35,37–39].

Initiation mutations consistently influence colony growth characteristics *in vitro* but incompletely direct global gene expression

In this chapter, I described transcriptomic comparisons between human HGSOC and the mouse OSE-SC transformants. Factors influencing human HGSOC cancer cells and cultured mouse OSE-SC transformants are incredibly different, but previously published data suggests that some cultured mouse HGSOC models can transcriptomically resemble human disease [13,14]. These supposed similarities led me to hypothesize that OSE-SC transcriptomic landscapes may resemble human cancer, and that this relationship may depend upon the identity of LentiCRISPR-induced mutations. I also hypothesized that OSE-SC transformants with identical sets of LentiCRISPR-targeted genes would transcriptomically converge and differ from transformants with different sets of LentiCRISPR-targeted genes.

In previous targeted mutagenesis experiments, I reported that specific sets of LentiCRISPR-targeted genes were significant determinants of OSE-SC colony number and size (Chapter 2, Figure 4). This result was consistent across numerous experiments and replicates, suggesting that the presence or absence of particular mutations influences cell fate. Surprisingly however, principal component analyses demonstrated that substantial variability existed among most transformants that had identical LentiCRISPR-targeted genes (Figure 2). Substantial overlap also existed between most groups (except for *Trp53*-/*Rb1*-/*Pten*- transformants) on the principal component plot despite differences in LentiCRISPR-targeted genes (Figure 2). These results cumulatively suggest that the identity of transformation-initiating mutations can

consistently influence initial transformant growth characteristics (Chapter 2, Figure 4). However, they are not the sole determinant of transcriptomic characteristics *in vitro*.

Completely *in vitro* modeling may be insufficient to recapitulate human disease characteristics

I also observed a lack of similarity between gene expression patterns in OSE-SC transformants and human HGSOC, suggesting that this completely *in vitro* approach cannot be transcriptomically compared to *in vivo* models or human samples. My methodology differed from previous comparisons of mouse HGSOC models and human HGSOC because my system did not incorporate an *in vivo* component. Maniati and colleagues (2020) performed RNA sequencing on tumors that grew *in vivo* following *in vitro* knockout of driver genes in OSE and TE [13]. Therefore, although the authors did employ cell culturing methodology prior to transcriptomic characterization, microenvironmental changes due to subsequent *in vivo* growth may have influenced transcriptomic characteristics. Other reports of cell lines that recapitulate human HGSOC transcriptomic characteristics involve tumor cells that initiated and developed *in vivo* prior to culture [14]. Consequently, these HGSOC-like cell lines may also be heavily influenced by *in vivo* growth conditions [14]. It's possible, therefore, that transcriptomic similarity to human disease may necessitate *in vivo* tumor growth or development.

Culturing conditions or inherent genomic instability may influence gene expression

Cells were cultured as briefly as possible during this investigation in order to avoid potential confounding variables associated with *in vitro* systems. Previous evidence in other culturing systems has suggested, for instance, that prolonged culture of cardiac progenitor cells is associated with global transcriptomic alterations relative to paired source tissues. The most significant changes following culture include enrichment of genes related to cell proliferation, cell cycle progression, upregulation of DNA damage response genes, and loss of some identity markers following five passages [37]. Similarly, culture and immortalization of lymphoblast cells from blood samples and fibroblasts from skin caused overexpression of cell cycle progression-related genes, upregulation of DNA damage response pathways, and upregulation of p53 and p53-related genes [39]. Many of the upregulated genes and pathways noted for both cultured cardiac progenitor cells and lymphoblast cells were also observed in OSE-SC transformants (Figures 4-6), and may therefore represent common mechanisms of cellular adaptation to the relatively harsh growth conditions of primary culture compared to the native microenvironment of *in vivo* growth [40].

Genomic drift represents an additional factor that may explain divergence of transformed OSE-SC with human disease and with other transformants with identical LentiCRISPR-targeted genes. Previous evidence suggests that transformants deficient for *Brca2, Fancd2*, or both should experience chronic DNA damage, especially during S phase, thereby causing potential genomic drift in OSE-SC samples deficient for those genes [41–44]. However, all transformant groups exhibited enrichment of DNA damage response genes in a manner that was independent of *Brca2* or *Fancd2* targeting, suggesting that all transformants may be responding to damage, regardless of genotype

(Figure 5). These factors may partially explain PC divergence between individual transformants with identical genotypes and acquisition of culture-influenced gene expression.

Non-HGSOC related pathways potentially suggest differential cancerous growth characteristics of different colonies

Despite overall underrepresentation of well-established HGSOC-related pathway enrichment in any OSE-SC transformant subtype, enrichment of several other canonical pathways implies that differences in growth characteristics may exist. Analyses using EdgeR found differentially expressed genes between *Trp53*-/*Rb1*-/*Brca2*-/*Wwox*-/*Fancd2*- or *Trp53*- transformants and *Trp53-Rb1*-/*Pten*- transformants. Both *Trp53*-/*Rb1*-/*Brca2*-/*Wwox*-/*Fancd2*- and *Trp53*- were enriched for factors known to support cell growth, invasion and mobility, suggesting a potentially more aggressive growth and metastasis-related phenotypes compared to *Trp53-Rb1*-/*Pten*- transformants.

Proper comparisons with human disease likely require *in vivo* methodologies

It's clear from transcriptomic analyses described here that future efforts to compare transformants to human HGSOC would require an alternative approach. If the approach were to remain fully *in vitro*, it's possible that culturing OSE-SC as organoids, rather than in 2D culture, would facilitate comparisons to *in vivo* datasets. There is a current field consensus that 3 dimensional culturing systems, or organoids, allow cultured tissues to recapitulate native microenvironment and most closely resemble the

in vivo organ from which the tissue was derived [45]. An alternative approach would be to intraperitoneally inject cells into congenic mice following the induction of transformation-inducing mutations. This approach proved successful for others [13], potentially due to growth and development of tumors *in vivo*, rather than in 2D cultures in vitro. An *in vivo* growth component may therefore be required for significant transcriptomic comparison to human HGSOC.

METHODS

3' RNA sequencing of ALDH+ OSE, ALDH- OSE, and transformed samples

Transformants were expanded in culture for collection of 500,000 cells per transformant. Library preparation was conducted using the QuantSeq 3' mRNR-Seq Library Prep Kit FWD for Illumina following the manufacturer's instructions (Lexogen). Samples were run on two lanes of an illumina NextSeq500 instrument with a read length of 75bp. STAR aligner (described by Dobin et al. 2013) was used to align samples to the mm10 genome [46]. The sequencing data were uploaded to the Galaxy web platform, the public server at usegalaxy.org was used to analyze the data [47]. EdgeR was used to for data normalization and determination of differentially expressed genes[21]. Heatmapper software was used to calculate z-scores and visualize data[48].

Gene set enrichment and pathway analyses

Gene set enrichment analysis was completed using software (version 4.0) described previously[49]. Differential expression determination was completed using

EdgeR [21,22], and differentially expressed genes with an insignificant FDR ($q < 0.05$) were removed. Pre-ranked enrichment analysis was performed on "classic" setting. Gene sets were derived from Maniati and colleagues (2020), TCGA [4,6], The Kyoto Encyclopedia of Genes and Genomes (KEGG) [50–52], Biocarta [53], Hallmark gene sets [54], and the Reactome database [55,56]. Gene set names are listed in Appendix 5.

Pathway analyses were completed through the use of IPA software (QIAGEN Inc., https://www.qiagenbioinformatics.com/products/ingenuitypathway-analysis)." Figures displaying information from IPA were generated using ggplot2 in R [57].

Primary culture of OSE-SC, OSE-NS, and transformants

OSE, OSE-SC and OSE-NS were cultured following previously described methodology [8]. Briefly, ovaries were isolated from *Trp53* heterozygous FVB/NJ adult females and placed into phosphate-buffered saline (PBS) without Ca^{2+} or Mg^{2+} on ice. Ovaries were washed three times with PBS under a laminar flow hood, and a sterile scalpel blade was used to separate ovaries from the bursa. OSE was separated from the ovary via treatment with a digestion buffer consisting of collagenase (Sigma-Aldrich; Cat#: 10269638001), dispase (Sigma-Aldrich; Cat#: 10269638001), DNaseI (Sigma-Aldrich; Cat#: 11284932001) and Bovine Serum Albumin (BSA) (Sigma-Aldrich; Cat#: A9418). Pellets from each ovary were then added to 2mL OSE medium on gelatin-coated 24 well culture plates (Corning Costar; Cat#: CLS3527-100EA. Epithelial lineage of isolated cells was determined via detection of CK8 expression using immunofluorescent microscopy (Figure S4B-D).

Primary OSE cultures and the OSN2 cell line[23] were maintained in culture in media containing DMEM (VWR; Cat#: 10-017-CM), Hams F12 (Thermo Fisher, Cat#: 11320033), 5% FBS (Atlanta Biologicals; Cat#: S11050H), hydrocortisone (Sigma-Aldrich; Cat#: H4001), insulin-transferrin-sodium selenite (Sigma Aldrich), non essential amino acids (NEAA) (Thermo Fisher; Cat#: 11140050), glutamate (Thermo Fisher; Cat#: 25030081), sodium pyruvate (Thermo Fisher; Cat#: 11360070), and penicillin-streptomycin (Thermo Fisher; Cat#: 15140122) on 0.2% gelatin-coated culture plates (Corning Costar; Cat#: 07-200-83). Cells were passaged up to two times using 0.25% Trypsin-EDTA with Phenol Red (Thermo Fisher; Cat#: 25200072) to remove adherent cells from plates.

Statistical information and analytical methods

Transcriptomic analyses were completed on 32 OSE-SC transformants, 10 OSE-NS transformants, 3 untransformed OSE-SC cultures (passage 1), and 3 untransformed OSE-NS cultured (passage 1). OSE-SC transformants included *Trp53*-/*Rb1*-/*Pten*-/*Crebbp*-/*Csmd3*- (n = 3), *Trp53*-/*Rb1*-/*Brca2*-/*Wwox*-/*Fancd2*- (n = 8), *Trp53*-/*Rb1*-/*Brca2*-/*Wwox*-/*Fancd2*-/*Pten*-/*Crebbp*- (n = 9), *Trp53*- (n = 5), *Trp53*-/*Rb1*-/ *Pten*- (n = 4), *Trp53*-/*Rb1*-/*Brca2*-/*Wwox*-/*Crebbp*- (n = 3) transformants. Significance of differential gene expression and z-scores were calculated using algorithms described by Robinson et al. (2010) [21]. Gene set enrichment and false discovery rate was calculated using methodology described by Subramanian et al. (2005) [49]. Significantly upregulated pathways were identified through the use of IPA software (QIAGEN Inc., https://www.qiagenbioinformatics.com/products/ingenuitypathway-analysis)."

REFERENCES

1. Perets, R. *et al.* Transformation of the fallopian tube secretory epithelium leads to high-grade serous ovarian cancer in Brca;Tp53;Pten models. *Cancer Cell* **24,** 751–765 (2013).
2. Zhai, Y. *et al.* High-grade serous carcinomas arise in the mouse oviduct via defects linked to the human disease. *J. Pathol.* **243,** 16–25 (2017).
3. Bowtell, D. D. L. The genesis and evolution of high-grade serous ovarian cancer. *Nat. Rev. Cancer* **10,** 803–808 (2010).
4. Cancer Genome Atlas Research Network *et al.* Integrated genomic characterization of endometrial carcinoma. *Nature* **497,** 67–73 (2013).
5. Nero, C., Ciccarone, F., Pietragalla, A. & Scambia, G. PTEN and gynecological cancers. *Cancers (Basel)* **11,** (2019).
6. Cancer Genome Atlas Research Network. Integrated genomic analyses of ovarian carcinoma. *Nature* **474,** 609–615 (2011).
7. Seidman, J. D., Cho, K. R., Ronnett, B. M. & Kurman, R. J. in *Blaustein's pathology of the female genital tract* (eds. Kurman, R. J., Ellenson, L. H. & Ronnett, B. M.) 679–784 (Springer US, 2011). doi:10.1007/978-1-4419-0489-8_14
8. Flesken-Nikitin, A. *et al.* Ovarian surface epithelium at the junction area contains a cancer-prone stem cell niche. *Nature* **495,** 241–245 (2013).
9. Petrucelli, N., Daly, M. B. & Pal, T. in *GeneReviews(®)* (eds. Pagon, R. A. et al.) (University of Washington, Seattle, 1993).
10. Risch, H. A. *et al.* Population BRCA1 and BRCA2 mutation frequencies and cancer penetrances: a kin-cohort study in Ontario, Canada. *J. Natl. Cancer Inst.* **98,** 1694–1706 (2006).
11. Szabova, L. *et al.* Perturbation of Rb, p53, and Brca1 or Brca2 cooperate in inducing metastatic serous epithelial ovarian cancer. *Cancer Res.* **72,** 4141–4153 (2012).
12. Chen, S. & Parmigiani, G. Meta-analysis of BRCA1 and BRCA2 penetrance. *J. Clin. Oncol.* **25,** 1329–1333 (2007).
13. Maniati, E. *et al.* Mouse ovarian cancer models recapitulate the human tumor microenvironment and patient response to treatment. *Cell Rep.* **30,** 525–540.e7 (2020).
14. Domcke, S., Sinha, R., Levine, D. A., Sander, C. & Schultz, N. Evaluating cell lines as tumour models by comparison of genomic profiles. *Nat. Commun.* **4,** 2126 (2013).

15. Elias, K. M. *et al.* Beyond genomics: critical evaluation of cell line utility for ovarian cancer research. *Gynecol. Oncol.* **139,** 97–103 (2015).

16. Liu, K. *et al.* Evaluating cell lines as models for metastatic breast cancer through integrative analysis of genomic data. *Nat. Commun.* **10,** 2138 (2019).

17. Brodaczewska, K. K., Szczylik, C., Fiedorowicz, M., Porta, C. & Czarnecka, A. M. Choosing the right cell line for renal cell cancer research. *Mol. Cancer* **15,** 83 (2016).

18. Yu, K. *et al.* Comprehensive transcriptomic analysis of cell lines as models of primary tumors across 22 tumor types. *Nat. Commun.* **10,** 3574 (2019).

19. Xie, X. *et al.* Effects of long-term culture on human embryonic stem cell aging. *Stem Cells Dev.* **20,** 127–138 (2011).

20. Vacanti, V. *et al.* Phenotypic changes of adult porcine mesenchymal stem cells induced by prolonged passaging in culture. *J. Cell Physiol.* **205,** 194–201 (2005).

21. Robinson, M. D., McCarthy, D. J. & Smyth, G. K. edgeR: a Bioconductor package for differential expression analysis of digital gene expression data. *Bioinformatics* **26,** 139–140 (2010).

22. McCarthy, D. J., Chen, Y. & Smyth, G. K. Differential expression analysis of multifactor RNA-Seq experiments with respect to biological variation. *Nucleic Acids Res.* **40,** 4288–4297 (2012).

23. Flesken-Nikitin, A., Choi, K.-C., Eng, J. P., Shmidt, E. N. & Nikitin, A. Y. Induction of carcinogenesis by concurrent inactivation of p53 and Rb1 in the mouse ovarian surface epithelium. *Cancer Res.* **63,** 3459–3463 (2003).

24. Knudson, A. G. Mutation and cancer: statistical study of retinoblastoma. *Proc. Natl. Acad. Sci. USA* **68,** 820–823 (1971).

25. ICGC/TCGA Pan-Cancer Analysis of Whole Genomes Consortium. Pan-cancer analysis of whole genomes. *Nature* **578,** 82–93 (2020).

26. Elmore, S. Apoptosis: a review of programmed cell death. *Toxicol. Pathol.* **35,** 495–516 (2007).

27. Satyanarayana, A. & Kaldis, P. Mammalian cell-cycle regulation: several Cdks, numerous cyclins and diverse compensatory mechanisms. *Oncogene* **28,** 2925–2939 (2009).

28. Tamura, R. E. *et al.* GADD45 proteins: central players in tumorigenesis. *Curr. Mol. Med.* **12,** 634–651 (2012).

29. Jacobs, K. *et al.* Higher-Density Culture in Human Embryonic Stem Cells Results in DNA Damage and Genome Instability. *Stem Cell Rep.* **6,** 330–341 (2016).

30. Spits, C. *et al.* Recurrent chromosomal abnormalities in human embryonic stem cells. *Nat. Biotechnol.* **26,** 1361–1363 (2008).

31. Tothill, R. W. *et al.* Novel molecular subtypes of serous and endometrioid ovarian cancer linked to clinical outcome. *Clin. Cancer Res.* **14,** 5198–5208 (2008).

32. Verhaak, R. G. W. *et al.* Prognostically relevant gene signatures of high-grade serous ovarian carcinoma. *J. Clin. Invest.* **123,** 517–525 (2013).

33. Wang, C. *et al.* Pooled Clustering of High-Grade Serous Ovarian Cancer Gene Expression Leads to Novel Consensus Subtypes Associated with Survival and Surgical Outcomes. *Clin. Cancer Res.* **23,** 4077–4085 (2017).

34. Wamunyokoli, F. W. *et al.* Expression profiling of mucinous tumors of the ovary identifies genes of clinicopathologic importance. *Clin. Cancer Res.* **12,** 690–700 (2006).

35. Katt, M. E., Placone, A. L., Wong, A. D., Xu, Z. S. & Searson, P. C. In vitro tumor models: advantages, disadvantages, variables, and selecting the right platform. *Front. Bioeng. Biotechnol.* **4,** 12 (2016).

36. Saeidnia, S., Manayi, A. & Abdollahi, M. From in vitro Experiments to in vivo and Clinical Studies; Pros and Cons. *Curr. Drug Discov. Technol.* **12,** 218–224 (2015).

37. Kim, T. *et al.* In situ transcriptome characteristics are lost following culture adaptation of adult cardiac stem cells. *Sci. Rep.* **8,** 12060 (2018).

38. Hirschhaeuser, F. *et al.* Multicellular tumor spheroids: an underestimated tool is catching up again. *J. Biotechnol.* **148,** 3–15 (2010).

39. Lopes-Ramos, C. M. *et al.* Regulatory network changes between cell lines and their tissues of origin. *BMC Genomics* **18,** 723 (2017).

40. Kapałczyńska, M. *et al.* 2D and 3D cell cultures - a comparison of different types of cancer cell cultures. *Arch. Med. Sci.* **14,** 910–919 (2018).

41. Feng, W. & Jasin, M. BRCA2 suppresses replication stress-induced mitotic and G1 abnormalities through homologous recombination. *Nat. Commun.* **8,** 525 (2017).

42. Kais, Z. *et al.* FANCD2 Maintains Fork Stability in BRCA1/2-Deficient Tumors and Promotes Alternative End-Joining DNA Repair. *Cell Rep.* **15,** 2488–2499 (2016).

43. Tian, Y. *et al.* Constitutive role of the Fanconi anemia D2 gene in the replication stress response. *J. Biol. Chem.* **292,** 20184–20195 (2017).

44. Hussain, S. *et al.* Direct interaction of FANCD2 with BRCA2 in DNA damage response pathways. *Hum. Mol. Genet.* **13,** 1241–1248 (2004).

45. Hynds, R. E. & Giangreco, A. Concise review: the relevance of human stem cell-derived organoid models for epithelial translational medicine. *Stem Cells* **31,** 417–

422 (2013).

46. Dobin, A. *et al.* STAR: ultrafast universal RNA-seq aligner. *Bioinformatics* **29,** 15–21 (2013).

47. Afgan, E. *et al.* The Galaxy platform for accessible, reproducible and collaborative biomedical analyses: 2016 update. *Nucleic Acids Res.* **44,** W3–W10 (2016).

48. Babicki, S. *et al.* Heatmapper: web-enabled heat mapping for all. *Nucleic Acids Res.* **44,** W147-53 (2016).

49. Subramanian, A. *et al.* Gene set enrichment analysis: a knowledge-based approach for interpreting genome-wide expression profiles. *Proc. Natl. Acad. Sci. USA* **102,** 15545–15550 (2005).

50. Kanehisa, M., Sato, Y., Furumichi, M., Morishima, K. & Tanabe, M. New approach for understanding genome variations in KEGG. *Nucleic Acids Res.* **47,** D590–D595 (2019).

51. Kanehisa, M. & Goto, S. KEGG: Kyoto Encyclopedia of Genes and Genomes. *Nucleic Acids Res.* **28,** 27–30 (2000).

52. Kanehisa, M. Toward understanding the origin and evolution of cellular organisms. *Protein Sci.* **28,** 1947–1951 (2019).

53. Nishimura, D. BioCarta. *Biotech Software & Internet Report* **2,** 117–120 (2001).

54. Liberzon, A. *et al.* The Molecular Signatures Database (MSigDB) hallmark gene set collection. *Cell Syst.* **1,** 417–425 (2015).

55. Fabregat, A. *et al.* The Reactome Pathway Knowledgebase. *Nucleic Acids Res.* **46,** D649–D655 (2018).

56. Jassal, B. *et al.* The Reactome Pathway Knowledgebase. *Nucleic Acids Res.* **48,** D498–D503 (2020).

57. Wickham, H. *ggplot2 - Elegant Graphics for Data Analysis* . (Springer-Verlag New York, 2016). doi:10.1007/978-0-387-98141-3

Chapter 4: Significance, Impact, and Future Directions

The following chapter summarizes findings detailed in Chapters 2 and 3, and Appendices 1 and 2. Immediate applications of the dissertation are assessed, and future directions are proposed. Finally, the impact of the dissertation and its findings in the context of cancer biology are reviewed.

Summary of findings

High grade serous ovarian carcinoma (HGSOC) is the most lethal gynecological malignancy and 5th leading cause of female death because it is almost never detected at an early, curable stage. Unlike many other cancers, there is substantial debate regarding both the initiating location of HGSOC (i.e. the cell of origin) and mutations necessary to initiate HGSOC within the context of specific cell types. Attempts to model early HGSOC development or develop novel screening methodologies are therefore burdened by a lack of information regarding crucial stages of disease development.

This dissertation represents the first effort to investigate both the HGSOC cell of origin and necessary initiating mutations in an unbiased manner. It is also the first effort to experimentally assess whether putative HGSOC driver genes published by the Cancer Genome Atlas Research Network (TCGA) are indeed drivers of ovarian tissue transformation alone, or in combination with others. My approach differed from previous models of HGSOC development because I did not pre-select specific mutation combinations for experimental assessment. Instead, I avoided bias by randomly evaluating all possible combinations of mutations in several different putative “cells of origin”. Results are therefore independent of preconceived biases derived from previously published HGSOC initiation theories.

The methodology described here led to a model of HGSOC initiation in which ovarian surface epithelial stem cells (OSE-SC) are more prone to transformation than non-stem OSE (OSE-NS). The model also suggests that most putative HGSOC driver mutations or deletions identified by TCGA are actually passenger mutations that convey no growth advantage onto ovarian tissues. Of the 20 TCGA driver genes assessed,

only disruption of *Trp53*, *Rb1*, and/or *Pten* were centrally important for OSE-SC transformation. Several previously uncharacterized mutation combinations further enhanced transformation but may do so via p53-related mechanisms.

This dissertation also contains a chapter (Chapter 3) and two appendices (Appendices 1 and 2) discussing methodological alternatives or addendums to *in vitro* HGSOC driver gene screening and provides suggestions regarding direct comparisons to human disease. Next generation sequencing analyses of *in vitro* OSE-SC transformants demonstrated crucial importance of *in vivo* modeling for parallels to be made with human cancer (See Chapter 3). *In vivo* growth strategies were also functionally assessed with results supporting the HGSOC transformation model proposed in Chapter 2 (See Appendix 2). Furthermore, complexities associated with the application of minilibrary driver screening methodologies toward extraovarian cell types were explored and discussed (See Appendix 1).

Together, the data presented in this dissertation represent a major first step in the development of mechanistic HGSOC initiation models based upon TCGA data and unbiased screening approaches. My model (See Chapter 2, Figure 6) has direct implications in discovery of novel therapeutic options and ascertainment of early screening methodologies. It also presents proof-of-concept datasets important for future investigations into HGSOC initiation mechanisms and proposes immediate applications of dissertation findings. Finally, the methodology utilized here (See Chapter 2) can serve as a rapid, reliable tool to screen for drivers of any cancer type for which putative cells of origin are known and culturing methodology exists.

Limitations

My dissertation provides valuable commentary regarding the limitations of fully *in vitro* approaches to model human disease in Chapter 3. Although transformation-initiating mutations impact transformation frequency and growth characteristics (See Chapter 2), global gene expression was largely influenced by cell culturing conditions. For instance, 3' RNA sequencing data suggested that even transformants with identical LentiCRISPR-induced mutations exhibited divergent global gene expression. *In vitro* screening may be most useful, therefore, as the first investigative step in differentiating driver and passenger mutations with follow-up validation experiments required *in vivo*.

Although *in vivo* experiments are likely required to recapitulate human disease characteristics, inefficiency of cellular transformation following LentiCRISPR minilibrary transduction may complicate future *in vivo* experiments and should be considered during experimental design. When transduced (MOI = 7) with a LentiCRISPR minilibrary targeting 20 putative HGOSOC driver genes, only 0.016% and 0.656% of OSE-NS and OSE-SC transformed, respectively. Surprisingly, transduction (MOI = 7) of OSE-SC with the most efficient transformation-inducting LentiCRISPR combination observed in Chapter 2 (those targeting *Trp53*, *Rb1*, *Cdkn2a* and *Pten* together) only caused 8.6% of cells to transform in soft agar. Therefore, even transformation-inducing mutations made in a transformation-prone cell type cannot cause most cells to exhibit adhesion independent growth in soft agar.

The minilibrary screening methodology also appears to require optimization for any novel cultured cell type, meaning that no single viral packaging protocol applies to any culturing system. I found that lentiviral concentrations which produce combinatorial

mutagenesis in one cell type may be insufficient for other cell types, resulting in single gene mutations only (Appendix 1). Inefficient minilibrary transduction was a contributing factor for failure to identify necessary transformation-initiating mutations in TE.

Another potential shortcoming of minilibrary mutagenesis screening is that only putative tumor suppressors were considered as potential drivers of transformation. Yet in TCGA data, over 20% of tumors exhibited focal amplification of the oncogenes *CCNE1*, *MYC*, and *MECOM* [1]. Several mouse models of HGSOC initiation have also implemented oncogene activation alongside mutations in tumor suppressors like *Trp53* and/or *Brca1* and have reported incidence of serous epithelial or undifferentiated ovarian tumors [2–4]. Evidence from both TCGA and mouse models together therefore suggests that oncogenes may also play potential roles in HGSOC initiation that may be overlooked via knockout screening alone.

Methodological implications

The fully *in vitro* screening pipeline described in this dissertation is a rapid, efficient method to functionally assess untested putative cancer drivers in any system for which culturing methodology exists. TCGA, for example, has sequenced over 20,000 primary tumor samples and has generated comprehensive lists of commonly mutated or deleted putative driver genes for 33 cancer types [5]. Many of the genes identified through these genomic analyses are novel mutations for particular cancers and have not been assessed experimentally. Animal modeling or targeted knockout assessment of TCGA-identified genes can be expensive or time consuming, but

LentiCRISPRv2 and next generation sequencing approaches allow for simultaneous assessment of thousands of combinations at once and have the potential to refine lists of candidate driver mutations. Longstanding cell transformation paradigms from various cancers can also be tested using the minilibrary pipeline to assess field dogma in an unbiased manner. The minilibrary screening approach may therefore help disentangle steps of neoplastic transformation in multiple malignancies.

Future Directions

Implications for modeling of HGSOC development

Results generated using the minilibrary screening pipeline in this dissertation have direct implications for exploration of early HGSOC initiation mechanisms through development of early stage HGSOC models. Both organoid models and mouse modeling systems have fundamental importance in ascertainment of cancer developmental mechanisms, development of early detection methodologies, and assessment of novel therapeutic options. I propose that the minimal model of HGSOC initiation proposed here in the context of the proper cell of origin can be used to generate mouse or organoid models of HGSOC initiation.

In vitro screening of putative HGSOC driver genes in the fallopian tubal epithelium

This dissertation described an investigation into mutations necessary for OSE-SC and OSE-NS transformation, two putative HGSOC cells of origin [6,7]. Importantly

however, HGSOC also has putative extraovarian origin in the distal TE [8]. Specifically, PAX8-expressing secretory cells and putative TE stem cells have been proposed as possible initiating cells [9–13]. In order to fully model HGSOC initiation, all possible cells of origin must be experimentally assessed.

Several groups have published recent reports of long term TE culture using traditional 2D culturing or organoid culturing methodologies. These reports suggest that TE cell identity can be maintained in long term culture [10,14–17]. Others have reported that TE stem cells can be enriched using flow cytometry and markers such as EPCAM or ALDH [12,17]. Therefore, previously published methodology to culture TE and TE stem cells can be implemented and optimized. The minilibrary screening pipeline described here can then be used to screen for mutations necessary to transform TE and TE stem cells to complete modeling of minimal HGSOC transformation requirements.

Transcriptomic characterization of tumors initiated via unique combinations of driver gene mutations

Minilibrary screening of OSE-SC *in vitro* produced several groups of transformants containing different sets of genome-integrated LentiCRISPRs. However, these analyses are not able to reveal whether different sets of LentiCRISPR-induced mutations in putative HGSOC driver genes cause transcriptomic convergence or divergence from human disease. Many of these *in vitro* transformants were transcriptomically characterized using 3' RNA seq, but transcriptomic characteristics were largely influenced by culturing methodology thereby preempting comparisons to

human HGSOC. Future attempts to compare LentiCRISPRv2-mutated transformants to human disease must therefore include *in vivo* transformation and growth.

Approaches to investigate transcriptomic similarities or differences between transformants with unique combinations of driver gene mutations may be modeled after methodology described by Maniati and colleagues (2020). The authors modeled peritoneal dissemination of HGSOC in human patients by introducing mutations in combinations of *Trp53*, *Rb1*, *Brca1* and *Pten* in either OSE or TE and then intraperitoneally injecting them into mice. Consequential tumors were then transcriptomically characterized and compared to human HGSOC. Striking similarity of gene expression profiles was noted between mouse tumors and human HGSOC, suggesting that *in vitro* models can recapitulate human disease characteristics [18].

To determine whether specific LentiCRISPR combinations conveys HGSOC-like characteristics, OSE-SC should be transduced with LentiCRISPR corresponding to putative driver mutations. Transduced cells can then be immediately intraperitoneally injected into mice to allow for histologic and transcriptomic analyses of resulting tumors. Such experiments would provide important insight into mechanistic function of putative HGSOC driver genes on disease development and cellular identity.

Preliminary proof-of-concept experiments were performed in Appendix 2. Transformants with unique combinations of LentiCRISPR-targeted genes were intraperitoneally injected into congenic mice, and efficient peritoneal tumorigenesis was observed following injection of specific transformants. These preliminary analyses therefore suggest that IP injections of cells transduced with LentiRISPRv2 constructs

can produce tumors which can later be subjected to transcriptomic and histologic characterization.

CRISPRa implementation into minilibrary screening methodology

In Chapter 2, lentiviral CRISPR/Cas9 was utilized for minilibrary screening efforts to induce random, combinatorial knockouts in putative tumor suppressors. While screening methodology employed in this dissertation is useful for assessment of tumor suppressors, it cannot directly identify oncogenes that may be involved in HGSOC initiation. Functional knockouts may result in indirect activation of oncogenes through disruption of tumor suppressors, but an inability to do so directly is a characteristic of mutation or knockout-based screening [19,20]. Direct gain-of-function activation mechanisms may instead be required to investigate the effect of oncogenes in HGSOC initiation [21].

CRISPRa is an alternative CRISPR system that utilizes a catalytically inactive Cas9 (dCas9) linked to transcriptional activators to enable gene expression. Like traditional CRSPR/Cas9 systems, CRISPRa can be guided to intended target sites using a single guide RNA and can be packaged into lentiviral vectors. However, they are targeted to the promoter region of endogenous genes to modulate gene expression rather than a coding exon, as is the case for traditional CRISPR/Cas9 [21]. CRISPRa-based screens have been used previously to activate positive regulators of cell proliferation such as oncogenes [22]. They have also been implemented in parallel with CRISPR-based knockdown or knockout screens to interrogate the effect of gene

activation or repression on phenotypes like growth, survival, drug resistance, or drug sensitivity [23–25].

Comprehensive functional assessment of necessary HGSOC initiation factors would benefit from interrogation of both tumor suppressors and oncogenes as potential factors contributing to cellular transformation. Because CRISPRa systems can also be packaged into lentiviral constructs, they can be included in future CRISPR-based screening attempts in putative HGSOC cells of origin, thereby allowing for combined random combinations of tumor suppressor knockouts and oncogene activations. This method would investigate whether the minimal transformation requirements identified in Chapter 2 are necessary in the presence of activated oncogenes. It would also reveal whether different putative HGSOC driver genes function synergistically with activated oncogenes to drive transformation in the context of multiple cell types.

Implementation of genome-wide CRISPR screening to identify genes associated with synthetic lethality in distinct transformant types

As was suggested in Chapter 2, a potential translational application of this dissertation is targeted therapy design. Mutations in several putative HGSOC driver genes resulted in growth inhibition rather than transformation enhancement. For example, LentiCRISPRv2 targeting of either *Prim2*, *Brca2*, *Rad51c*, *Fancd2*, *Apc* or *Fat3* alongside *Trp53* and *Cdkn2a* (or *Rb1*) resulted in significantly less cellular transformation and often smaller colony size. It's possible, therefore, that the potential

synthetic lethality or growth deterrence following disruption of these genes may be relevant targeted therapy development.

Although single mutations in several genes can cause growth inhibition, I also observed that several growth-inhibiting genes actually promoted cellular transformation or colony size when mutated alongside specific synergistic genes. While assessment of these genes as potential druggable targets may still be viable, complications regarding synergistic mutations may necessitate a more comprehensive search for druggable targets in transformants. Genome-wide CRISPR/Cas9 screening has been frequently implemented as a method to accomplish high throughput assessment of synthetically lethal genes [19,26–28]. Genome-wide synthetic lethality screens may therefore be performed in transformants with specific sets of transformation-initiating mutations to identify genotype-specific therapies.

Significance in Cancer Biology

Cancer has become a leading cause of human mortality in recent history, but its prominence a major cause of death is a relatively recent development. Prior to the mid 20th century, deaths due to cancer were greatly surpassed by those from infectious disease or injury[29]. Human lifespans were consequently much lower, but innovations such as sulfa drugs and antibiotics in past 100 years resulted in less infection- or injury-related death and steadily increased lifespans[29]. Unfortunately, cancer is an age-related malady, so improved life expectancy also positively correlates with the

probability of one's cells receiving random mutations or experiencing environmental mutagens that cause carcinogenesis[29–31].

Although cancer has only become a leading cause of human mortality in the past century, physicians and scientists have studied cancer and searched for potential cures throughout much of human history. The earliest documented case of human tumors was found between 1500 and 1600 B.C. in ancient Egypt detailing characteristics of probable breast tumors [32]. The disease was first termed "carcinos", or "crab" by Hippocrates in ancient Greece due to physical resemblance to a crab, and was translated as "cancer" by the Roman physician Celsus between the year 28 and 50 B.C. Such reports and subsequent research have been accompanied by speculation regarding a cure for the disease[33].

Despite unifying hallmarks shared by all cancers, the term "cancer" has evolved in recent years from its original designation as a single disease[34]. It is now considered to be a collection of diverse maladies that vary tremendously in their origin, genetics, progression, causative factors, response to treatment, and prognosis [35]. Because these individual diseases acquire and manifest universal cancer hallmarks in a different manner, it's unlikely that one single cure, or "golden bullet", exists for all cancers. Instead, that individual cures could be developed and optimized for each type of cancer[36].

The prospect of individual cancer cures or treatments may appear daunting, but successful treatment or prevention strategies have been implemented with incredible success for several thoroughly characterized cancer types. For example, only 68% of patients diagnosed with prostate cancer survived over five years following initial

diagnoses between 1975 and 1977. However, early detection methodologies and optimized treatment strategies have increased the five year survival rate to 99% [30]. Acute Lymphoblastic Leukemia (ALL) childhood survival is another prominent success story as prognosis has improved from 6 month average survival to 85% of patients being cured of detectible disease [37]. Subtype-specific cancer treatments, and even "cures", are therefore possible given thorough understanding of cancer subtype developmental mechanisms.

Unfortunately, ovarian cancer differs from the aforementioned examples because little progress has been made over the past several decades in improving patient prognoses. Ovarian cancer consists of several distinct diseases that diverge in their genetics, risk factors, cell of origin, and progression, but subtypes are often clinically treated as a single disease due to shared localization in the female reproductive tract [38–41]. The current "gold standard" for treatment is a harsh regimen of debulking surgery and administration of cytotoxic chemotherapeutics like cisplatin, but relapse rates are high, especially for aggressive subtypes like HGSOC [42].

Although the differences between HGSOC cases may appear to make targeted treatment options difficult, it's possible that exploitation of these differences may actually be the key to improving HGSOC prognoses. 20% of HGSOC cases, for example, exhibit inhibited DNA damage repair responses due to mutations in *BRCA1* or *BRCA2*. These *BRCA*-related HGSOC cases may be particularly susceptible to PARP inhibitors, which exploit cellular stress due to impaired DNA damage response and cause apoptosis in BRCA-deficient cells [43,44]. Future options for ovarian cancer treatment may

therefore benefit from ascertainment of drug targets that cause synthetic lethality in cells with specific mutation spectra.

To therapeutically exploit further differences between HGOSC tumors, mechanistic models of tumorigenesis must be developed in a manner that embraces the heterogeneity that characterizes HGSOC tumors. Ultimately, the unbiased approaches described in this dissertation were undertaken to understand the diversity of HGSOC initiating mechanisms, develop an array of possible mutagenic profiles, and contribute to the body of mechanistic knowledge that is critical for future subtype-specific therapeutic manipulation. As an unintended side effect of screening, some of the genes evaluated in targeted mutagenesis assays actually caused decreased transformation of ovarian tissues harboring specific mutational loads. This observation demonstrates that specific transformed cell genotypes may be susceptible to growth inhibition via targeted therapeutics.

Although this dissertation focused on ovarian cancer, the methodology proposed in Chapter 2 can be immediately implemented as a high throughput pipeline to assess of cancer initiation mechanism for any cancer for which culturing methodology exists. These methods can lead to mechanistic understanding of specific cancer subtypes and create opportunity for development of subtype-specific therapies. Therefore, while no particular therapy can be completely effective for all cancers, this dissertation provides a foundational tool that can be implemented as a first step towards the development of new therapies or cures for distinct cancers.

REFERENCES

1. Cancer Genome Atlas Research Network. Integrated genomic analyses of ovarian carcinoma. *Nature* **474,** 609–615 (2011).
2. Xing, D. & Orsulic, S. A mouse model for the molecular characterization of brca1-associated ovarian carcinoma. *Cancer Res.* **66,** 8949–8953 (2006).
3. Orsulic, S. *et al.* Induction of ovarian cancer by defined multiple genetic changes in a mouse model system. *Cancer Cell* **1,** 53–62 (2002).
4. Bobbs, A. S., Cole, J. M. & Cowden Dahl, K. D. Emerging and evolving ovarian cancer animal models. *Cancer Growth Metastasis* **8,** 29–36 (2015).
5. Gao, G. F. *et al.* Before and after: comparison of legacy and harmonized TCGA genomic data commons' data. *Cell Syst.* **9,** 24–34.e10 (2019).
6. Auersperg, N. The origin of ovarian cancers--hypotheses and controversies. *Front. Biosci. (Schol. Ed)* **5,** 709–719 (2013).
7. Flesken-Nikitin, A. *et al.* Ovarian surface epithelium at the junction area contains a cancer-prone stem cell niche. *Nature* **495,** 241–245 (2013).
8. Piek, J. M. *et al.* Dysplastic changes in prophylactically removed Fallopian tubes of women predisposed to developing ovarian cancer. *J. Pathol.* **195,** 451–456 (2001).
9. Adler, E., Mhawech-Fauceglia, P., Gayther, S. A. & Lawrenson, K. PAX8 expression in ovarian surface epithelial cells. *Hum. Pathol.* **46,** 948–956 (2015).
10. Paik, D. Y. *et al.* Stem-like epithelial cells are concentrated in the distal end of the fallopian tube: a site for injury and serous cancer initiation. *Stem Cells* **30,** 2487–2497 (2012).
11. Perets, R. *et al.* Transformation of the fallopian tube secretory epithelium leads to high-grade serous ovarian cancer in Brca;Tp53;Pten models. *Cancer Cell* **24,** 751–765 (2013).
12. Rose, I. *et al.* WNT and inflammatory signaling distinguish human Fallopian tube epithelial cell populations. *BioRxiv* (2020). doi:10.1101/2020.01.15.908293
13. Schmoeckel, E. *et al.* LEF1 is preferentially expressed in the tubal-peritoneal junctions and is a reliable marker of tubal intraepithelial lesions. *Mod. Pathol.* **30,** 1241–1250 (2017).
14. Levanon, K. *et al.* Primary ex vivo cultures of human fallopian tube epithelium as a model for serous ovarian carcinogenesis. *Oncogene* **29,** 1103–1113 (2010).
15. Kessler, M. *et al.* The Notch and Wnt pathways regulate stemness and differentiation in human fallopian tube organoids. *Nat. Commun.* **6,** 8989 (2015).

16. Lawrenson, K. *et al.* In vitro three-dimensional modeling of fallopian tube secretory epithelial cells. *BMC Cell Biol.* **14,** 43 (2013).

17. Xie, Y., Park, E.-S., Xiang, D. & Li, Z. Long-term organoid culture reveals enrichment of organoid-forming epithelial cells in the fimbrial portion of mouse fallopian tube. *Stem Cell Res.* **32,** 51–60 (2018).

18. Maniati, E. *et al.* Mouse ovarian cancer models recapitulate the human tumor microenvironment and patient response to treatment. *Cell Rep.* **30,** 525–540.e7 (2020).

19. Wang, T., Wei, J. J., Sabatini, D. M. & Lander, E. S. Genetic screens in human cells using the CRISPR-Cas9 system. *Science* **343,** 80–84 (2014).

20. Doench, J. G. Am I ready for CRISPR? A user's guide to genetic screens. *Nat. Rev. Genet.* **19,** 67–80 (2018).

21. Konermann, S. *et al.* Genome-scale transcriptional activation by an engineered CRISPR-Cas9 complex. *Nature* **517,** 583–588 (2015).

22. Luo, J. Crispr/cas9: from genome engineering to cancer drug discovery. *Trends Cancer* **2,** 313–324 (2016).

23. Gilbert, L. A. *et al.* Genome-scale CRISPR-mediated control of gene repression and activation. *Cell* **159,** 647–661 (2014).

24. le Sage, C. *et al.* Dual direction CRISPR transcriptional regulation screening uncovers gene networks driving drug resistance. *Sci. Rep.* **7,** 17693 (2017).

25. Boettcher, M. *et al.* Dual gene activation and knockout screen reveals directional dependencies in genetic networks. *Nat. Biotechnol.* **36,** 170–178 (2018).

26. Shalem, O. *et al.* Genome-scale CRISPR-Cas9 knockout screening in human cells. *Science* **343,** 84–87 (2014).

27. Dhanjal, J. K., Radhakrishnan, N. & Sundar, D. Identifying synthetic lethal targets using CRISPR/Cas9 system. *Methods* **131,** 66–73 (2017).

28. Martin, T. D. *et al.* A Role for Mitochondrial Translation in Promotion of Viability in K-Ras Mutant Cells. *Cell Rep.* **20,** 427–438 (2017).

29. Armstrong, G. L., Conn, L. A. & Pinner, R. W. Trends in infectious disease mortality in the United States during the 20th century. *JAMA* **281,** 61–66 (1999).

30. Siegel, R. L., Miller, K. D. & Jemal, A. Cancer statistics, 2020. *CA Cancer J Clin* **70,** 7–30 (2020).

31. Nachman, M. W. & Crowell, S. L. Estimate of the mutation rate per nucleotide in humans. *Genetics* **156,** 297–304 (2000).

32. Faguet, G. B. A brief history of cancer: age-old milestones underlying our current knowledge database. *Int. J. Cancer* **136,** 2022–2036 (2015).

33. Mukherjee, S. *The Emperor Of All Maladies: A Biography Of Cancer*. 592 (Scribner, 2010).

34. Hanahan, D. & Weinberg, R. A. Hallmarks of cancer: the next generation. *Cell* **144,** 646–674 (2011).

35. Cooper, G. *The Cell: A Molecular Approach*. 689 (Sinauer Associates Inc, 2000).

36. Shin, S. H., Bode, A. M. & Dong, Z. Precision medicine: the foundation of future cancer therapeutics. *npj Precision Onc.* **1,** 12 (2017).

37. O'Leary, M., Krailo, M., Anderson, J. R., Reaman, G. H. & Children's Oncology Group. Progress in childhood cancer: 50 years of research collaboration, a report from the Children's Oncology Group. *Semin. Oncol.* **35,** 484–493 (2008).

38. Cho, K. R. & Shih, I.-M. Ovarian cancer. *Annu. Rev. Pathol.* **4,** 287–313 (2009).

39. Köbel, M. *et al.* Ovarian carcinoma subtypes are different diseases: implications for biomarker studies. *PLoS Med.* **5,** e232 (2008).

40. Lisio, M.-A., Fu, L., Goyeneche, A., Gao, Z.-H. & Telleria, C. High-Grade Serous Ovarian Cancer: Basic Sciences, Clinical and Therapeutic Standpoints. *Int. J. Mol. Sci.* **20,** (2019).

41. Tothill, R. W. *et al.* Novel molecular subtypes of serous and endometrioid ovarian cancer linked to clinical outcome. *Clin. Cancer Res.* **14,** 5198–5208 (2008).

42. Seidman, J. D., Ronnett, B. M., Shih, I.-M., Cho, K. R. & Kurman, R. J. in *Blaustein's pathology of the female genital tract* (eds. Kurman, R. J., Hedrick Ellenson, L. & Ronnett, B. M.) 841–966 (Springer International Publishing, 2019). doi:10.1007/978-3-319-46334-6_14

43. Curtin, N. J. & Szabo, C. Therapeutic applications of PARP inhibitors: anticancer therapy and beyond. *Mol. Aspects Med.* **34,** 1217–1256 (2013).

44. Liu, J. F., Konstantinopoulos, P. A. & Matulonis, U. A. PARP inhibitors in ovarian cancer: current status and future promise. *Gynecol. Oncol.* **133,** 362–369 (2014).

Appendix 1: *In Vitro* Transformation of Fallopian Tubal Epithelial Cells

This appendix documents attempted application of LentiCRISPR minilibrary-based screening methodologies to investigate putative transformation-associated genes in the distal fallopian tubal epithelium (TE). Several factors, including culturing methodology and inefficient TE viral transduction, preempted analyses of putative transformation-initiating mutations. However, these limitations are discussed in this appendix, along with suggestions for methodological improvement. These results have not been submitted for publication.

INTRODUCTION

The ovarian surface epithelium (OSE) is a longstanding High Grade Serous Ovarian Carcinoma (HGSOC) putative “cell of origin” due to HGSOC localization at the OSE, transcriptomic similarity with many HGSOC tumors, and previously-demonstrated transformation *in vivo* [1–8]. However, evidence for other extraovarian HGSOC initiating locations was first proposed in 2001 by Piek and colleagues, who questioned the predominant OSE initiation paradigm [9]. The authors observed high frequency of dysplastic or hyperplastic lesions in the fimbriae of distal fallopian tube(s) in high risk patients who underwent preventative surgery [9]. These lesions, called Serous Tubal Intraepithalial Carcinomas (STICs), were found to coincide with ovarian serous carcinomas about 50-70% of cases [10–12]. These early data suggested that STICs may represent an early stage of HGSOC and that HGSOC potentially originates in the distal fallopian tubal epithelium (TE). STIC occurrence also potentially explains the extremely infrequent detection of HGSOC precursor lesions at the OSE [13].

The distal TE is composed of both ciliated and secretory cells, but only TE secretory cells are considered a putative HGSOC cell of origin. These secretory cells express well-characterized markers of HGSOC that have not been observed in the OSE [14]. PAX8, for instance, is an established secretory marker that is not expressed in the OSE, but is expressed in both the TE and HGSOC [15–17]. Monolayers of $PAX8^+$ cells can also express high levels of p53 called “p53 signatures” in which p53 is usually mutated. p53 signatures potentially correlate HGSOC initiation and TE lesions, as TP53 mutations are nearly ubiquitous in human HGSOC and are necessary core initiating mutations for ovarian tissue transformation (Chapter 2, Figure 6). These lesions are

considered an early phase of tubal epithelial disease due to a general lack of cellular atypia and low proliferative index [12,18] [19]. p53 signatures in secretory distal TE may therefore be a relatively benign initiating step in HGSOC development.

In HGSOC models, $PAX8^+$ cells in the distal TE have been shown to transform and produce HGSOC-like lesions following induction of oncogenic mutations. In one prominent genetically engineered mouse model (GEMM), PAX8 was demonstrated to be expressed specifically in the TE, not OSE, and to therefore drive tissue-specific expression of Cre recombinase. Cre-driven knockouts of *Trp53*, *Brca1* (or *Brca2*), and *Pten* in $Pax8^+$ TE cells can cause HGSOC-like tumors in mice [20,21]. These results are complemented by another model of TE transformation in which the SV40 large T-antigen is expressed using the Mullerian-specific *Ovgp-1* promoter, resulting in p53 signatures, STICs, and HGSOC-like tumors in the fallopian tube with metastasis to the ovary [22]. Mouse models of TE transformation therefore suggest that the TE is a putative HGSOC tissue of origin.

Several theories regarding the increased transformation propensity of the distal vs proximal TE potentially offer unifying characteristics between OSE and TE-derived HGSOC. One involves classic theories of HGSOC initiation following repeated cycles of ovulation and consequential ovarian surface repair [1,23,24]. Inflammatory factors and microenvironmental changes following follicular rupture are suspected to facilitate OSE transformation initiation and differentiation toward secretory phenotypes [1,13,25]. Authors have speculated that the TE may similarly experience follicular rupture-related inflammatory factors and microenvironmental changes that facilitate transformation due to the close proximity of the distal TE and OSE [13,26]. The OSE-TE juxtaposition would

also provide a route by which HGSOC precursor lesions can migrate toward the ovary following accumulation of further oncogenic characteristics in a process that may be dependent upon inflammation [26–28].

The ovarian stem cell theory of HGSOC initiation offers a second corollary between HGSOC induction in the OSE and TE. There has been longstanding suspicion that stem cells and transitional zones are particularly susceptible to oncogenesis [7,29–32]. Flesken-Nikitin and colleagues (2013) identified a slow cycling $ALDH^+$, $LEF1^+$ ovarian stem cell (OSE-SC) population in a transition zone in the ovarian hilum between the OSE, TE, and mesothelium. OSE-SC form more colonies in culture than $ALDH^-$ non-stem OSE (OSE-NS) and are especially prone to transformation following knockout of *Trp53* and *Rb1*. The distal fallopian tubal epithelium also contains a putative stem cell niche that may further explain its propensity for oncogenesis. Distal TE cells within the tubal-peritoneal junction share OSE-SC stem cell markers such as ALDH and LEF1. They also exhibit high degrees of Wnt signaling, experience inflammatory signaling, and possess greater colony formation capacity in culture than $ALDH^-$ cells from the proximal TE [33–35]. Although the relative contribution of TE-SC and TE-SC to HGSOC initiation has yet to be elucidated, markers of TE-SC like high LEF1 expression confer poorer five year patient survival, suggesting that stem cell characteristics may influence disease prognosis [34].

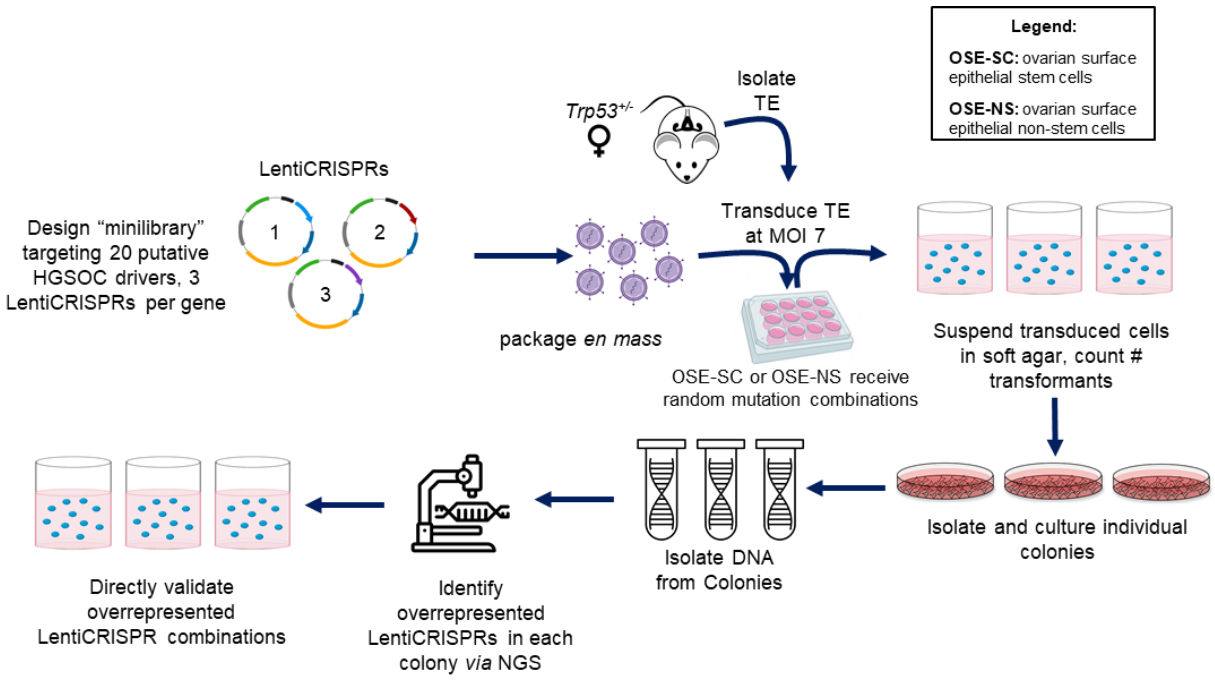

Figure 1. Strategy for identifying HGSOC tumor suppressor combinations. A total of 60 constructs were made in the vector LentiCRISPRv2, constituting the "minilibrary". TE cells were transduced with functionally-validated LentiCRISPRs and then plated in soft agar. Individual transformants/colonies were isolated and individually cultured. Genome-integrated LentiCRISPRs from each transformant were identified by sequencing, and overrepresented combinations later validated in directed soft agar transformation assays. TE, distal tubal epithelial cells; NGS, next-generation sequencing.

Although HGSOC-like tumors have been initiated at the distal TE using tissue-specific promoters, these studies have not assessed most genes identified by TCGA as commonly mutated or deleted in HGSOC [19]. Transcriptomic analyses of human HGSOC tumors have also suggested that initiation may have occurred in either the OSE or TE, but little information exists regarding whether the OSE and TE require the same mutations to undergo transformation [36,37]. To address these unknowns, I investigated which combinations of HGSOC-associated mutations are necessary to cause *in vitro* transformation of cultured distal mouse TE. The distal TE was chosen due to aforementioned evidence of transformation propensity, its putative stem cell subpopulation, and its propensity to form STICs in human patients.

Distal TE from Trp53$^{+/-}$ FVB/N mice (hereafter referred to as "TE") were cultured and transduced with a validated LentiCRISPRv2 minilibrary targeting 20 genes found to be significantly mutated or commonly deleted in human HGSOC tumors by TCGA [38] [19]. My goal was to identify and validate overrepresented combinations mutations associated with TE adhesion independent growth, a well-established hallmark of cellular oncogenic transformation (hereafter, colonies exhibiting adhesion independent growth will be termed "transformants") [39–44]. Another goal was to identify both shared and differing transformation drivers between OSE-SC (chapter 2), OSE-NS (chapter 2), and TE.

Efforts to perform screening of putative HGSOC driver genes on cultured TE were preempted by limitations in culturing and viral transduction-related methodology. I found that that TE are transduced with lentivirus less efficiently than are OSE, despite similar viral titer and cell quantity. Some transduced TE did exhibit adhesion

independent growth in soft agar. However, these colonies quickly senesced after their formation. LentiCRISPRs associated with TE adhesion independent growth were consequentially not identified. Different culturing methodology may therefore be necessary to assess drivers of TE transformation *in vitro*.

RESULTS

Trp53$^{+/-}$ TE cells inefficiently form colonies in soft agar following minilibrary transduction

Minilibrary functional titer calculations were originally completed via transduction of OSE with various concentrations of minilibrary virus (Chapter 2, Figure 1). LentiCRISPRv2 confers puromycin resistance, so the quantity of cells that can survive puromycin treatment following transduction with minilibrary virus correlates positively with the concentration of viral particles. Using this relationship, minilibrary virus was produced and concentrated to a functional titer of 7 for OSE (Chapter 2, Methods). *Trp53*$^{+/-}$ distal TE were transduced with the same concentration of minilibrary virus to concurrently target genes in the same manner. As detailed in Chapter 2, I adapted a strategy analogous to the one described by Zender and colleagues [45,46] to validate candidate tumor suppressors in a sensitized cell type. *Trp53*$^{+/-}$ distal TE were therefore utilized for all experiments described here.

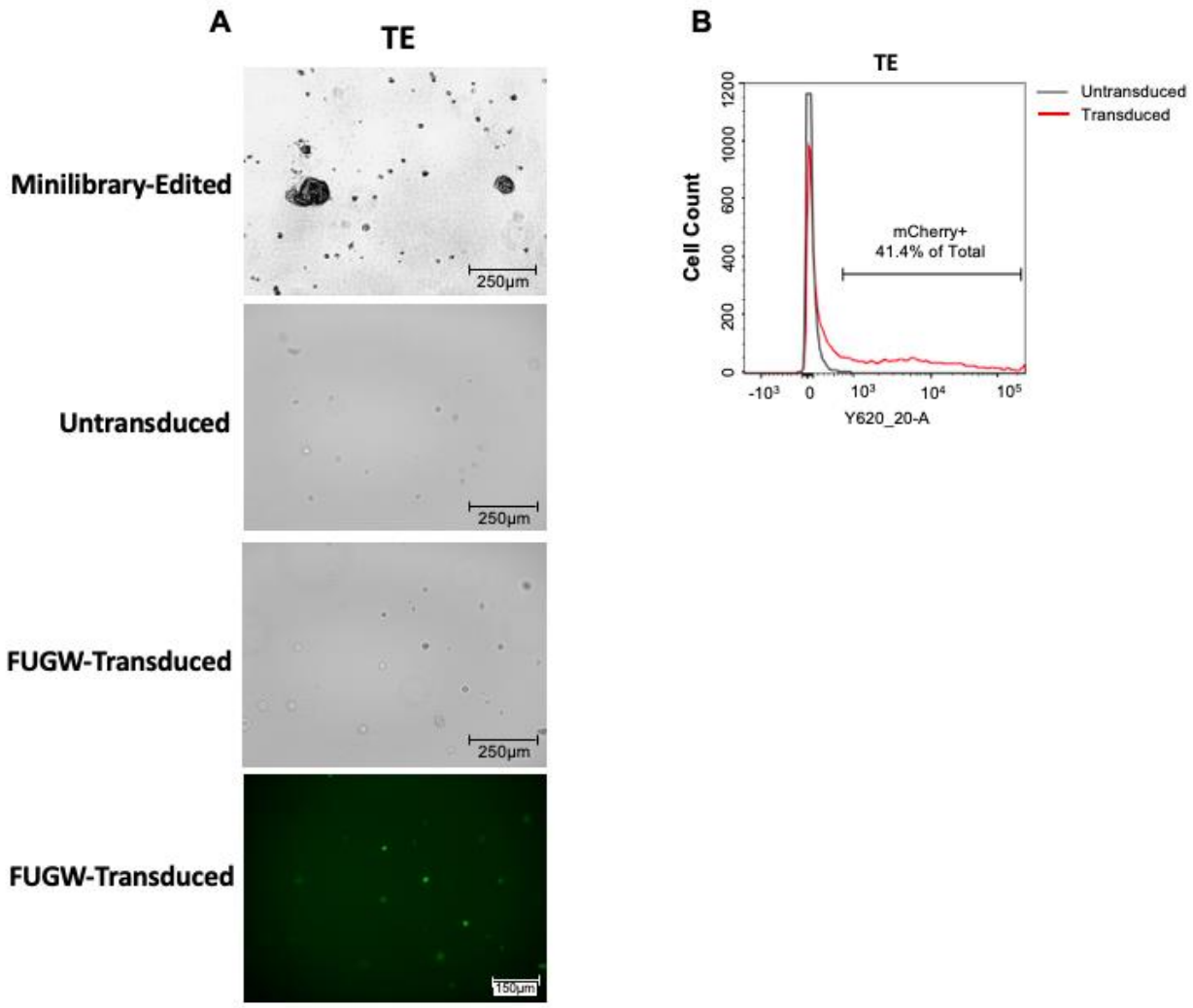

Figure 2. Minilibrary transduction, but not FUGW (GFP-expressing lentivirus) transduction, causes transformation of *Trp53*$^{+/-}$ TE. (A) The x axis indicates the cell type being tested (TE). The y axis indicates the treatment given to the corresponding cell type. Only minilibrary virus transduction resulted in colony growth for all groups. FUGW transduction resulted in GFP expression, but no adhesion independent growth. Cells also do not transform if untransduced. **(B)** FUGW-mCherry (mCherry-expressing lentivirus) transduction efficiency in TE. Flow cytometry was used to count mCherry^{+} cells following transduction with FUGW-mCherry lentivirus. Percentages indicate the

propotion of total cells that are mCherry^{+}. The dark grey lines represent cell counts of untransduced cells. The red line represents cell counts of FUGW-mCherry cells.

Following transduction with minilibrary lentivirus, TE were suspended in soft agar for assessment of colony growth. Though colonies were observed (figure 2A), TE exhibited infrequent adhesion independent growth. Of 2 million plated cells, only 24 colonies were observed and collected. None of the 24 plated colonies grew upon collection and transfer into a 2D culturing system. These results suggest that different culturing methodology may be required for stable long-term culture of mouse fallopian tubal epithelial cells.

Lentiviral transduction of cultured TE is inefficient relative to transduction of OSE

The infrequent rate of minilibrary-induced TE adhesion independent growth suggests that TE lentiviral transduction efficiency may differ from that of OSE. To assess relative viral transduction rates between TE and OSE, OSE-SC, OSE-NS, and TE were transduced with equal concentrations of FUGW-mCherry (mCherry-expressing) lentivirus. The quantity of $mCherry^+$ cells in each group following viral transduction was determined using flow cytometry. I found that most OSE-SC and OSE-NS expressed mCherry, and that mCherry expression rates were similar between the two cell types (72.9% and 85.6%, respectively) (Chapter 2, Figure 2). However, only 41.4% of TE expressed mCherry following lentiviral transduction, suggesting that viral transduction was much less efficient for TE than OSE (Figure 2B). Given a transduction rate of 41.4%, single infection percentage would also be exceptionally high, resulting primarily single gene mutations and few combinatorial mutations [47,48]. These results suggest that the relatively low rate of TE adhesion independent growth

may be in part due to inefficient lentiviral transduction rates. Induction of mutation combinations in TE may therefore require higher minilibrary virus titer.

DISCUSSION

In this dissertation, I've addressed fundamental unknowns regarding necessary HGSOC initiating mutations by implementing a LentiCRISPRv2 minilibrary-based screening approach to initiate random combinations of putative HGSOC driver mutations in cultured OSE (Chapter 2, Figure 6). However, work by others has suggested that HGSOC can initiate from both the OSE and distal TE [8,9,36,37,49,50], thereby necessitating screening of cancer drivers in both tissues. It's possible that divergent sets of mutations are critical for transformation of either tissue.

Minilibrary screening of putative HGSOC driver genes in OSE populations was an efficient process resulting in multiple LentiCRISPR construct integrations per cell (Chapter 2, Figure 3), transformation of both OSE-SC and OSE-NS (Chapter 2, Figures 2,3,5), and reproducible LentiCRISPR construct-specific effects on OSE-SC transformation (Chapter 2, Figure 4). Despite the success of minilibrary screening methodology in OSE, however, the methodology proved insufficient for functional screening of putative transformation drivers in TE. TE were treated with LentiCRISPRv2 minilibrary using the same methodology described in Chapter 2, but several potentially complicating factors related to TE culturing, population composition, and viral transduction efficiency may have negatively influenced TE screening efforts.

Following minilibrary transduction of TE, I observed that a few colonies formed, but all senesced shortly after growth in soft agar. One potential explanation for colony senescence is inadequacy of culturing methodologies to maintain TE in a state of growth and not senescence. I utilized a previously published culturing method that has been successfully implemented for brief TE culture (see Methods), but that has not been assessed for long term growth of TE [38]. Use of this culturing system, therefore, may have contributed to TE senescence. Implementation of organoid culture systems as an alternative *in vitro* approach may address issues related to long term TE culture. Recently published methods to culture both human and mouse TE utilizing organoid culture suggest that organoid-based methodology may facilitate longer term TE maintenance while also supporting inherent characteristics of distal fallopian tube structure and distinct cellular identities [35,51,52]. Although no LentiCRISPR-driven screens have been reported for TE organoids, organoid lentiviral transduction methodologies are common for other organoid tissue systems and may therefore be applicable to the screening of TE transformation-inducing mutations [53,54].

The presence of several TE cell subpopulations may have also complicated efforts to screen for transformation drivers, as was observed for OSE (Chapter 2, Figure 2). In minilibrary screening of OSE subpopulations, stem cell characteristics substantially influenced transformation frequency. OSE-SC transformed 41-fold more frequently than OSE-NS following transduction with minilibrary virus (MOI = 7). Regardless of the higher OSE-SC transformation rate, however, transformation was a rare event overall. Only 0.66% and 0.02% of OSE-SC and OSE-NS transformed, respectively. Because OSE-NS transformation was so rare, very few colonies were

collected overall and few conclusions were made regarding overrepresented LentiCRISPR driver combinations. It's possible that the low rate of TE transformation observed here is also a consequence of an overrepresented non-stem cell population. The bulk TE transduced with minilibrary virus greatly enriched for non-stem cells because stem cells only constitute a minority of the epithelia's population [33]. As an alternative approach, enrichment of TE stem cells using documented markers like ALDH or EPCAM [33,51] may result in increased transformation due to high propensity of many stem cell niches to transform.

Distal fallopian tubal epithelium also consists of both secretory and ciliated cells. However, only PAX8-expressing secretory TE are prone to transformation and are putative HGSOC cells of origin [15–17,20,21,36,55]. The distal TE isolated for minilibrary screening described here contained both secretory and ciliated populations because no methodology was implemented to preferentially culture distinct populations. The relative unlikelihood of ciliated cell transformation may have further decreased the efficiency of minilibrary screening, as a significant portion of the cultured TE population was unlikely to transform following minilibrary transduction. Therefore, the inherent heterogeneity of the TE, along with failure to enrich cultured TE for stem-like cells, may contribute to inefficient transformation following minilibrary-induced mutagenesis.

Technical issues related to TE viral transduction efficiency may have also preempted productive screening of necessary TE transformation driver genes. Upon transduction with FUGW-mCherry virus, only 41% of TE transduced FUGW-mCherry were mCherry^{+}. In comparison, most OSE-SC and OSE-NS receiving equal quantities of FUGW-mCherry virus exhibited mCherry expression (Chapter 2, Figure 2). This

discrepancy suggests that LentiCRISPR transduction efficiencies differ in distinct cell types and that future optimization of LentiCRISPR titer may be necessary to achieve multiple infections per TE cell.

Substantial evidence that the TE is a putative HGSOC cell of origin necessitates future functional screening of mutations necessary for TE transformation. Although screening of putative TE transformation driver genes was not successful, this preliminary approach provides insights into factors necessary for *in vitro* TE culture, efficient viral transduction, and TE subpopulations potentially susceptible to transformation. Future attempts to model HGSOC development will require elucidation of mutations necessary to transform all potential HGSOC cells of origin and identification of differences between the transformation initiation requirements these different populations.

METHODS

For descriptions of minilibrary construction methodology, OSE culture, creation of a $Trp53^{+/-}$ FVB/N mouse line, viral packaging methodology, soft agar assay approach, flow cytometry and details regarding brightfield microscopy, see the methods section in Chapter 2.

TE isolation and culture

TE were isolated and maintained in culture following methodology described by Nikitin and colleagues (2016) [38]. Mouse tubal epithelium growth medium contains HAM's DMEM F12 (Thermo Fisher; Cat#: 31765035), 2mM L-Glutamine (Thermo Fisher; Cat#: 21051024), 1mM sodium pyruvate (Thermo Fisher; Cat#: 11360070), 10ng/mL epidermal growth factor (Millipore Sigma; Cat#: E9644-.2MG), 10ng/mL basic fibroblast growth factor-2 (Millipore Sigma; Cat#: SRP4038), 500ng/mL hydrocortisone (Millipore Sigma; Cat#: H0888-1G), 5 ug/mL insulin (Sigma Aldrich; Cat#: 11074547001), 5ug/mL transferrin (Sigma Aldrich; Cat#: 11074547001), 5ug/mL sodium selenite (Sigma Aldrich; Cat#: 11074547001), 0.10% bovine albumin (Millipore Sigma; Cat#: A9418), 100ug/mL penicillin/streptomycin (Thermo Fisher; Cat#: 15070063), 0.1mM minimal essential medium eagle non-essential amino acids (Millipore Sigma; Cat#: M5650), and 10^{-4} beta-mercaptoethanol (Fisher Scientific; Cat#: 21985023). 5% FBS (Sigma Aldrich; Cat#: F2442) was also used in some cultures to assess changes to TE growth.

REFERENCES

1. Godwin, A. K. *et al.* Spontaneous transformation of rat ovarian surface epithelial cells: association with cytogenetic changes and implications of repeated ovulation in the etiology of ovarian cancer. *J. Natl. Cancer Inst.* **84,** 592–601 (1992).
2. Testa, J. R. *et al.* Spontaneous transformation of rat ovarian surface epithelial cells results in well to poorly differentiated tumors with a parallel range of cytogenetic complexity. *Cancer Res.* **54,** 2778–2784 (1994).
3. Orsulic, S. *et al.* Induction of ovarian cancer by defined multiple genetic changes in a mouse model system. *Cancer Cell* **1,** 53–62 (2002).
4. Auersperg, N., Woo, M. M. M. & Gilks, C. B. The origin of ovarian carcinomas: A developmental view. *Gynecol. Oncol.* **110,** 452–454 (2008).
5. Scully, R. E. *Tumors Of The Ovary, Maldeveloped Gonads, Fallopian Tube, And Broad Ligament*. (Armed Forces Institute Of Pathology Available From The American Registry Of Pathology, Armed Forces Institute Of Pathology, 1999).
6. Flesken-Nikitin, A., Choi, K.-C., Eng, J. P., Shmidt, E. N. & Nikitin, A. Y. Induction of carcinogenesis by concurrent inactivation of p53 and Rb1 in the mouse ovarian surface epithelium. *Cancer Res.* **63,** 3459–3463 (2003).
7. Flesken-Nikitin, A. *et al.* Ovarian surface epithelium at the junction area contains a cancer-prone stem cell niche. *Nature* **495,** 241–245 (2013).
8. Kim, J. *et al.* Cell Origins of High-Grade Serous Ovarian Cancer. *Cancers (Basel)* **10,** (2018).
9. Piek, J. M. *et al.* Dysplastic changes in prophylactically removed Fallopian tubes of women predisposed to developing ovarian cancer. *J. Pathol.* **195,** 451–456 (2001).
10. Kindelberger, D. W. *et al.* Intraepithelial carcinoma of the fimbria and pelvic serous carcinoma: Evidence for a causal relationship. *Am. J. Surg. Pathol.* **31,** 161–169 (2007).
11. Bowtell, D. D. L. The genesis and evolution of high-grade serous ovarian cancer. *Nat. Rev. Cancer* **10,** 803–808 (2010).
12. Lee, Y. *et al.* A candidate precursor to serous carcinoma that originates in the distal fallopian tube. *J. Pathol.* **211,** 26–35 (2007).
13. Auersperg, N. Ovarian surface epithelium as a source of ovarian cancers: unwarranted speculation or evidence-based hypothesis? *Gynecol. Oncol.* **130,** 246–251 (2013).
14. Perets, R. & Drapkin, R. It's totally tubular....riding the new wave of ovarian cancer research. *Cancer Res.* **76,** 10–17 (2016).

15. Adler, E., Mhawech-Fauceglia, P., Gayther, S. A. & Lawrenson, K. PAX8 expression in ovarian surface epithelial cells. *Hum. Pathol.* **46,** 948–956 (2015).

16. Tacha, D., Zhou, D. & Cheng, L. Expression of PAX8 in normal and neoplastic tissues: a comprehensive immunohistochemical study. *Appl Immunohistochem Mol Morphol* **19,** 293–299 (2011).

17. Ozcan, A., Liles, N., Coffey, D., Shen, S. S. & Truong, L. D. PAX2 and PAX8 expression in primary and metastatic müllerian epithelial tumors: a comprehensive comparison. *Am. J. Surg. Pathol.* **35,** 1837–1847 (2011).

18. Leonhardt, K., Einenkel, J., Sohr, S., Engeland, K. & Horn, L.-C. p53 signature and serous tubal in-situ carcinoma in cases of primary tubal and peritoneal carcinomas and serous borderline tumors of the ovary. *Int J Gynecol Pathol* **30,** 417–424 (2011).

19. Cancer Genome Atlas Research Network. Integrated genomic analyses of ovarian carcinoma. *Nature* **474,** 609–615 (2011).

20. Perets, R. *et al.* Transformation of the fallopian tube secretory epithelium leads to high-grade serous ovarian cancer in Brca;Tp53;Pten models. *Cancer Cell* **24,** 751–765 (2013).

21. Maniati, E. *et al.* Mouse ovarian cancer models recapitulate the human tumor microenvironment and patient response to treatment. *Cell Rep.* **30,** 525–540.e7 (2020).

22. Sherman-Baust, C. A. *et al.* A genetically engineered ovarian cancer mouse model based on fallopian tube transformation mimics human high-grade serous carcinoma development. *J. Pathol.* **233,** 228–237 (2014).

23. Murdoch, W. J. & Martinchick, J. F. Oxidative damage to DNA of ovarian surface epithelial cells affected by ovulation: carcinogenic implication and chemoprevention. *Exp. Biol. Med.* **229,** 546–552 (2004).

24. Katabuchi, H. & Okamura, H. Cell biology of human ovarian surface epithelial cells and ovarian carcinogenesis. *Med. Electron Microsc.* **36,** 74–86 (2003).

25. Auersperg, N., Wong, A. S., Choi, K. C., Kang, S. K. & Leung, P. C. Ovarian surface epithelium: biology, endocrinology, and pathology. *Endocr. Rev.* **22,** 255–288 (2001).

26. Seidman, J. D., Ronnett, B. M., Shih, I.-M., Cho, K. R. & Kurman, R. J. in *Blaustein's pathology of the female genital tract* (eds. Kurman, R. J., Hedrick Ellenson, L. & Ronnett, B. M.) 841–966 (Springer International Publishing, 2019). doi:10.1007/978-3-319-46334-6_14

27. Seidman, J. D., Cho, K. R., Ronnett, B. M. & Kurman, R. J. in *Blaustein's pathology of the female genital tract* (eds. Kurman, R. J., Ellenson, L. H. & Ronnett, B. M.)

679–784 (Springer US, 2011). doi:10.1007/978-1-4419-0489-8_14

28. Jia, D., Nagaoka, Y., Katsumata, M. & Orsulic, S. Inflammation is a key contributor to ovarian cancer cell seeding. *Sci. Rep.* **8,** 12394 (2018).

29. Greene, D. R., Wheeler, T. M., Egawa, S., Dunn, J. K. & Scardino, P. T. A comparison of the morphological features of cancer arising in the transition zone and in the peripheral zone of the prostate. *J. Urol.* **146,** 1069–1076 (1991).

30. Ferraro, F., Celso, C. L. & Scadden, D. Adult stem cels and their niches. *Adv. Exp. Med. Biol.* **695,** 155–168 (2010).

31. Mcnairn, A. J. & Guasch, G. Epithelial transition zones: merging microenvironments, niches, and cellular transformation. *Eur J Dermatol* **21 Suppl 2,** 21–28 (2011).

32. Flesken-Nikitin, A., Odai-Afotey, A. A. & Nikitin, A. Y. Role of the stem cell niche in the pathogenesis of epithelial ovarian cancers. *Molecular & Cellular Oncology* **1,** e963435 (2014).

33. Rose, I. *et al.* WNT and inflammatory signaling distinguish human Fallopian tube epithelial cell populations. *BioRxiv* (2020). doi:10.1101/2020.01.15.908293

34. Schmoeckel, E. *et al.* LEF1 is preferentially expressed in the tubal-peritoneal junctions and is a reliable marker of tubal intraepithelial lesions. *Mod. Pathol.* **30,** 1241–1250 (2017).

35. Paik, D. Y. *et al.* Stem-like epithelial cells are concentrated in the distal end of the fallopian tube: a site for injury and serous cancer initiation. *Stem Cells* **30,** 2487–2497 (2012).

36. Lawrenson, K. *et al.* A Study of High-Grade Serous Ovarian Cancer Origins Implicates the SOX18 Transcription Factor in Tumor Development. *Cell Rep.* **29,** 3726–3735.e4 (2019).

37. Hao, D. *et al.* Integrated Analysis Reveals Tubal- and Ovarian-Originated Serous Ovarian Cancer and Predicts Differential Therapeutic Responses. *Clin. Cancer Res.* **23,** 7400–7411 (2017).

38. Flesken-Nikitin, A., Harlan, B. A. & Nikitin, A. Y. Transplantation into the mouse ovarian fat pad. *J. Vis. Exp.* (2016). doi:10.3791/54444

39. Horibata, S., Vo, T. V., Subramanian, V., Thompson, P. R. & Coonrod, S. A. Utilization of the soft agar colony formation assay to identify inhibitors of tumorigenicity in breast cancer cells. *J. Vis. Exp.* e52727 (2015). doi:10.3791/52727

40. Borowicz, S. *et al.* The soft agar colony formation assay. *J. Vis. Exp.* e51998 (2014). doi:10.3791/51998

41. Puck, T. T., Marcus, P. I. & Cieciura, S. J. Clonal growth of mammalian cells in

vitro; growth characteristics of colonies from single HeLa cells with and without a feeder layer. *J. Exp. Med.* **103,** 273–283 (1956).

42. Roberts, A. B. *et al.* Type beta transforming growth factor: a bifunctional regulator of cellular growth. *Proc. Natl. Acad. Sci. USA* **82,** 119–123 (1985).

43. de Larco, J. E. & Todaro, G. J. Growth factors from murine sarcoma virus-transformed cells. *Proc. Natl. Acad. Sci. USA* **75,** 4001–4005 (1978).

44. Hamburger, A. W. & Salmon, S. E. Primary bioassay of human tumor stem cells. *Science* **197,** 461–463 (1977).

45. Zender, L. *et al.* Identification and validation of oncogenes in liver cancer using an integrative oncogenomic approach. *Cell* **125,** 1253–1267 (2006).

46. Zender, L. *et al.* Cancer gene discovery in hepatocellular carcinoma. *J. Hepatol.* **52,** 921–929 (2010).

47. Sanjana, N. E., Shalem, O. & Zhang, F. Improved vectors and genome-wide libraries for CRISPR screening. *Nat. Methods* **11,** 783–784 (2014).

48. Shalem, O. *et al.* Genome-scale CRISPR-Cas9 knockout screening in human cells. *Science* **343,** 84–87 (2014).

49. Harlan, B. A. & Nikitin, A. Y. A quest for better mouse models of breast and ovarian cancers. *EBioMedicine* **2,** 1268–1269 (2015).

50. Zhang, S. *et al.* Both fallopian tube and ovarian surface epithelium are cells-of-origin for high-grade serous ovarian carcinoma. *Nat. Commun.* **10,** 5367 (2019).

51. Xie, Y., Park, E.-S., Xiang, D. & Li, Z. Long-term organoid culture reveals enrichment of organoid-forming epithelial cells in the fimbrial portion of mouse fallopian tube. *Stem Cell Res.* **32,** 51–60 (2018).

52. Kessler, M. *et al.* The Notch and Wnt pathways regulate stemness and differentiation in human fallopian tube organoids. *Nat. Commun.* **6,** 8989 (2015).

53. Maru, Y., Orihashi, K. & Hippo, Y. Lentivirus-Based Stable Gene Delivery into Intestinal Organoids. *Methods Mol. Biol.* **1422,** 13–21 (2016).

54. Van Lidth de Jeude, J. F., Vermeulen, J. L. M., Montenegro-Miranda, P. S., Van den Brink, G. R. & Heijmans, J. A protocol for lentiviral transduction and downstream analysis of intestinal organoids. *J. Vis. Exp.* (2015). doi:10.3791/52531

55. Neel, B. G. *et al.* Both Fallopian Tube and Ovarian Surface Epithelium Can Act as Cell-of-Origin for High Grade Serous Ovarian Carcinoma. *BioRxiv* (2018). doi:10.1101/481200

Appendix 2: *In Vivo* Characterization of OSE Transformant Tumorigenesis

This appendix documents preliminary *in vivo* tumorigenesis experiments. OSE-SC transformants containing different LentiCRISPRv2 combinations were intraperitoneally injected into mice, and tumor formation frequency was documented. These results have not been submitted for publication and are intended to explore methodological alternatives or additions to the *in vitro* approaches detailed in Chapter 2 and Appendix 1.

INTRODUCITON

Each chapter of this thesis concerns *in vitro* characterization of mutations necessary for cellular transformation using a LentiCRISPRv2-based minilibrary screen. Screening revealed putative minimal “core mutations” necessary for transformation of OSE-SC and suggested that OSE-SC transform more readily than OSE-NS (Chapter 2, Figure 2). It also revealed novel mutations combinations associated with increased OSE-SC transformation and colony growth (Chapter 2, Figures 3,4). However, 3’ RNA sequencing results suggested that few transcriptional similarities existed between OSE-SC transformants, human HGSOC, or other ovarian cancer subtypes (See Chapter 3). Lack of transcriptomic similarity with human HGSOC was not unique to transformants with a specific set of genome-integrated LentiCRISPRs and was rather a universal characteristic of all transformants. Transcriptomic analyses also revealed that transformants with identical genome-integrated LentiCRISPRs transcriptomically diverged from one another (Chapter 3, Figure 2). These results cumulatively imply that factors other than LentiCRISPR-induced mutations, like cell culturing conditions, dictate the transcriptomic identity of transformants.

Prominent recent analyses seeking to compare transcriptomic and genomic characteristics between human HGSOC and mouse models differ from the methodology described Chapters 2 and 3 due to implementation of *in vivo* tumor growth and development [1–4]. The success of these approaches are consistent with observed phenotypic divergence between cultured cells and *in vivo* tissues [5–10], suggesting that *in vivo* approaches most precisely recapitulate human disease characteristics. Given the advantages of *in vivo* tumor development for translational applications, future efforts to

characterize novel HGSOC transformation-initiating mutations likely require *in vivo* methodologies.

I performed intraperitoneal injections of OSE-SC transformants (generated in Chapter 2) to investigate the effect of LentiCRISPR-induced mutations on *in vivo* tumorigenesis and assess validity of *in vitro* growth assay results. Results demonstrate that some *in vitro* transformation and growth characteristics correlate with *in vivo* tumorigenesis rates. For instance, Trp53 and Rb1 were minimal requirements for tumorigenesis, and the addition of Cdkn2a mutations was associated with more efficient tumor formation. However, some differences between *in vivo* and *in vitro* results were observed and are reported here. Together, these preliminary *in vivo* data suggest viability of *in vivo* tumorigenesis assays of OSE-SC cells with LentiCRISPR-induced mutation and have implications for future modeling of HGSOC initiation.

RESULTS

I hypothesized that differential *in vitro* growth characteristics conveyed by specific LentiCRISPR combinations (Chapter 2, Figures 3,4) correlate with similar growth characteristics of the same transformants *in vivo*. To address this hypothesis, I intraperitoneally injected mouse OSE-SC transformants containing differing sets of genome-integrated LentiCRISPRs into congenic FVB/N mice. All injected OSE-SC cells transformed previously (see Chapter 2) *in vitro* and were briefly expanded in culture prior to IP injection.

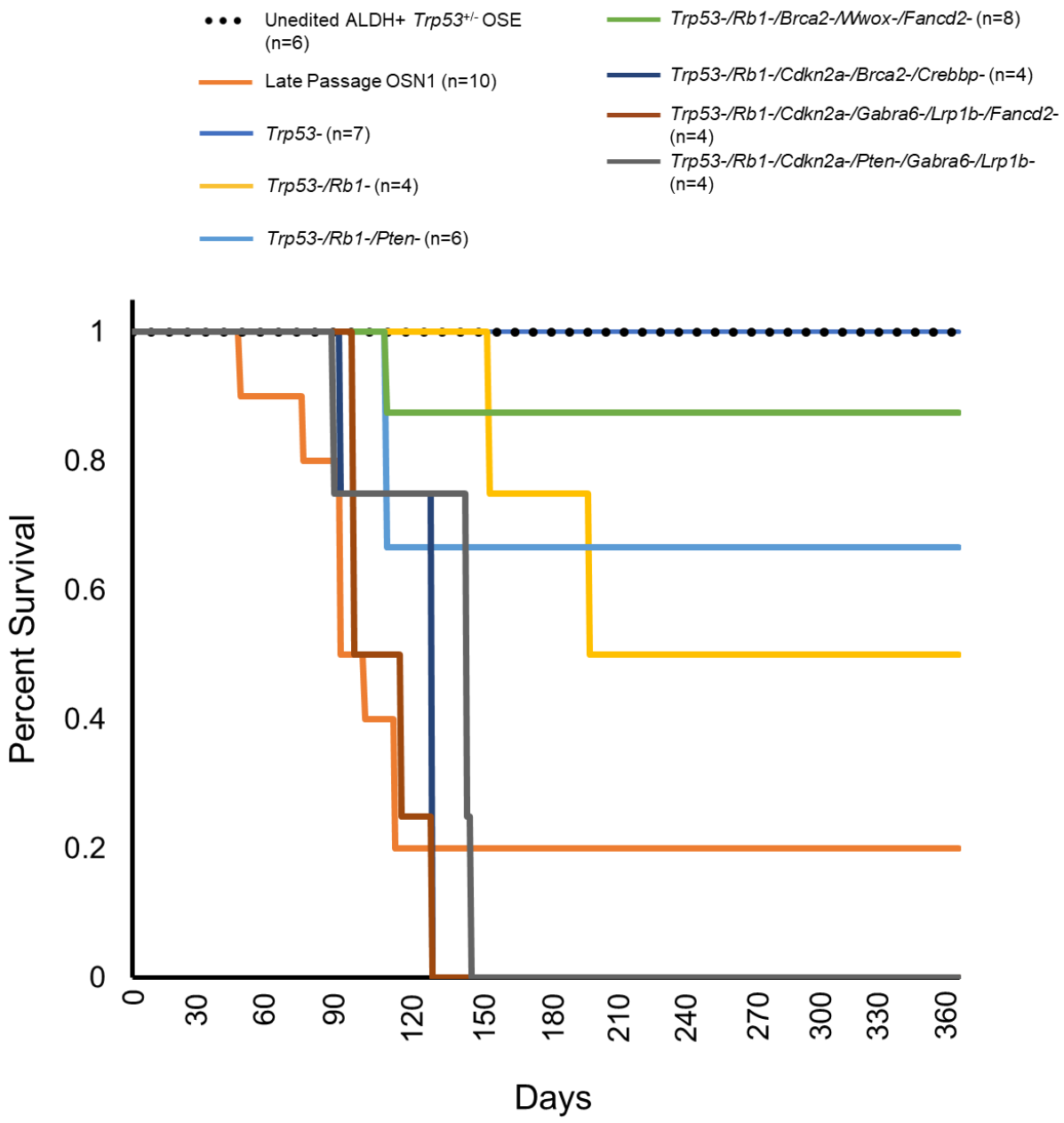

Figure 1. Combined LentiCRISPR targeting of *Trp53*, *Rb1*, and *Cdkn2a* is associated with rapid tumorigenesis. A Kaplan-Meier curve was constructed for mouse survival following intraperitoneal injection of OSE-SC transformants. Mice were sacrificed immediately following detection of tumors via physical palpation.

Trp53 and *Rb1* mutations are minimal requirements to cause tumorigenesis *in vivo*

In agreement with a previous *in vitro* growth assays (Chapter 2, Figure 4), no tumors were observed in 7 mice injected with *Trp53*- OSE-SC transformants (Hereafter OSE-SC transformants will be simply referred to as transformants) (Figure 1). These results support previous reports that *Trp53* knockouts alone cause infrequent transformation of mouse OSE [11]. The addition of LentiCRISPRs targeting *Rb1* alone, or both *Rb1* and *Pten*, to *Trp53* resulted in tumor formation, albeit infrequently (Figure 1). Of the four mice injected with *Trp53*-/*Rb1*- transformants, two formed small tumors (Figure 1). Two of the six mice injected with *Trp53*-/*Rb1*-/*Pten*- transformants also formed small tumors (Figure 1), suggesting that *Pten* mutations did not enhance tumorigenesis of *Trp53*-/*Rb1*- cells.

As a positive tumorigenesis control, late passage OSN1 ovarian epithelial cells from congenic mice were also IP injected. Late passage OSN1 share null mutations in *Trp53* and *Rb1* with *Trp53*-/*Rb1*- OSE-SC transformants, but have likely accumulated mutations over many passages [11]. Most mice (8 of 10) that received OSN1 injections presented with larger tumors that were over 8mm in diameter (Figure 1). This result potentially reflects differences between recent transformants and late passage cells. Injection of *Trp53*$^{+/-}$ ALDH+ OSE-SC (untransformed) was completed as a negative control and resulted in no tumors (n = 6).

Transformants with LentiCRISPRs targeting *Trp53*, *Rb1* and *Cdkn2a* frequently form tumors *in vivo*

To assess the effect of additional LentiCRISPR-induced mutations on tumorigenicity, I injected mice with transformants containing LentiCRISPRs targeting combinations of *Brca2, Crebbp, Wwox, Fancd2, Gabra6, Lrp1b*, and *Pten* in addition to *Trp53* and *Rb1*. Surprisingly, the addition of *Brca2*, *Wwox*, and *Fancd2* to *Trp53* and *Rb1* (*Trp53*-/*Rb1*-/*Brca2*-/*Wwox*-/*Fancd2*-) resulted in low tumorigenicity, with only a single mouse (n = 8) presenting with a tumor (Figure 1). Disruption of *Cdkn2a* in combination with *Trp53* and *Rb1*, however, yielded much higher degrees of tumor growth. All (4/4) mice injected with *Trp53*-/*Rb1*-/*Cdkn2a*-/*Brca2*-/*Crebbp*- OSE-SC transformants formed large tumors (Figure 1). Similar results were observed for transformants lacking *Brca2* LentiCRISPRs but containing *Cdkn2a* LentiCRISPRs. Efficient tumorigenesis was observed for *Trp53*-/*Rb1*-/*Cdkn2a*-/*Gabra6*-/*Lrp1b*-/*Fancd2*- and *Trp53*-/*Rb1*-/*Cdkn2a*-/*Pten*-/*Gabra6*-/*Lrp1b*- OSE-SC, as all (n=4) injected mice formed large tumors (Figure 1). These results cumulatively suggest that *Trp53*, *Rb1* and *Cdkn2a* function synergistically to promote *in vivo* tumorigenesis in mice.

DISCUSSION

Trp53 and Rb1 disruption are minimal requirements for *in vivo* OSE-SC tumorigenesis

Tumor incidence following IP injection of transformants largely supported the hypothesis that LentiCRISPR combinations associated with increased *in vitro* transformation would cause greater rates of tumorigenesis *in vivo*. For instance, *in vitro* targeted mutagenesis assays suggested that *Trp53* mutations alone cause inefficient colony formation (Chapter 2, Figure 4A). Correlatively, none of the mice (n = 7) injected

with *Trp53*- transformants formed tumors. *In vitro* assays also suggested that combined disruption of *Trp53*, *Rb1*, and/or *Pten* are minimal ("core") requirements for significant rates of *in vitro* OSE-SC transformation (Chapter 2, Figure 4), and that the addition of specific mutations can significantly increase transformation rates beyond those observed for *Trp53*-/*Rb1*- OSE-SC (Chapter 2, Figure 4B). These data were supported by occasional tumorigenesis of mice injected with *Trp53*-/*Rb1*- or *Trp53*-/*Rb1*-/*Pten*- transformants (Figure 1), and near ubiquitous tumorigenesis in transformants with specific sets of additional mutations (Figure 1).

Like *Trp53*-/*Rb1*- OSE-SC transformants, late passage OSN1 cells also have *Trp53* and *Rb1* null mutations but differ due to accumulation of unknown additional mutations over many passages. They were chosen as a positive tumorigenesis control due to previously published reports from Nikitin and colleagues demonstrating that consistent carcinogenicity of OSN1 cells occurs *in vivo* [12,13]. IP injection of late passage OSN1 cells caused tumorigenesis *in vivo* much more frequently than either *Trp53*-/*Rb1*- or *Trp53*-/*Rb1*-/*Pten*- transformants, suggesting additional gene disruptions increase tumorigenesis rates of *Trp53*-/*Rb1*- OSE (Figure 1).

<u>*Brca2* and/or *Fancd2* disruption neither promote nor inhibit OSE-SC transformant tumorigenesis</u>

Infrequent tumor growth observed following injection of *Trp53*-/*Rb1*-/*Brca2*-/*Wwox*-/*Fancd2*- OSE-SC may, at first glance, suggest that *Brca2*, *Wwox*, and/or *Fancd2* negatively influence tumorigenic properties of injected cells (Figure 1). These

potential growth-inhibitory effects due to disruption of either gene have been previously assessed in this thesis (Chapter 2 Figure 4C) and in other previously published reports [14–19]. However, combined *Brca2* and *Fancd2* mutagenesis in *Trp53*-/*Rb1*- OSE-SC actually increased *in vitro* transformation compared to *Trp53*-/*Rb1*- OSE-SC, suggesting that *Brca2* and *Fancd2* co-mutagenesis may not inhibit OSE-SC growth (Chapter 2, Figure 4C).

Despite previously published reports of growth inhibition following *Brca2* and *Fancd2* mutagenesis, neither gene appeared to cause *in vivo* growth inhibition among IP injected transformants containing a *Brca2* or *Fancd2* genome-integrated lentiCRISPR. *Fancd2* was targeted in the absence of *Brca2* in both *Trp53*-/*Rb1*-/*Cdkn2a*-/*Gabra6*-/*Lrp1b*-/*Fancd2*- and *Trp53*-/*Rb1*-/*Cdkn2a*-/*Pten*-/*Gabra6*-/*Lrp1b*-/*Fancd2*- OSE-SC, yet efficient tumorigenesis was observed in both cases (Figure 1). Similarly, a transformant with a *Brca2*-targeting LentiCRISPRs and no *Fancd2*-targeting LentiCRISPR (*Trp53*-/*Rb1*-/*Cdkn2a*-/*Brca2*-/*Crebbp*-) had a 100% tumor formation rate following injection (n=4) (Figure 1). Together, *in vivo* tumorigenesis results demonstrate that *Brca2* and *Fancd2* LentiCRISPRs neither promote nor inhibit OSE-SC transformant tumorigenesis. *Brca2* and *Fancd2* therefore function as passenger mutations in the *in vivo* scenarios assessed here.

<u>*Trp53*, *Rb1*, and *Cdkn2a*, but not *Pten, Lrp1b*, *Wwox*, *Crebbp*, or *Gabra6*, are associated with frequent tumorigenesis</u>

IP injection results suggest that *Lrp1b*, *Wwox*, *Crebbp*, and *Gabra6* may not strongly influence tumorigenesis in the groups tested here, since tumorigenesis occurred efficiently with or without mutations in these genes (Figure 1). Because disruption of *Lrp1b*, *Wwox*, *Crebbp*, *Gabra6, Brca2,* and *Fancd2* could not explain differential *in vivo* tumorigenesis rates, some combination of the remaining disrupted genes, namely *Trp53*, *Rb1*, *Pten*, and *Cdkn2a*, must influence tumorigenesis efficiency. Although *Pten* was found to increase *in vitro* transformation when disrupted alongside *Trp53* and *Rb1* (Chapter 2, Figure 4A,B), *Trp53*-/*Rb1*-/*Pten*- IP injected transformants did not cause more tumorigenesis than *Trp53*-/*Rb1*- transformants (Figure 1). *Pten* mutations in IP-injected cell lines therefore could not explain divergent tumorigenesis rates between transformant types. *Cdkn2a* mutagenesis, however, occurred in all IP injected transformants that formed tumors in most cases, suggesting that *Cdkn2a* mutations may convey an aggressive *in vivo* growth phenotype alongside mutations *Trp53* and *Rb1* (Figure 1). These additive effects of *Trp53*, *Rb1* and *Cdkn2a* mutagenesis were apparent *in vivo* via high tumorigenesis resulting from *Trp53*-/*Rb1*-/*Cdkn2a*-/*Gabra6*-/*Lrp1b*-/*Fancd2*- and *Trp53*-/*Rb1*-/*Cdkn2a*-/*Pten*-/*Gabra6*-/*Lrp1b*-/*Fancd2*- transformant IP injections (Figure 1).

Putative *in vivo* growth phenotypes resulting from *Cdkn2a* mutagenesis are supported by *in vitro* transformation assay data. Combined disruption of *Trp53*, *Rb1*, *Pten* and *Cdkn2a* during *in vitro* transformation assays resulted in significantly greater colony formation than *Trp53*-, *Trp53*-/*Rb1*-, *Trp53*-/*Cdkn2a*-, or *Trp53*-/*Rb1*-/*Pten*- OSE-SC (Chapter 2, Figure 4A). *Cdkn2a* is a known regulator of both *Trp53* and *Rb1*, so it's possible that its mutagenesis further disrupts the tumor suppressor functionality of both

Trp53 and *Rb1*. It's also conceivable that some LentiCRISPR-induced mutations in *Trp53* and/or *Rb1* are silent mutations, so co-mutagenesis of *Cdkn2a* compensates for non-loss of function mutations [20–22].

Regardless of the mechanism, the high degrees of transformation observed in cells with *Trp53*, *Rb1* and *Cdkn2a* LentiCRISPRs suggest nonredundant, additive roles for each mutation in *Trp53*-/*Rb1*/-*Cdkn2a*- OSE-SC. These observations are also supported by patient survival data compiled by TCGA. Patients with mutations in *CDKN2A* experienced much shorter survival and progression-free survival rates compared to individuals with no alterations in *CDKN2A* [23–25].

Significance and conclusions

In vitro screening of putative transformation-initiating mutations in OSE-SC is a rapid means of generating large sample size and identifying statistically overrepresented transformation-associated mutations. However, clear differences between *in vivo* and *in vitro* growth conditions suggested that *in vivo* assessment of putative initiating mutations may be required following *in vitro* screening. The intraperitoneal injection methodology described here offers a technically simplistic means of validating screening "hits". However, further characterization of transformant-derived tumors using methods like RNA sequencing, histology, and immunohistochemistry may be required for proper comparison to human HGSOC.

METHODS

For descriptions of minilibrary construction methodology, OSE culture, creation of a Trp53+/- FVB/N mouse line, viral packaging methodology, soft agar assay approach, flow cytometry and details regarding brightfield microscopy, see the methods section in Chapter 2.

Intraperitoneal injection of OSE-SC transformants into FVB/NJ Mice

Ten million cells were intraperitoneally injected into FVB/NJ mice for each transformant type. Cells were expanded in culture following colony growth in soft agar. Prior to injection, ten million cells were counted using a hemocytometer, washed three times in PBS, and then resuspended in 1mL PBS. Cells were temporarily stored on ice prior to injection into mice and were injected into FVB/NJ mice using a 26ga needle and 3mL syringe.

Cultured *Trp53*$^{+/-}$ ALDH+ OSE from FVB/NJ mice (passage 3 or 4) and PBS (with no cells) were used as negative tumorigenesis controls. Late passage OSN1 cells were a gift from Alexander Nikitin and were used as a positive control for tumorigenesis.

Mouse Care and Monitoring for Tumorigenesis

Ten-week-old FVB/N female mice were intraperitoneally injected with controls or transformants and were housed for up to one year. All mice were checked daily for tumors using physical palpation. Euthanasia using CO_2 was employed at the first sign

of tumors, if mice appeared distressed or unhealthy, or after one year. All mice were dissected immediately following euthanasia, and all tumors were collected. Samples from each tumor were frozen for potential RNA or DNA isolation. Samples were also placed in paraformaldehyde.

REFERENCES

1. Maniati, E. *et al.* Mouse ovarian cancer models recapitulate the human tumor microenvironment and patient response to treatment. *Cell Rep.* **30,** 525–540.e7 (2020).
2. Perets, R. *et al.* Transformation of the fallopian tube secretory epithelium leads to high-grade serous ovarian cancer in Brca;Tp53;Pten models. *Cancer Cell* **24,** 751–765 (2013).
3. Sherman-Baust, C. A. *et al.* A genetically engineered ovarian cancer mouse model based on fallopian tube transformation mimics human high-grade serous carcinoma development. *J. Pathol.* **233,** 228–237 (2014).
4. Kim, J. *et al.* Cell Origins of High-Grade Serous Ovarian Cancer. *Cancers (Basel)* **10,** (2018).
5. Kim, T. *et al.* In situ transcriptome characteristics are lost following culture adaptation of adult cardiac stem cells. *Sci. Rep.* **8,** 12060 (2018).
6. Lopes-Ramos, C. M. *et al.* Regulatory network changes between cell lines and their tissues of origin. *BMC Genomics* **18,** 723 (2017).
7. Fasterius, E. & Al-Khalili Szigyarto, C. Analysis of public RNA-sequencing data reveals biological consequences of genetic heterogeneity in cell line populations. *Sci. Rep.* **8,** 11226 (2018).
8. Kapałczyńska, M. *et al.* 2D and 3D cell cultures - a comparison of different types of cancer cell cultures. *Arch. Med. Sci.* **14,** 910–919 (2018).
9. Kasai, F., Hirayama, N., Ozawa, M., Iemura, M. & Kohara, A. Changes of heterogeneous cell populations in the Ishikawa cell line during long-term culture: Proposal for an in vitro clonal evolution model of tumor cells. *Genomics* **107,** 259–266 (2016).
10. Jacobs, K. *et al.* Higher-Density Culture in Human Embryonic Stem Cells Results in DNA Damage and Genome Instability. *Stem Cell Rep.* **6,** 330–341 (2016).
11. Flesken-Nikitin, A., Choi, K.-C., Eng, J. P., Shmidt, E. N. & Nikitin, A. Y. Induction of carcinogenesis by concurrent inactivation of p53 and Rb1 in the mouse ovarian surface epithelium. *Cancer Res.* **63,** 3459–3463 (2003).
12. Corney, D. C., Flesken-Nikitin, A., Godwin, A. K., Wang, W. & Nikitin, A. Y. MicroRNA-34b and MicroRNA-34c are targets of p53 and cooperate in control of cell proliferation and adhesion-independent growth. *Cancer Res.* **67,** 8433–8438 (2007).
13. Williams, R. M. *et al.* Strategies for high-resolution imaging of epithelial ovarian cancer by laparoscopic nonlinear microscopy. *Transl Oncol* **3,** 181–194 (2010).

14. Kuznetsov, S. G., Haines, D. C., Martin, B. K. & Sharan, S. K. Loss of Rad51c leads to embryonic lethality and modulation of Trp53-dependent tumorigenesis in mice. *Cancer Res.* **69,** 863–872 (2009).

15. Hinz, J. M., Helleday, T. & Meuth, M. Reduced apoptotic response to camptothecin in CHO cells deficient in XRCC3. *Carcinogenesis* **24,** 249–253 (2003).

16. Kondrashova, O. *et al.* Secondary Somatic Mutations Restoring RAD51C and RAD51D Associated with Acquired Resistance to the PARP Inhibitor Rucaparib in High-Grade Ovarian Carcinoma. *Cancer Discov.* **7,** 984–998 (2017).

17. Thompson, E. L. *et al.* FANCI and FANCD2 have common as well as independent functions during the cellular replication stress response. *Nucleic Acids Res.* **45,** 11837–11857 (2017).

18. Tian, Y. *et al.* Constitutive role of the Fanconi anemia D2 gene in the replication stress response. *J. Biol. Chem.* **292,** 20184–20195 (2017).

19. Feng, W. & Jasin, M. BRCA2 suppresses replication stress-induced mitotic and G1 abnormalities through homologous recombination. *Nat. Commun.* **8,** 525 (2017).

20. Nielsen, G. P., Burns, K. L., Rosenberg, A. E. & Louis, D. N. CDKN2A gene deletions and loss of p16 expression occur in osteosarcomas that lack RB alterations. *Am. J. Pathol.* **153,** 159–163 (1998).

21. Zhao, R., Choi, B. Y., Lee, M.-H., Bode, A. M. & Dong, Z. Implications of genetic and epigenetic alterations of CDKN2A (p16(ink4a)) in cancer. *EBioMedicine* **8,** 30–39 (2016).

22. Li, J., Poi, M. J. & Tsai, M.-D. Regulatory mechanisms of tumor suppressor P16(INK4A) and their relevance to cancer. *Biochemistry* **50,** 5566–5582 (2011).

23. Cancer Genome Atlas Research Network. Integrated genomic analyses of ovarian carcinoma. *Nature* **474,** 609–615 (2011).

24. Gao, J. *et al.* Integrative analysis of complex cancer genomics and clinical profiles using the cBioPortal. *Sci. Signal.* **6,** pl1 (2013).

25. Cerami, E. *et al.* The cBio cancer genomics portal: an open platform for exploring multidimensional cancer genomics data. *Cancer Discov.* **2,** 401–404 (2012).

Appendix 3: Supplemental figures and captions for Chapter 2

The following appendix contains supplemental figures and captions for Chapter 2 of this dissertation and a manuscript submitted to Cell Reports (manuscript number CELL-REPORTS-D-20-00575)

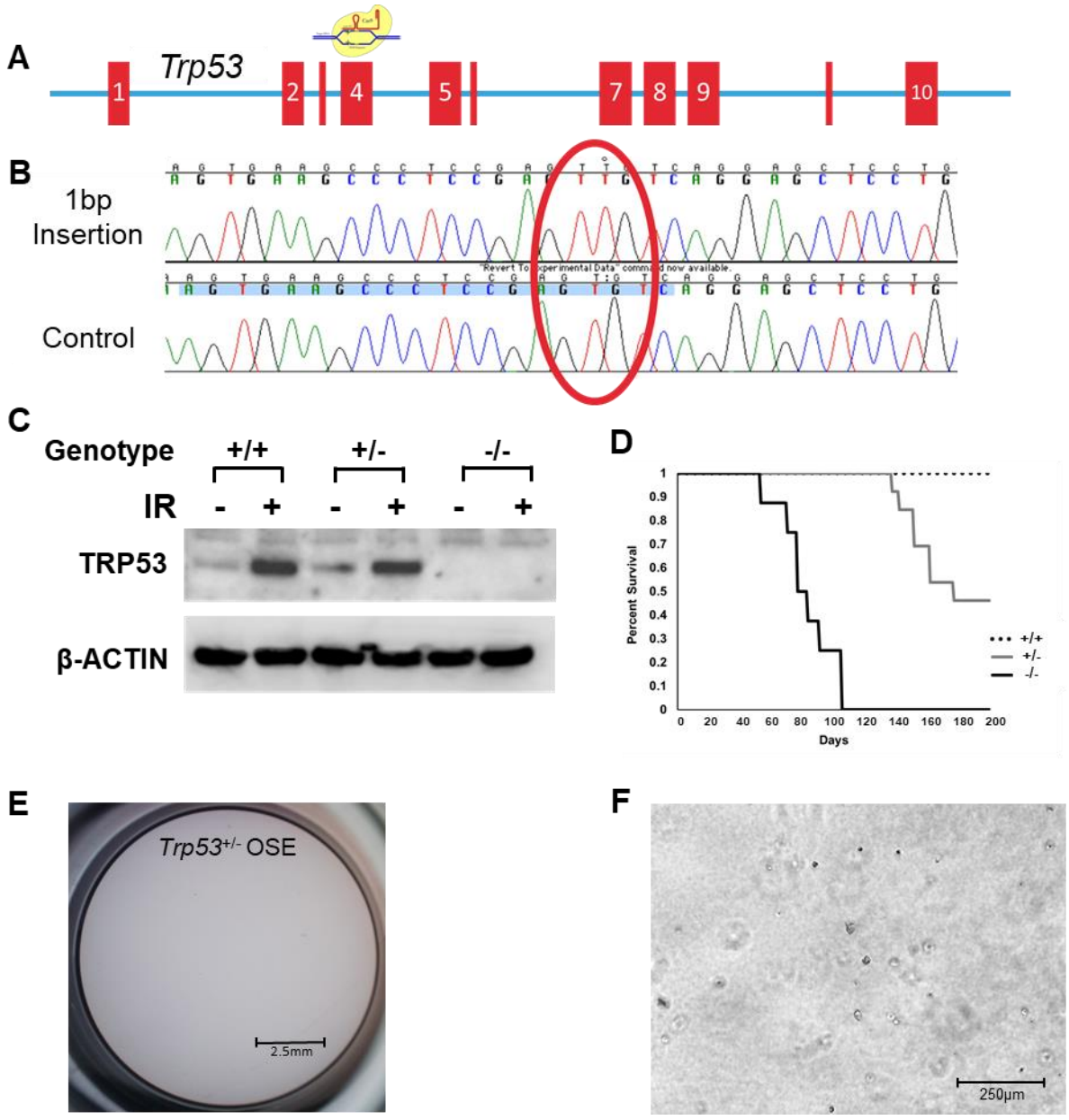

Supplemental Figure 1: Generation of a *Trp53* null mouse line congenic in strain FVB/NJ by genome editing and validation. (A) Schematic of mouse *Trp53* gene and CRISPR/Cas9 targeting of exon 4, which precedes the DNA binding domain of TRP53. **(B)** Sanger sequencing chromatogram of the founder animal used to establish the line. The CRISPR/Cas9 target site is highlighted in blue, and the 1bp insertion in circled in red. **(C)** Western blot analysis of TRP53 levels in MEFs treated (or not) with 10 Gy of

ionizing irradiation (IR). Increased TP53 (due to stabilization) was evident in WT and heterozygous MEFs, but the protein was completely absent in homozygous mutants. ACTB (β-actin) was also detected as a control for equal loading. **(D)** Kaplan-Meier survival plots of female *Trp53*$^{+/+}$, *Trp53*$^{+/-}$, and *Trp53*$^{-/-}$. **(E,F)** *Trp53*$^{+/-}$ ovarian surface epithelium (OSE) cells do not transform in the soft agar assay. No adhesion independent growth was noted for *Trp53*$^{+/-}$ OSE after 14 days.

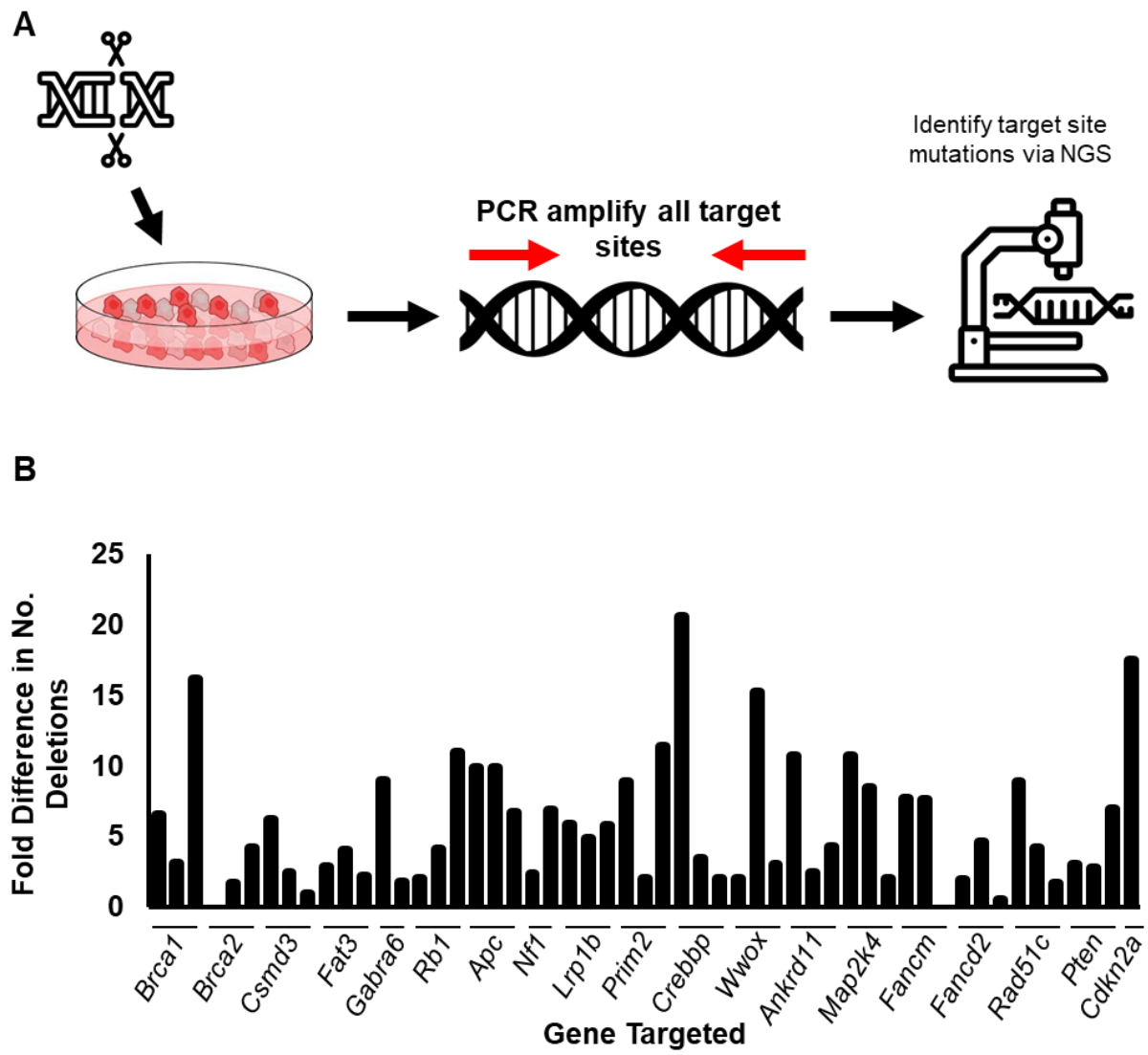

Supplemental Figure 2. Next generation sequencing of minilibrary LentiCRISPRv2 target sites suggests that most constructs cause indels at target sites. (A) Schematic representation of minilibrary validation strategy. **(B)** Fold difference in number of 4+ base pair indels at minilibrary target sites between minilibrary-transduced OSN2 and untransduced OSN2. All minilibrary target sites were PCR-amplified and sequenced using NGS. Each gene name on the X axis represents an individual LentiCRISPRv2 target site. All target sites were assessed except for *Trp53* because OSN2 cells lack *Trp53* alleles. All three *Cdkn2a* target sites are contained

within the same amplicon. Most minilibrary target sites in transduced cells exhibited two-fold or more indels vs target sites in untransduced cells. Constructs unable to cause two-fold or more deletions in target sites vs controls were considered “non-functional” and were redesigned. Target sites that were not amplified or not sequenced were also later validated or redesigned. (NGS = Next Generation Sequencing)

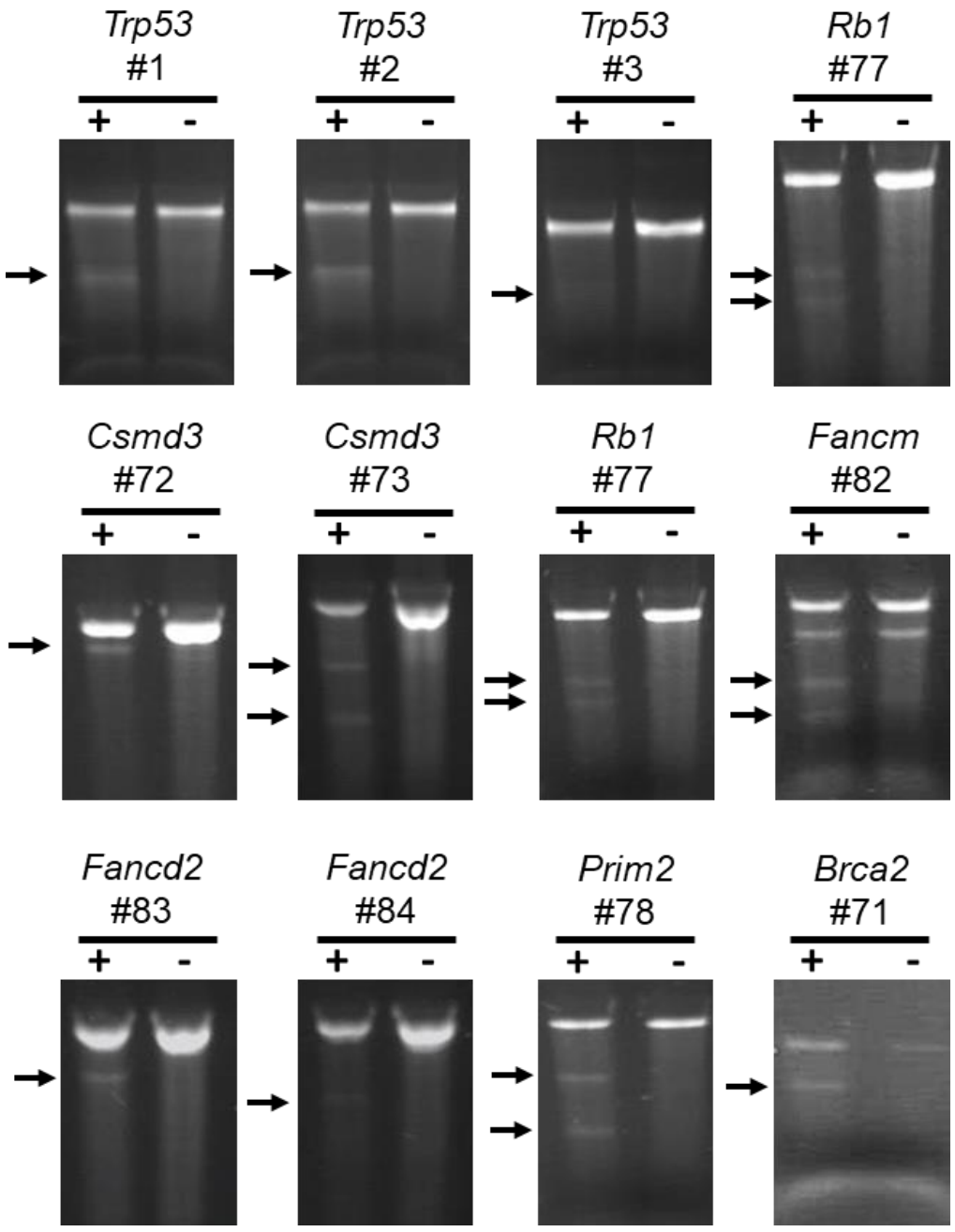

Supplementary Figure 3. Redesigned LentiCRISPRs and LentiCRISPRs targeting Trp53 cause mutations in target sites. LentiCRISPRv2 target sites were PCR-amplified, and mutations were detected using the Surveyor mutagenesis assay (See Methods). The “+” lane represents Surveyor-treated heteroduplexes between edited target site amplicons and corresponding unedited target site amplicons. The “-” lane

contains Surveyor-treated re-annealed amplicons from control, unedited cell DNA. Bands in the “+” lane suggest that a LentiCRISPRv2-induced mutation was present within the edited amplicon, resulting in mismatched DNA and digestion by Surveyor nuclease. Bands in the “-” lane represent background digestion by Surveyor. Arrows indicate bands unique to edited samples, suggesting that mutagenesis following LentiCRISPRv2 targeting occurred.

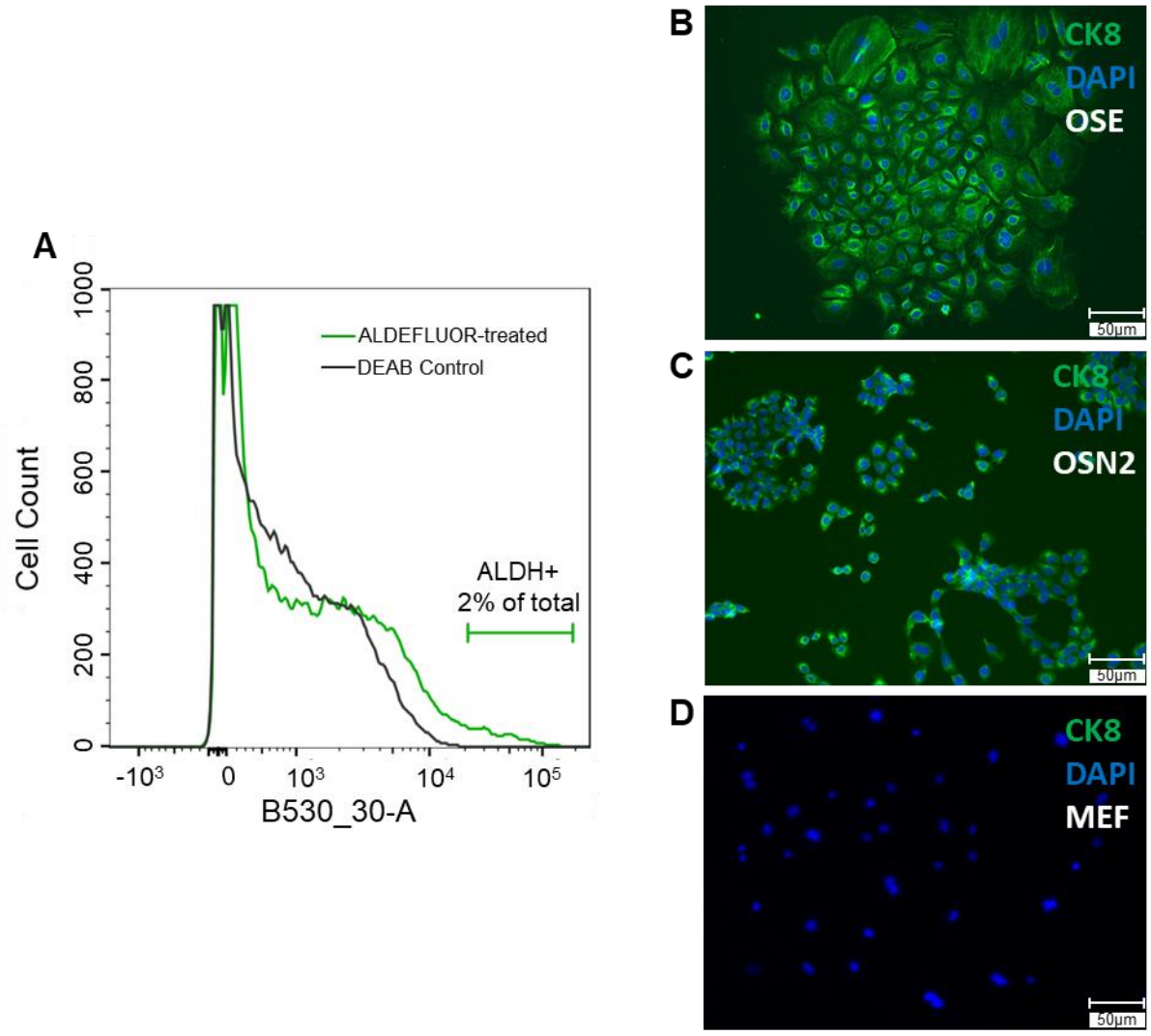

Supplemental Figure 4: OSE contains a small population of ALDH^{+} cells and express the CK8 epithelial marker in culture. (**A)** Isolation of OSE-SC and OSE-NS via FACS sorting. OSE cells were treated with ALDEFLUOR reagent (green line) or ALDEFLUOR plus the DEAB ALDH inhibitor (grey line) (see Methods). ALEFLUOR-treated cells that fluoresced more than DEAB control cells were isolated as an OSE-SC enriched population. Cells with low levels of fluorescence were isolated as OSE-NS. **(B-D)** CK8 epithelial cell marker expression in OSE. OSE was isolated from *Trp53*$^{+/-}$ FVB/N mice. OSN2 cells are an ovarian surface epithelial cell line and a positive control

for CK8 expression, and MEFs from *Trp53*$^{+/-}$ FVB/NJ mice were chosen as a negative control. CK8 was expressed in OSN2 cells and OSE, but not in MEFs.

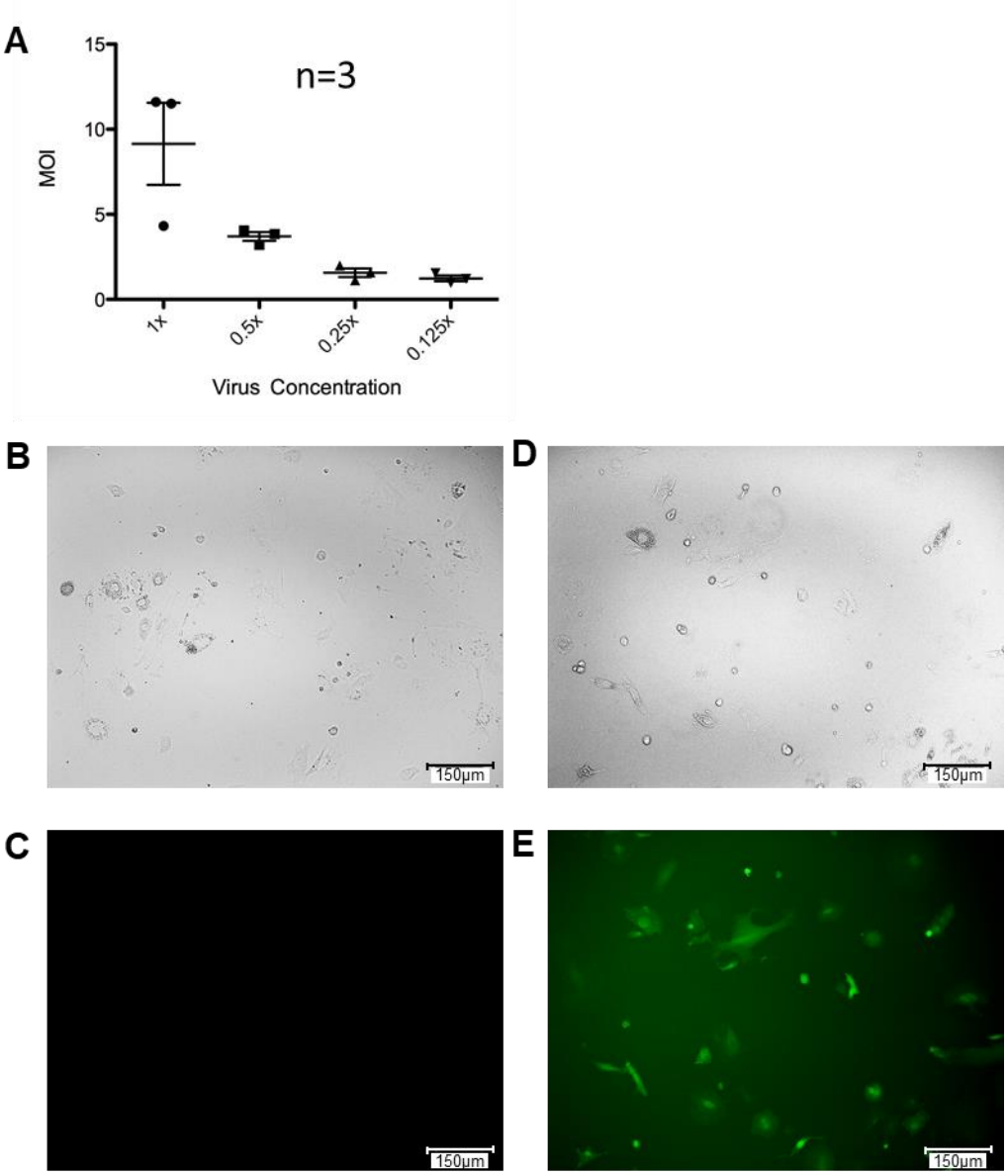

Supplemental Figure 5. Assessment of minilibrary viral titer and FUGW (GFP-expressing lentiviral construct) transduction efficiency. (A) LentiCRISPRv2 MOI in response to serial dilution of concentrated lentivirus. **(B-E)** Expression of GFP in OSE cells transduced with FUGW (GFP-expressing) lentivirus. OSE cells were transduced with FUGW **(D,E)** or remained untransduced as a control **(B,C).** FUGW-transduced

OSE **(D,E)** ubiquitously expressed GFP. No fluorescence was observed for untransduced OSE following imaging using the same exposure time **(B,C).**

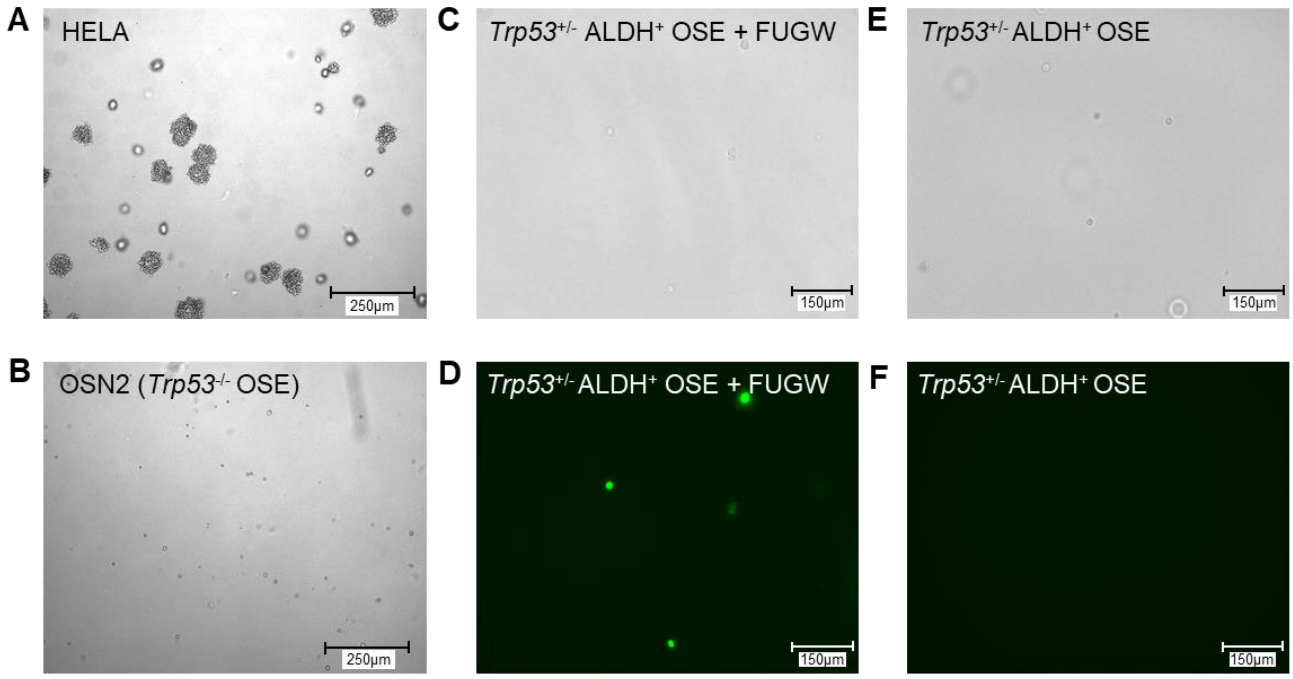

Supplemental Figure 6: *Trp53* mutations and lentiviral transduction are not sufficient for adhesion independent growth of OSE. HELA cells **(A)**, *Trp53*$^{+/-}$ OSE-SC **(E,F)**, *Trp53*$^{-/-}$ OSE (OSN2) **(B)**, and FUGW-transduced (GFP-expressing lentivirus) *Trp53*$^{-/-}$ OSE-SC **(C,D)** were plated in soft agar. Colony growth was noted for HELA cells **(A)**, but not for any OSE genotype or treatment group **(B-F)**. No colonies were observed following FUGW transduction, but GFP expression was noted **(C,D)**. No GFP expression was observed for untransduced *Trp53*$^{+/-}$ OSE-SC **(F)**.

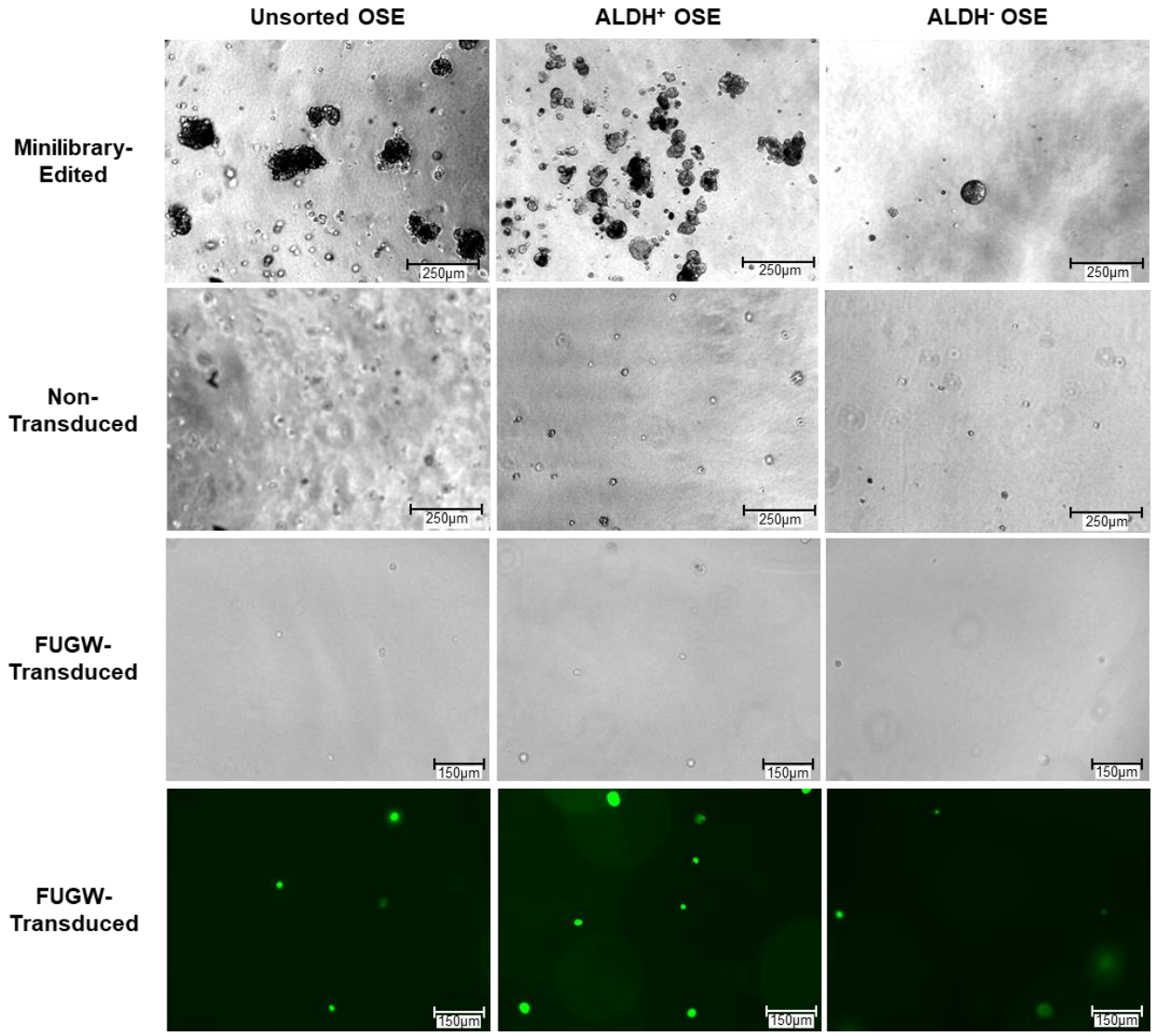

Supplemental Figure 7. Minilibrary transduction, but not FUGW (GFP-expressing lentivirus) transduction, causes transformation of *Trp53*$^{+/-}$ unsorted OSE, OSE-SC, and OSE-NS. The x axis indicates the OSE population being treated. The y axis indicates the treatment given to a corresponding OSE population. Only minilibrary virus transduction resulted in colony growth for all groups. FUGW transduction resulted in GFP expression but no adhesion independent growth. Cells also do not transform if untransduced.

A

Determination of Single Infection Percentage (SIP), n Viral Particles, and Multiplicity of Infection (MOI):

SIP and MOI were calculated using the Poisson Distribution.
m = MOI
n = Number of viral particles
P(survival) = puromycin survival

$$P(n) = \frac{m^n e^{-m}}{n!}$$

$$p(survival) = P(n > 0) = 1 - P(n = 0) = 1 - e^{-m}$$

Solving for SIP as a function of survival:

$$SIP = \frac{P(n = 1)}{P(n \geq 1)} = \frac{P(n = 1)}{P(n > 0)} = \frac{\big(1 - p(survival)\big)\ln(1 - p(survival))}{p(survival)}$$

B

Probability of a single gene being targeted at random:

$$\frac{Ways\ to\ get\ at\ least\ 1\ of\ 3\ LentiCRISPRs from\ 60\ total}{Total\ Number\ of\ Possibilities} = \frac{60^7 - 57^7}{60^7} = 0.302$$

Probability of GFP being targeted in any cell:

$$\frac{\#\ ways\ to\ get\ 1\ of\ 60\ LentiCRISPRs}{Total\ Number\ of\ Possibilities} = \frac{60^7 - 59^7}{60^7} = 0.111$$

Supplemental Figure 8. Calculation of MOI (multiplicity of infection), SIP (single infection percentage) and random gene targeting frequency. **(A)** Determining MOI and SIP as a function of LentiCRISPR-transduced cell puromycin survival. **(B)** Probability of random gene targeting in a population of cells transduced with virus with a MOI of 7.

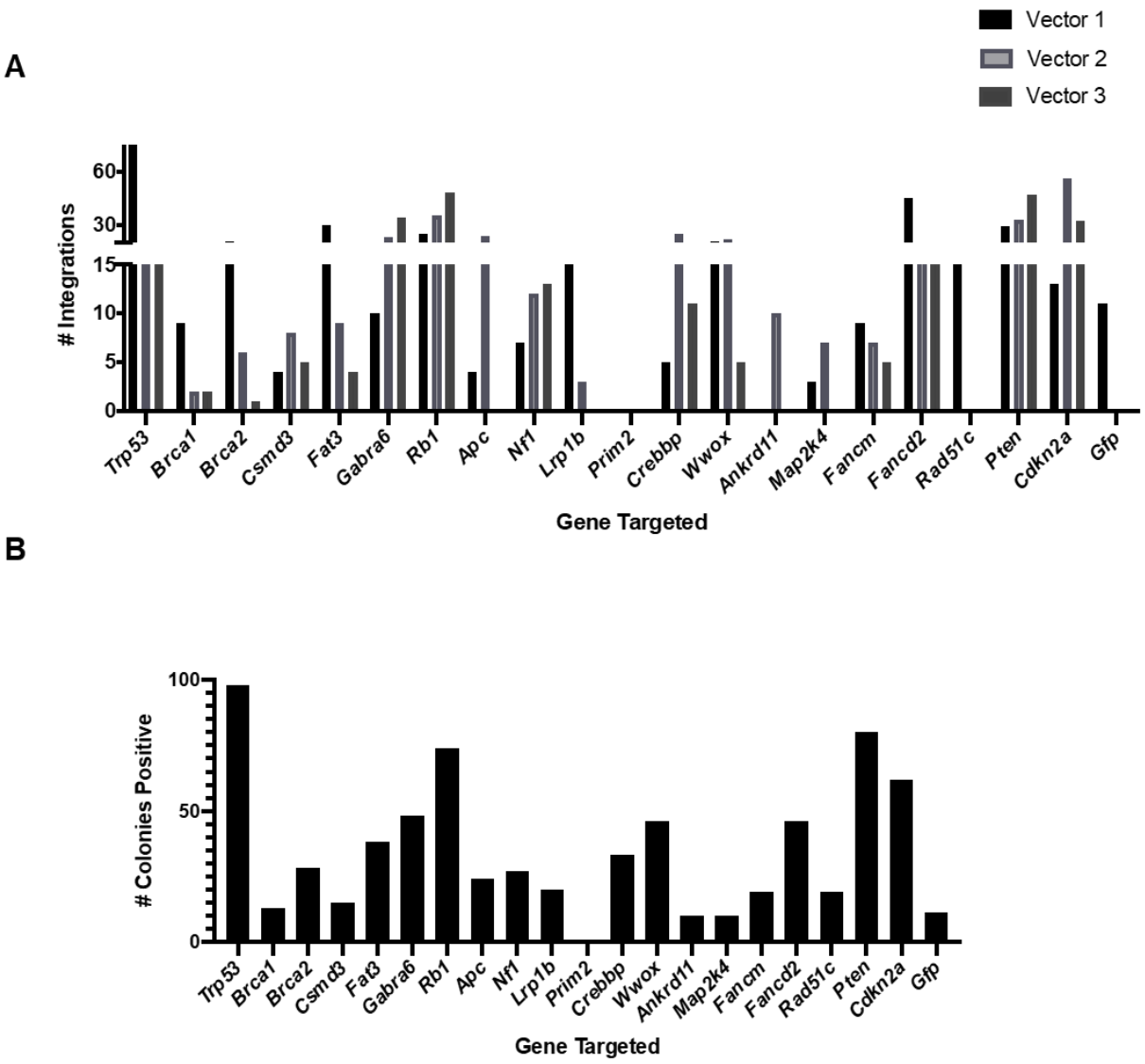

Supplemental Figure 9: Frequently gene "hits" in OSE-SC transformants were targeted by three unique LentiCRISPRv2 constructs. (A) Quantification of individual LentiCRISPRv2 construct genome integrations in OSE-SC transformants. Each bar corresponding to a target gene (x axis) represents an individual LentiCRISPRv2 construct. All genes that were targeted in 30% or more of OSE-SC samples had representation from all three gene-targeting LentiCRISPR constructs. **(B)** Gene targeting frequency among all OSE-SC transformants. LentiCRISPRv2 constructs

targeting each putative HGSOC driver gene were identified in OSE-SC colonies using next generation sequencing. The frequency by which individual genes were targeted by at least one LentiCRISPRv2 construct among all OSE-SC transformants was tallied.

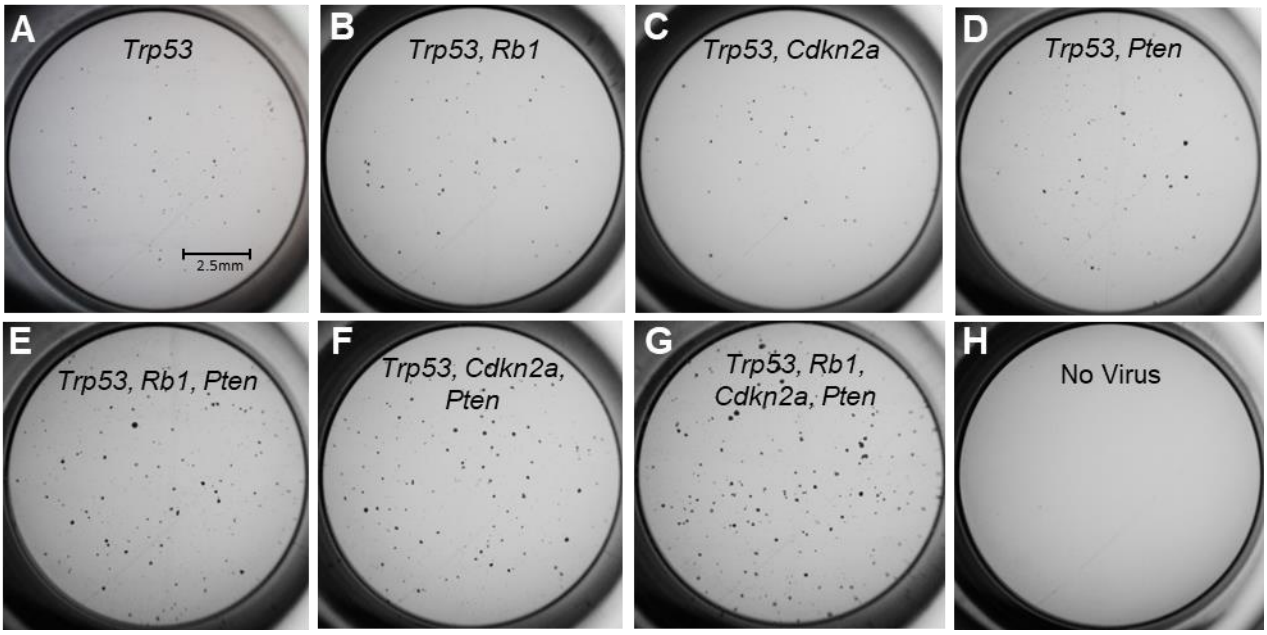

Supplementary Figure 10. *Trp53, Rb1, Cdkn2a, and Pten* function synergistically in OSE-SC transformation initiation. Cells were transduced with LentiCRISPRs targeting *Trp53* alone **(A)**, *Trp53* and *Rb1* **(B)**, *Trp53* and *Cdkn2a* **(C)**, *Trp53* and *Pten* **(D)**, *Trp53*, *Rb1* and *Pten* **(E)**, *Trp53*, *Cdkn2a* and *Pten* **(F)**, *Trp53*, *Rb1*, *Cdkn2a*, and *Pten* **(G)**, or were not transduced as a negative control **(H)**. Adhesion independent growth was observed for all groups except for the untransduced control. The quantity of transformants in each group was tallied for each replicate (n=6). Significant increases in adhesion independent growth vs *Trp53* alone were noted for groups **E, F** and **G** (Students t-test, $p<0.05$).

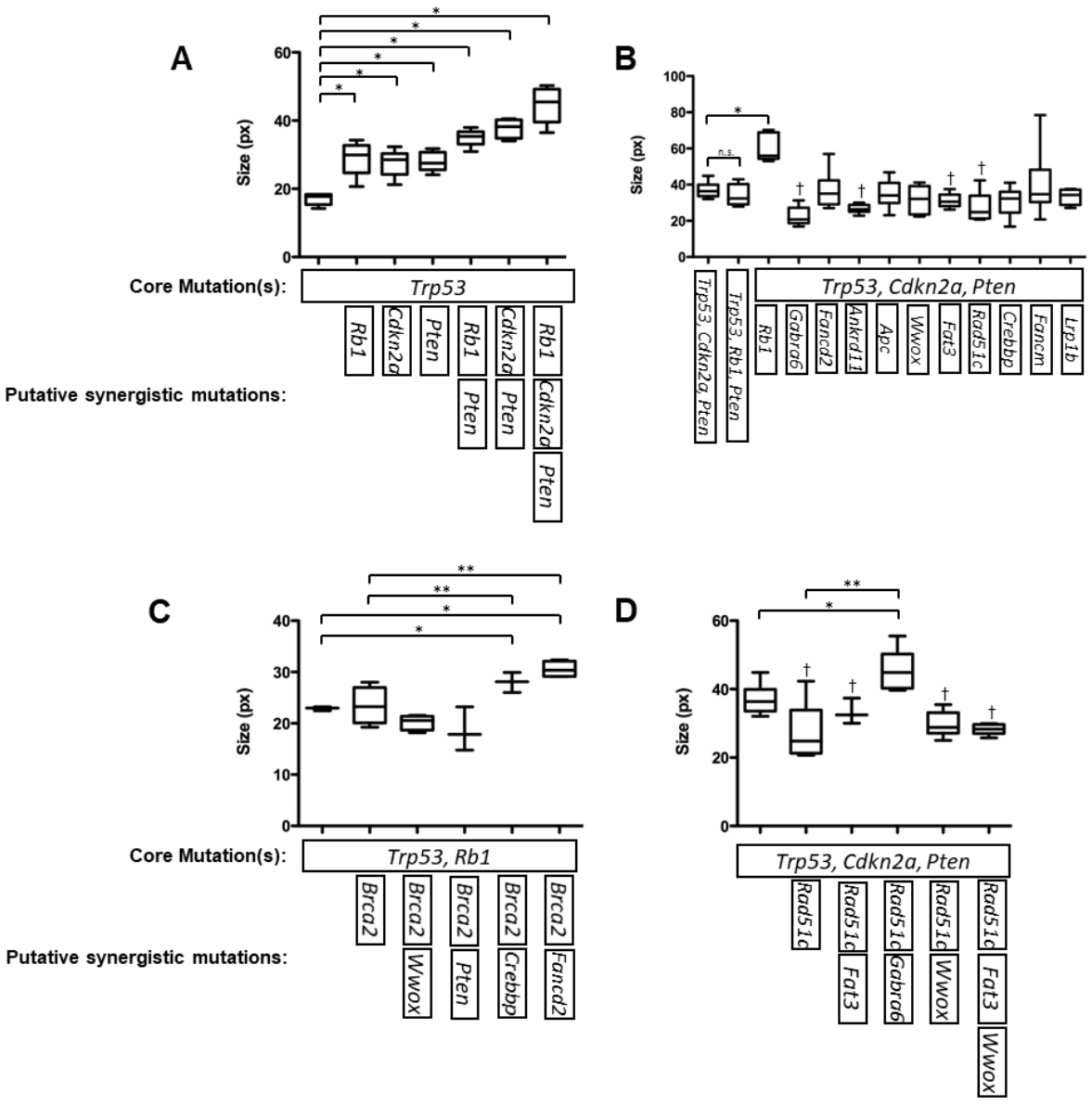

Supplemental Figure 11. Colony size resulting from OSE-SC transformation with targeted sets of LentiCRISPRv2 constructs. A baseline level of adhesion independent growth was first assessed via induction of specific “core mutations”. Additional minilibrary target genes were then mutated alongside core mutations to assess whether they act synergistically to promote adhesion independent growth. **(A)** Targeted transduction of *Trp53*, *Rb1*, *Pten* and *Cdkn2a* LentiCRISPRs in OSE-SC.

(n=6). **(B)** Targeted transduction of *Trp53*, *Cdkn2a* and *Pten* LentiCRISPRs plus putative transformation enhancers. **(C)** Targeted transduction of *Brca2* LentiCRISPRs and *Brca2*-associated LentiCRISPRs. **(D)** Targeted mutagenesis of *Rad51c* LentiCRISPRs and *Rad51c*-associated LentiCRISPRs. Values higher than baseline with Students' two-tailed t-test $p<0.05$ are labeled with an asterisk (*), and those lower than baseline are labeled with an obelisk (†). Standard error of the mean (SEM) error bars. N = 6 in all cases.

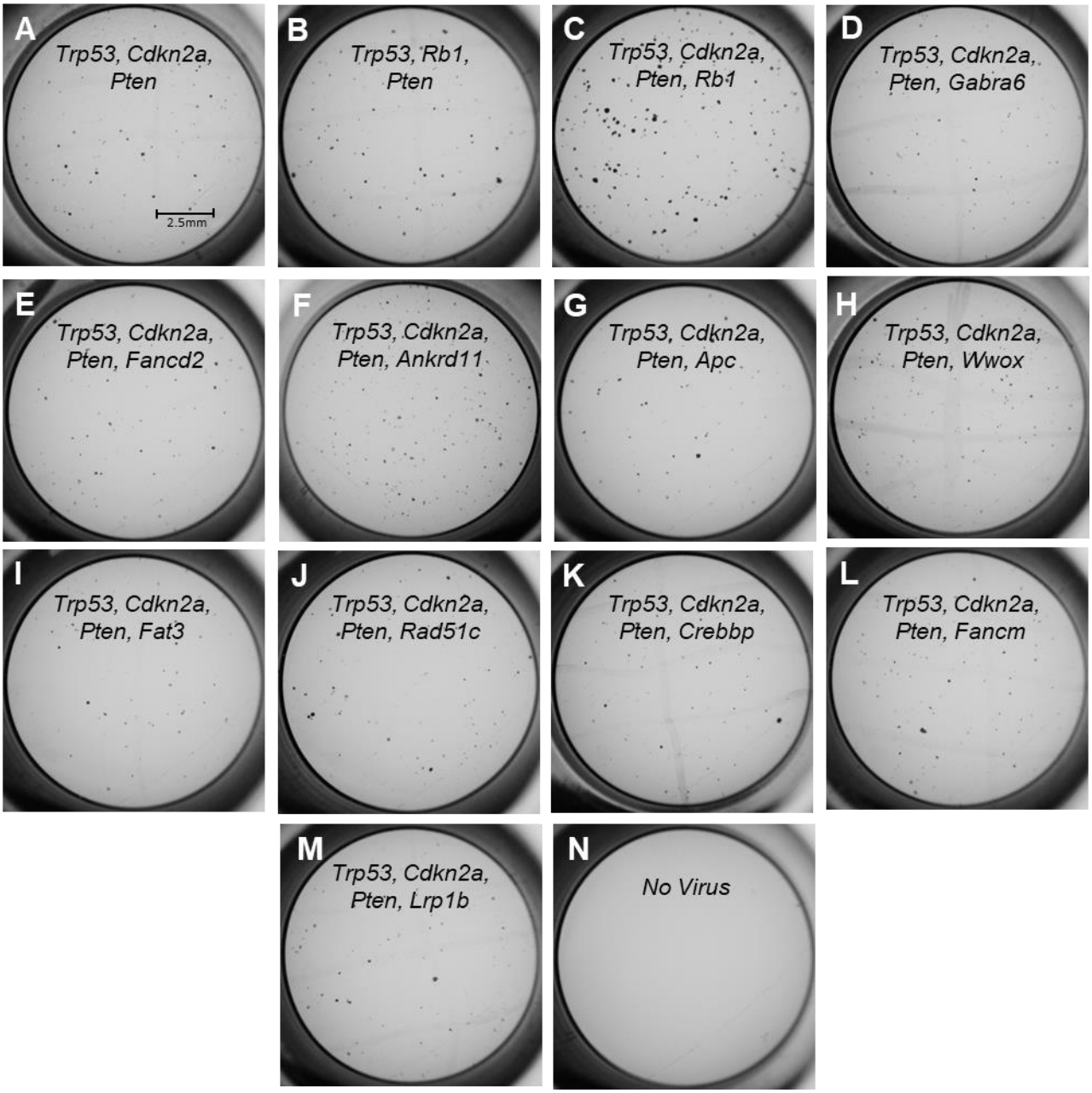

Supplemental Figure 12: LentiCRISPRv2 targeting of *Ankrd11* or *Wwox* alongside *Trp53, Cdkn2a*, and *Pten* causes significant increases in adhesion independent growth vs combined mutagenesis of *Trp53, Cdkn2a*, and *Pten*. Cells were transduced with core mutations in *Trp53*, *Cdkn2a* and *Pten* plus *Rb1* **(C)**, *Gabra6* **(D)**,

Fancd2 **(E)**, *Ankrd11* **(F)**, *Apc* **(G)**, *Wwox* **(H)**, *Fat3* **(I)**, *Rad51c* **(J)**, *Crebbp* **(K)**, *Fancm* **(L)**, *Lrp1b* **(M)**, or were untransduced **(N)**. Adhesion independent growth was noted for all groups except for the untransduced control. The quantity of transformants in each group was tallied for each replicate (n=6). Significant increases in adhesion independent growth were observed following the addition of LentiCRISPRs targeting *Rb1*, *Wwox* or *Ankrd11* (Students t-test, $p<0.05$). Significant decreases in adhesion independent growth were noted following the addition of Fancd2, Apc, Fat3, or Rad51c (Students t-test, $p<0.05$).

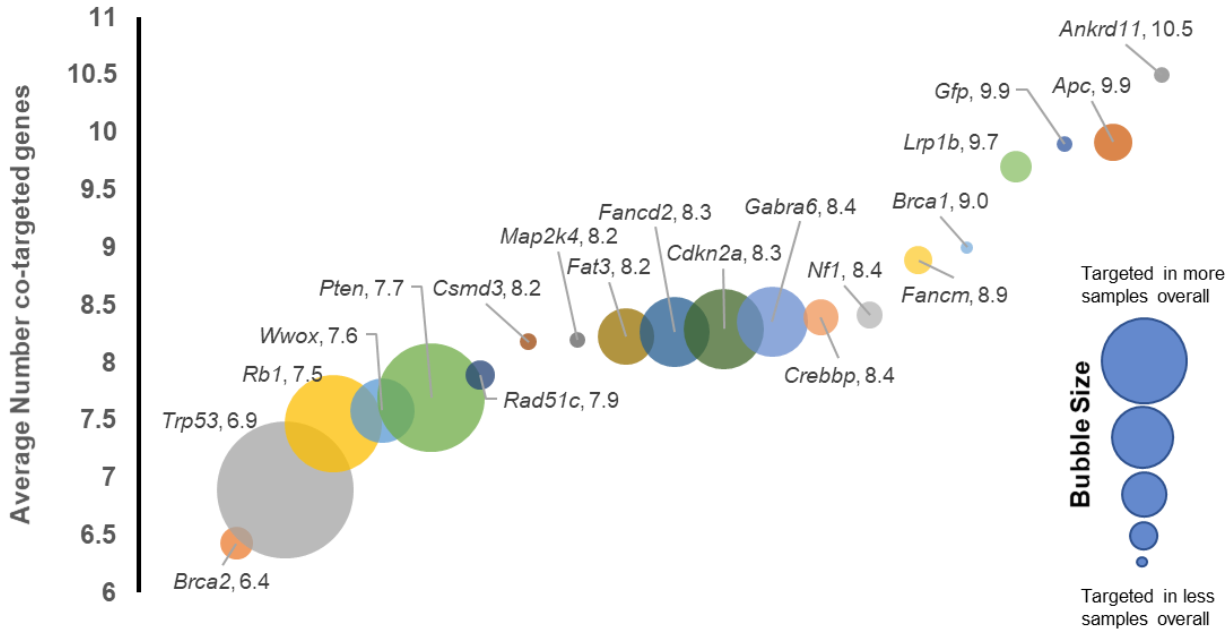

Supplemental Figure 13. Underrepresented minilibrary target genes are frequently found in colonies with greater overall quantities of targeted genes in OSE-SC. The Y axis represents the average number of genes targeted alongside the corresponding gene in the X axis. Bubble size corresponds to the overall number of samples that contain LentiCRISPRs targeting a given gene. Smaller bubbles therefore indicate that a gene is targeted infrequently in OSE-SC samples overall, while a larger bubble indicates that a given gene is frequently targeted. Genes targeted in few samples overall were associated with greater quantities of concurrently targeted genes.

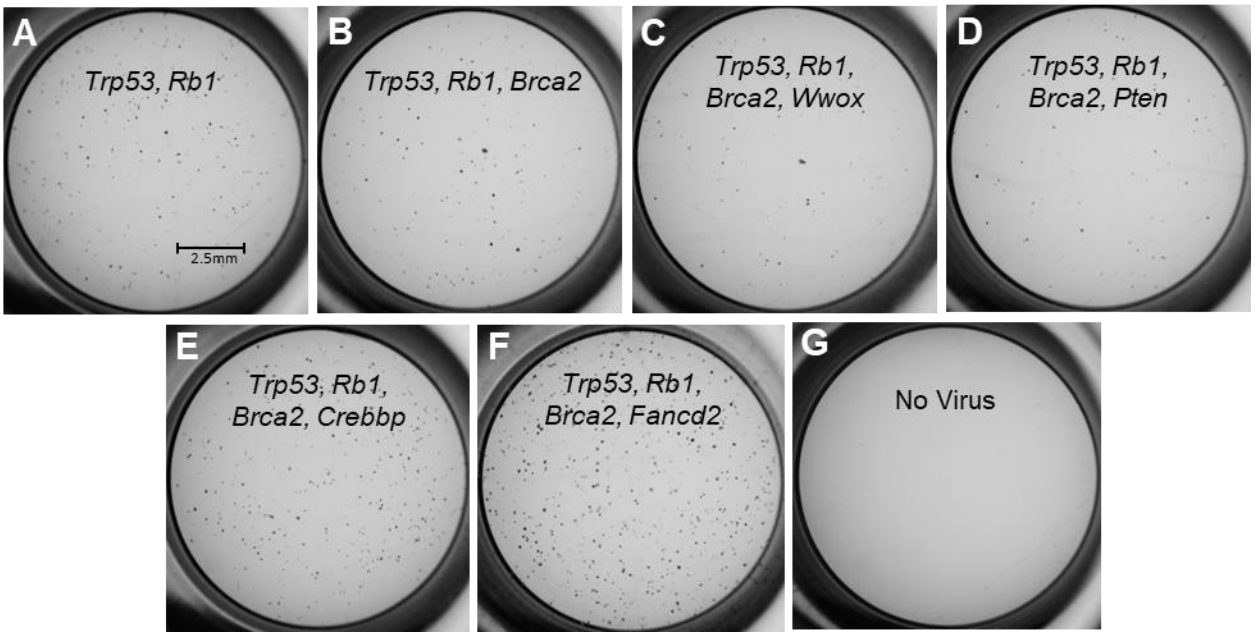

Supplemental Figure 14. *Fancd2* and *Brca2* function synergistically to promote OSE-SC adhesion independent growth. Cells were transduced with LentiCRISPRs targeting *Trp53* and *Rb1* **(A)**, *Trp53*, *Rb1* and *Brca2* **(B)**, *Trp53*, *Rb1*, *Brca2* and *Wwox* **(C)**, *Trp53*, *Rb1*, *Brca2* and *Pten* **(D)**, *Trp53*, *Rb1*, *Brca2* and *Crebbp* **(E)**, *Trp53*, *Rb1*, *Brca2* and *Fancd2* **(F)**, or were not transduced as a negative control **(G).** Adhesion independent growth was observed for all groups except for the untransduced control. The quantity of transformants in each group was tallied for each replicate (n=5). Significant increases in adhesion independent growth vs combined mutagenesis of *Trp53* and *Rb1* were noted only for group **F**. Group **B** had significantly less colonies than combined mutagenesis of *Trp53* and *Rb1* (Students t-test, $p<0.05$).

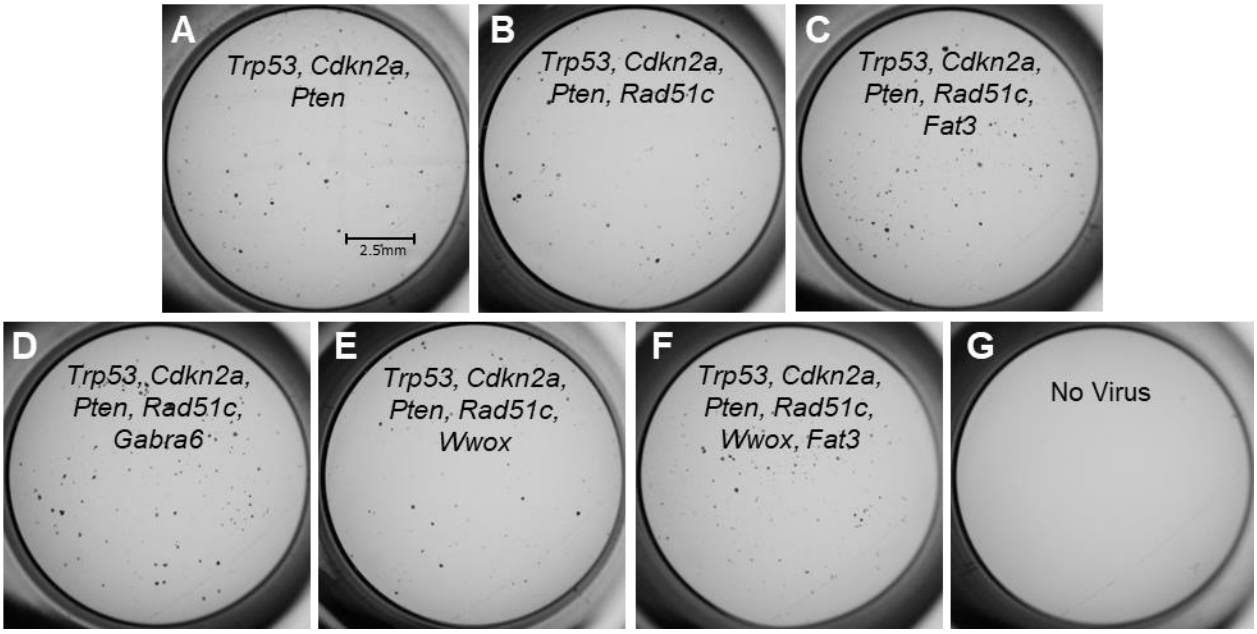

Supplemental Figure 15. Combinatorial mutagenesis of *Trp53*, *Cdkn2a*, *Pten*, *Rad51c* and either *Fat3* or *Gabra6* causes significantly greater colony growth vs disruption of *Trp53*, *Cdkn2a*, *Pten*, and *Rad51c*. Cells were transduced with LentiCRISPRs targeting core genes *Trp53*, *Cdkn2a* and *Pten* **(A)** or *Trp53*, *Cdkn2a*, *Pten* and *Rad51c* **(B)** to establish a baseline degree of adhesion independent growth. OSE-SC were also transduced with LentiCRISPRs targeting *Trp53*, *Cdkn2a*, *Pten, Rad51c* and *Fat3* **(C)**, *Trp53*, *Cdkn2a*, *Pten, Rad51c* and *Gabra6* **(D)**, *Trp53*, *Cdkn2a*, *Pten, Rad51c* and *Wwox* **(E)**, *Trp53*, *Cdkn2a*, *Pten, Rad51c, Wwox* and *Fat3* **(F)** or no virus as a negative control **(G)**. Colonies were observed for all groups except the negative control. Significant increases in adhesion independent growth compared to cells transduced with *Trp53*, *Cdkn2a*, *Pten* and *Rad51c* were noted for groups **C** and **D** (Students t-test, $p<0.05$).

Appendix 4: Supplemental tables for Chapter 2

The following appendix contains supplemental tables for Chapter 2 of this dissertation and a manuscript submitted to Cell Reports (manuscript number CELL-REPORTS-D-20-00575

Table S1: Primers for next generation sequencing used for minilibrary validation

Gene_exon_primer version	Sequence: illumina overhang_primer
BRCA1_4_1	TCGTCGGCAGCGTCAGATGTGTATAAGAGACAGTTTTTCTGCTTATGCAGCATCT
BRCA1_4_1_rev	GTCTCGTGGGCTCGGAGATGTGTATAAGAGACAGAGTCAGAGGCCTTGTGCCTA
BRCA1_6_1	TCGTCGGCAGCGTCAGATGTGTATAAGAGACAGCAGAGACCCTCCTGCTTCTG
BRCA1_6_1_rev	GTCTCGTGGGCTCGGAGATGTGTATAAGAGACAGAGAACACTTGTCCAGCCACT
BRCA1_7_1	TCGTCGGCAGCGTCAGATGTGTATAAGAGACAGTTCATAGTTCTTTCCCTCTGTTCC
BRCA1_7_1_rev	GTCTCGTGGGCTCGGAGATGTGTATAAGAGACAGACCAAAACTCCATGCAACAC
BRCA2_2_1	TCGTCGGCAGCGTCAGATGTGTATAAGAGACAGGTAGCCACTTGGTTGGAAGC
BRCA2_2_1_rev	GTCTCGTGGGCTCGGAGATGTGTATAAGAGACAGGAGAAGTCCACCTGCCTCTG
BRCA2_3_1	TCGTCGGCAGCGTCAGATGTGTATAAGAGACAGCCCCCATGACACAATAATGA
BRCA2_3_1_rev	GTCTCGTGGGCTCGGAGATGTGTATAAGAGACAGTTCTCTGAAAGGCGACTGGT
BRCA2_4_1	TCGTCGGCAGCGTCAGATGTGTATAAGAGACAGGTGCACACCATCCCTTGAG
BRCA2_4_1_rev	GTCTCGTGGGCTCGGAGATGTGTATAAGAGACAGGCAAGATGACGGTTCATGACT
CSMD3_1_1	TCGTCGGCAGCGTCAGATGTGTATAAGAGACAGCCGTTGGAGAGATGGTTGAG
CSMD3_1_1_rev	GTCTCGTGGGCTCGGAGATGTGTATAAGAGACAGAGCTTGCTAGCCTCTCTCAGG
FAT3_1_1	TCGTCGGCAGCGTCAGATGTGTATAAGAGACAGTTGACCGACACACACCAGTT
FAT3_1_1_rev	GTCTCGTGGGCTCGGAGATGTGTATAAGAGACAGCTTTGTCTTTGGCCCTGACT
FAT3_2_1	TCGTCGGCAGCGTCAGATGTGTATAAGAGACAGTGTTAATCTTCTCCTATTTGCCAAG
FAT3_2_1_rev	GTCTCGTGGGCTCGGAGATGTGTATAAGAGACAGAGTTCTGTGGGTTTCCACTTGT
FAT3_4_1	TCGTCGGCAGCGTCAGATGTGTATAAGAGACAGTGAAATGGCCCAGTGAGTAA
FAT3_4_1_rev	GTCTCGTGGGCTCGGAGATGTGTATAAGAGACAGACTCCCTGCTGTGAATTGCT
Gabra_2and2B	TCGTCGGCAGCGTCAGATGTGTATAAGAGACAGGGGATAGTGTGGCTGGTGTC
Gabra_2and2Brev	GTCTCGTGGGCTCGGAGATGTGTATAAGAGACAGTGGTCAGTGATTGAGGAAGG
GABRA_4_1	TCGTCGGCAGCGTCAGATGTGTATAAGAGACAGTGCTGTCTTGATTAAATTTGGAA
GABRA_4_1_rev	GTCTCGTGGGCTCGGAGATGTGTATAAGAGACAGCAATCAGCGTTGATGGTGAG
RB1_1_2	TCGTCGGCAGCGTCAGATGTGTATAAGAGACAGGGGGACGTTCCCATTATTTT
RB1_1_2_rev	GTCTCGTGGGCTCGGAGATGTGTATAAGAGACAGCTCCCTTCCCTTCCCTTCT
RB1_2_1	TCGTCGGCAGCGTCAGATGTGTATAAGAGACAGAAAACTGTGCTGGTGTGTGC
RB1_2_1_rev	GTCTCGTGGGCTCGGAGATGTGTATAAGAGACAGCCACTGCCATCATCACCAT
RB1_4_1	TCGTCGGCAGCGTCAGATGTGTATAAGAGACAGATACTAGGGCCTGGGTTGCT
RB1_4_1_rev	GTCTCGTGGGCTCGGAGATGTGTATAAGAGACAGGCAAAATGGATAAGGCTAGGG
APC_4_1_4B_1	TCGTCGGCAGCGTCAGATGTGTATAAGAGACAGGCAGGGCAAGTTTTAACTATTCT
APC_4_1_4Brev	GTCTCGTGGGCTCGGAGATGTGTATAAGAGACAGCCCACTCCCCTGTTACCTTT
APC_6_1	TCGTCGGCAGCGTCAGATGTGTATAAGAGACAGTTTGGGTTTCTCAAGCATGG
APC_6_1_rev	GTCTCGTGGGCTCGGAGATGTGTATAAGAGACAGTAATGTCCAACAGCCACGAG
NF1_3_1	TCGTCGGCAGCGTCAGATGTGTATAAGAGACAGAGCTTGGAAATTTATTTTTAGGG
NF1_3_1_rev	GTCTCGTGGGCTCGGAGATGTGTATAAGAGACAGTGGGATTTATAAAAGCTGAGAGAA
NF1_4_next	TCGTCGGCAGCGTCAGATGTGTATAAGAGACAGAGCTGTGTGGCTGTTCCTTC
NF1_4_next_rev	GTCTCGTGGGCTCGGAGATGTGTATAAGAGACAGCCTTCAAAAACCCAGATGTCA

LRP_1_1	TCGTCGGCAGCGTCAGATGTGTATAAGAGACAGCTTTCGCTCACCTTCCACAT
LRP_1_1_rev	GTCTCGTGGGCTCGGAGATGTGTATAAGAGACAGGCACTCTGGCACCTAGTTCA
LRP_2_1	TCGTCGGCAGCGTCAGATGTGTATAAGAGACAGGGAGTCAAGTCTGCCAAAGC
LRP_2_1_rev	GTCTCGTGGGCTCGGAGATGTGTATAAGAGACAGAGGCTTCCCATTTCTCTGGT
LRP_3_1	TCGTCGGCAGCGTCAGATGTGTATAAGAGACAGTTTTTGGTGATCAGAACTGTGC
LRP_3_1_rev	GTCTCGTGGGCTCGGAGATGTGTATAAGAGACAGTTGAAGTTCATACTGAGAGACTGGA
PRIM_2_1	TCGTCGGCAGCGTCAGATGTGTATAAGAGACAGTCAGCCTTTTTCCGTCATTT
PRIM_2_1_rev	GTCTCGTGGGCTCGGAGATGTGTATAAGAGACAGATGGGCTGCTGAACAAAGAG
Prim_3_1	TCGTCGGCAGCGTCAGATGTGTATAAGAGACAGCTGCGGAAACAAAGTTGTTAAT
Prim_3_1_rev	GTCTCGTGGGCTCGGAGATGTGTATAAGAGACAGGAGGGTGGGAAACTGCTGTA
Prim_4_1	TCGTCGGCAGCGTCAGATGTGTATAAGAGACAGTGACTGATGGAAGGCAGTTG
Prim_4_1_rev	GTCTCGTGGGCTCGGAGATGTGTATAAGAGACAGATATTCAGCCCATGGCACTC
CREBBP_2_1	TCGTCGGCAGCGTCAGATGTGTATAAGAGACAGTTTTTCTTGTTTTACCTCCCTAAA
CREBBP_2_1_rev	GTCTCGTGGGCTCGGAGATGTGTATAAGAGACAGCCTAAGCTGGCCATGTTTGTA
CREBBP_3_1	TCGTCGGCAGCGTCAGATGTGTATAAGAGACAGTGAGTGAAACTTGTCCTTTCACA
CREBBP_3_1_rev	GTCTCGTGGGCTCGGAGATGTGTATAAGAGACAGGCTTTTCACTGTGAGCACCA
Wwox_2_1	TCGTCGGCAGCGTCAGATGTGTATAAGAGACAGCTGCCCTGCAAGATTCCTT
Wwox_2_1_rev	GTCTCGTGGGCTCGGAGATGTGTATAAGAGACAGGACATCCTTCTGTCCACCTCA
Wwox_3_1	TCGTCGGCAGCGTCAGATGTGTATAAGAGACAGGAGTGCAACAGGGTTTTGGT
Wwox_3_1_rev	GTCTCGTGGGCTCGGAGATGTGTATAAGAGACAGAAGGGTGGAAAACTGCAGAC
Wwox_4_1	TCGTCGGCAGCGTCAGATGTGTATAAGAGACAGTCCAGAGGCCAGAAGGTAGA
Wwox_4_1_rev	GTCTCGTGGGCTCGGAGATGTGTATAAGAGACAGGAGTCACCACCAACGTTTCA
Ankrd11_5_1	TCGTCGGCAGCGTCAGATGTGTATAAGAGACAGACTTCCCCTCATAGGCCTTC
Ankrd11_5_1_rev	GTCTCGTGGGCTCGGAGATGTGTATAAGAGACAGGAACCTCAAGACCCAACCAT
ANKRD11_6_1	TCGTCGGCAGCGTCAGATGTGTATAAGAGACAGGGTCTTGAGGTTCCCATGAA
ANKRD11_6_1_rev	GTCTCGTGGGCTCGGAGATGTGTATAAGAGACAGCGCCCCCAATAAGAAAAAGA
ANKRD11_7_1	TCGTCGGCAGCGTCAGATGTGTATAAGAGACAGATTATGCAAAGCGCCACAAT
ANKRD11_7_1_rev	GTCTCGTGGGCTCGGAGATGTGTATAAGAGACAGCACAAAGCTCACTTCCCAGTC
MAP2K4_1_2	TCGTCGGCAGCGTCAGATGTGTATAAGAGACAGCTCGGCTCTTCACTTCCAAC
MAP2K4_1_2_rev	GTCTCGTGGGCTCGGAGATGTGTATAAGAGACAGACAGCGTTCACCGAAACC
MAP2K4_5_1	TCGTCGGCAGCGTCAGATGTGTATAAGAGACAGCAAGCTAAAGGTTCAGCAGAGG
MAP2K4_5_1_rev	GTCTCGTGGGCTCGGAGATGTGTATAAGAGACAGTGAAGAATGTTCCTCAGATCCA
FancM_1_1	TCGTCGGCAGCGTCAGATGTGTATAAGAGACAGAGAACGCTCTTCCAGACGTG
FancM_1_1_rev	GTCTCGTGGGCTCGGAGATGTGTATAAGAGACAGCCTGTCATTTCAGCCATGTG
FancM_2_1	TCGTCGGCAGCGTCAGATGTGTATAAGAGACAGCCCGGCTTCACTGTTAATTT
FancM_2_1_rev	GTCTCGTGGGCTCGGAGATGTGTATAAGAGACAGCAGCACCCTCTGTTCTGACA
FancM_3_1	TCGTCGGCAGCGTCAGATGTGTATAAGAGACAGATGATTGGTGGTCGTTCCAT
FancM_3_1_rev	GTCTCGTGGGCTCGGAGATGTGTATAAGAGACAGACCTTTAATCCCGGCACTTG
FancD2_2_1	TCGTCGGCAGCGTCAGATGTGTATAAGAGACAGCATTTGGGTGGTTTGGACAG
FancD2_2_1_rev	GTCTCGTGGGCTCGGAGATGTGTATAAGAGACAGAAGCCCTAAGTGGCATTTGA
FancD2_5_1	TCGTCGGCAGCGTCAGATGTGTATAAGAGACAGCTGTGGTGCTTCTGCTTCTG
FancD2_5_1_rev	GTCTCGTGGGCTCGGAGATGTGTATAAGAGACAGTTCCAGTTCTTTGCAATCCA

FancD2_6_1	TCGTCGGCAGCGTCAGATGTGTATAAGAGACAGAACTCATAGCGGGCTGCTT
FancD2_6_1_rev	GTCTCGTGGGCTCGGAGATGTGTATAAGAGACAGTGGCAGATCAACCAGCCTAA
Rad51c_2_1	TCGTCGGCAGCGTCAGATGTGTATAAGAGACAGCCATGCCAGGCTCTGAGTTA
Rad51c_2_1_rev	GTCTCGTGGGCTCGGAGATGTGTATAAGAGACAGTGTATGCTTCTTGGTTTCCTGA
Rad51c_3_1	TCGTCGGCAGCGTCAGATGTGTATAAGAGACAGTTAGACATCTCTTTTGCCTTGG
Rad51c_3_1_rev	GTCTCGTGGGCTCGGAGATGTGTATAAGAGACAGTTTTGCAACAAAAGTATTGGAGA
Rad51c_5_1	TCGTCGGCAGCGTCAGATGTGTATAAGAGACAGTCCAGCACCATCAAAAACTG
Rad51c_5_1_rev	GTCTCGTGGGCTCGGAGATGTGTATAAGAGACAGCCACAAGAACAACCACCAGA
Pten_1_1	TCGTCGGCAGCGTCAGATGTGTATAAGAGACAGGAGAAGCAGGCCCAGTCTC
Pten_1_1_rev	GTCTCGTGGGCTCGGAGATGTGTATAAGAGACAGATCTAGAAATGCGCCCAGAA
Pten_2_1	TCGTCGGCAGCGTCAGATGTGTATAAGAGACAGAGTGAGTGGCTGACTGTCCA
Pten_2_1_rev	GTCTCGTGGGCTCGGAGATGTGTATAAGAGACAGCCAGTTCTCATCCAGTGACG
Pten_5_1	TCGTCGGCAGCGTCAGATGTGTATAAGAGACAGTCTTACACTGGGATTATCTTTTTGC
Pten_5_1_rev	GTCTCGTGGGCTCGGAGATGTGTATAAGAGACAGCAGTTCTCAAAGCATCACACTG
CDK_2A_1	TCGTCGGCAGCGTCAGATGTGTATAAGAGACAGCAACGTTCACGTAGCAGCTC
CDK_2A_1_rev	GTCTCGTGGGCTCGGAGATGTGTATAAGAGACAGCCTAGGCCTTGACCAGGAG
CDK_2B_1	TCGTCGGCAGCGTCAGATGTGTATAAGAGACAGAGAATTCCAAGGCGGGACTA
CDK_2B_1_rev	GTCTCGTGGGCTCGGAGATGTGTATAAGAGACAGCAGCGGAACACAAAGAGCAC
CDK_2C_1	TCGTCGGCAGCGTCAGATGTGTATAAGAGACAGGGCCGTGATCCCTCTACTTT
CDK_2C_1_rev	GTCTCGTGGGCTCGGAGATGTGTATAAGAGACAGGGGTTGCTTCTTCTTTTTCTGA
CSMD3_2_1	TCGTCGGCAGCGTCAGATGTGTATAAGAGACAGTTTGTCTTGTGTTGCAGGATTT
CSMD3_2_1_rev	GTCTCGTGGGCTCGGAGATGTGTATAAGAGACAGTGAAAAACATATTCTTCGCATGA
CSMD3_4_1	TCGTCGGCAGCGTCAGATGTGTATAAGAGACAGGGAGTTCCACCCAAAGGTGT
CSMD3_4_1_rev	GTCTCGTGGGCTCGGAGATGTGTATAAGAGACAGGTTATGCTTTATTTAACAGGTTTTCA
CREBBP_1_1	TCGTCGGCAGCGTCAGATGTGTATAAGAGACAGGTGAAGATGGCCGAGAACTT
CREBBP_1_1_rev	GTCTCGTGGGCTCGGAGATGTGTATAAGAGACAGGCCTCTGGTCGCATTCTCT
MAP2K4_2_1	TCGTCGGCAGCGTCAGATGTGTATAAGAGACAGAAGGCATGTTTCTCTCTTTTTCA
MAP2K4_2_1_rev	GTCTCGTGGGCTCGGAGATGTGTATAAGAGACAGATCAGTCCCTTGCTTTGCAT

Table S2: Primers for surveyor assay

Gene_exon_primer version	Sequence: illumina overhang_primer
TRP53_4_1	TTGTTTTCCAGACTTCCTCCA
TRP53_4_1_rev	GCATTGAAAGGTCACACGAA
TRP53_5_1	TGGTGCTTGGACAATGTGTT
TRP53_5_1_rev	ACGCTGTGGCGAAAAGTCT
TRP53_6_1	GCCATGGCCATCTACAAGAA
TRP53_6_1_rev	GGCAGCTTGCACCTCTAAG
RY_RB1_3_2	GCTTACTCAAAGTTTCCAAAGGA
RY_RB1_3_2_rev	TGCACATGGTGCACTTACCT
RY_CSMD3_5_2	TGAAATGATTAAATGTTTCTCACTGG
RY_CSMD3_5_2_rev	TCTCCCAGTTCTGACAATGC
RY_CSMD3_6_2	TGAAGAATTCTACTTTGCAAGTTTGT
RY_CSMD3_6_2_rev	TTTGTAGCATGCTTTCTGCTG
RY_FancM_2_2	ATAGAGCGAGCTAGCCGTGA
RY_FancM_2_2_rev	CAGCACCCTCTGTTCTGACA
RY_FancD2_8_2	ATTTGGAAGAGCAGCCAGTG
RY_FancD2_8_2_rev	GGCTGTCCTGGAACTCACTC
RY_FancD2_9_2	CCCCTGAACTCACACTCACA
RY_FancD2_9_2_rev	ATGAACAAGTTCCCCTGGTG
RY_PRIM2_6_2	GCCCCATGTAGTGCTAGGAA
RY_PRIM2_6_2_rev	ATCCAGGAGCTTCAGCAATG
RY_BRCA2_5_2	CATGAACCGTCATCTTGCAT
RY_BRCA2_5_2_rev	TACAGGCAGCTCACAACCAC

Table S3: Minilibrary sgRNA sequences and exon targeted

Minilib ID	Sequence	Exon
RY_TRP53_4_1	AGTGAAGCCCTCCGAGTGTC	4
RY_TRP53_5_1	GAAGTCACAGCACATGACGG	5
RY_TRP53_6_1	AAATTTGTATCCCGAGTATC	6
RY_BRCA1_4_1	ATTGTGAAGGCCCTTTCTTC	4
RY_BRCA1_6_1	GGCGTCGATCATCCAGAGCG	6
RY_BRCA1_7_1	GGTGTCCAGCTGTCTAACCT	7
RY_BRCA2_5F	TCTTACTCTGCGGTGCACAC	5
RY_BRCA2_3_1	TAGGACCGATAAGCCTCAAT	3
RY_BRCA2_4_1	GGACTAGCAACATCTACCAC	4
RY_CSMD3_1_1	TTAGCGCATCTTCGCGTGCC	1
RY_CSMD3_5F	TTCATTAGGAAAACCCGGGC	5
RY_CSMD3_6F	GGTAGGGAGCACTAAATCCT	6
RY_FAT3_1_1	GACCTTCACGCTGTAGCTAC	1
RY_FAT3_2_1	AATAGAGAGGGACCACGCCC	2
RY_FAT3_4_1	TTCTGGATGAAAACGACAAC	4
RY_GABRA_2_1	TATGACAACCGTCTACGGCC	2
GABRA_2B_1	AAGGCTATGACAACCGTCTA	2
RY_GABRA_4_1	CCTGACACTTTTTTCCGGAA	4
RY_RB1_3F	TGTAGCTCAGTAAAAGTGAA	3
RY_RB1_2_1	TTGGGAGAAAGTTTCATCCG	2
RY_RB1_4_1	AGAAATCGATACCAGTACCA	4
RY_APC_4_1	AGATCCTTCCCGACTTCCGT	4
RY_APC_4B_1	GGATCTGTATCCAGCCGTTC	4
RY_APC_6_1	GTGCACGCTTCTCCATGTCC	6
RY_NF1_3_1	GTTGATCATATTGGATACAC	3
RY_NF1_4_1	TCCGAAGTTCGGCTGCATGT	4
RY_NF1_4B_1	ACCAACATGCAGCCGAACTT	4
RY_LRP_1_1	GGGATTATTGCCTAACGCTG	1
RY_LRP_2_1	TCGTGGCAAAGAAATTCGCC	2
RY_LRP_3_1	GTCAAAACTGTGCAACGGAG	3
RY_PRIM_2_1	CCGGAAGAAGCTGCGATTGG	2
RY_PRIM2_6F	CCATGATATCCTGTTCCCGA	6
RY_PRIM_4_1	ATGAGTATGAGCCACGGCGA	4
CREBBP_1_1	GTTGTCATTCGCGGAGAAGC	1
CREBBP_2_1	CCATTGGGGATCAGCTCATC	2
CREBBP_3_1	GGACAACCCTTTAGTCAAAC	3

RY_WWOX_2_1	AACATCCGAAAACCGGCAAG	**2**
RY_WWOX_3_1	TTTGCCGTATGGATGGGAAC	**3**
RY_WWOX_4_1	CTTCGTCGGATTATCGTCCA	**4**
ANKRD11_5_1	GTCCGGGCTGTTGTTCGGCA	**5**
ANKRD11_6_1	TGATGAGTTCCTTGATGCGC	**6**
ANKRD11_7_1	TGGCGATGTCGTAATAGCCC	**7**
RY_MAP_1_1	CCAGAAGCTGGAGGTCCGAT	**1**
RY_MAP_2_1	CACCTGTCAAATCGACAGCA	**2**
RY_MAP_5_1	TGTGTTAGATGACGTTATTC	**5**
RY_FancM_1_1	GTCCAGCTGGTAGTCGCGCA	**1**
RY_FancM_2_1	CACCCACGTAAAGTGTCTTG	**2**
RY_FancM_2F	TTACCATGACCTGCGGTGTC	**2**
RY_FancD2_8F	TAGTTGATTGATAATGAGTC	**8**
RY_FANCD_5_1	GCTGTCTTGTGAGCGCCTGC	**5**
RY_FancD2_9F	ACTGCATCATCTGGGCCGTG	**9**
RY_RAD51_2_1	TCTCGAGCAAGAGCATACCC	**2**
RY_RAD51_3_1	GCCACGCCCCCAAAACATTC	**3**
RY_RAD51_5_1	CATTTAGTAATCGAGTACGA	**5**
RY_PTEN_1_1	GCTAACGATCTCTTTGATGA	**1**
RY_PTEN_2_1	AAAGACTTGAAGGTGTATAC	**2**
RY_PTEN_5_1	TGTGCATATTTATTGCATCG	**5**
RY_CDK_2A_1	GTGCGATATTTGCGTTCCGC	**2**
RY_CDK_2B_1	CGGTGCAGATTCGAACTGCG	**2**
RY_CDK_2C_1	GGCTGGATGTGCGCGATGCC	**2**
Minilib 556 GFP1a	GAGCTGGACGGCGACGTAAA	**GFP**

Appendix 5: Supplemental tables for Chapter 3

The following appendix contains supplemental tables for Chapter 3 of this dissertation.

Table S1: HGSOC-associated gene sets published by Maniati et al. (2020)

Gene Sets
GO_POSITIVE_REGULATION_OF_CYTOKINE_SECRETION
GO_CELLULAR_RESPONSE_TO_MECHANICAL_STIMULUS
GO_POSITIVE_REGULATION_OF_PEPTIDYL_TYROSINE_PHOSPHORYLATION
GO_POSITIVE_REGULATION_OF_CELL_DIVISION
GO_RESPONSE_TO_TRANSFORMING_GROWTH_FACTOR_BETA
KEGG_ECM_RECEPTOR_INTERACTION
REACTOME_CELLULAR_RESPONSE_TO_HYPOXIA
GO_WOUND_HEALING
GO_CELL_MATRIX_ADHESION
GO_AXON_GUIDANCE
GO_EXTRACELLULAR_MATRIX
GO_ANGIOGENESIS
GO_ACTIVATION_OF_IMMUNE_RESPONSE
GO_POSITIVE_REGULATION_OF_ADAPTIVE_IMMUNE_RESPONSE
GO_INFLAMMATORY_RESPONSE
GO_POSITIVE_REGULATION_OF_CELL_PROLIFERATION
KEGG_CYSTEINE_AND_METHIONINE_METABOLISM
KEGG_LYSINE_DEGRADATION
KEGG_TYROSINE_METABOLISM
KEGG_BETA_ALANINE_METABOLISM
KEGG_GLYCOSAMINOGLYCAN_BIOSYNTHESIS_CHONDROITIN_SULFATE
KEGG_GLYCOSPHINGOLIPID_BIOSYNTHESIS_GLOBO_SERIES
KEGG_AMINOACYL_TRNA_BIOSYNTHESIS
KEGG_DRUG_METABOLISM_CYTOCHROME_P450
KEGG_DRUG_METABOLISM_OTHER_ENZYMES
KEGG_RNA_DEGRADATION
KEGG_ERBB_SIGNALING_PATHWAY
PID_NFKAPPAB_CANONICAL_PATHWAY
GO_RNA_SURVEILLANCE
GO_MRNA_TRANSPORT
PID_FOXO_PATHWAY
KEGG_P53_SIGNALING_PATHWAY
KEGG_SNARE_INTERACTIONS_IN_VESICULAR_TRANSPORT
GO_REGULATION_OF_ENDOPLASMIC_RETICULUM_UNFOLDED_PROTEIN_RESPONSE
KEGG_ENDOCYTOSIS
KEGG_MTOR_SIGNALING_PATHWAY
REACTOME_REGULATION_OF_RHEB_GTPASE_ACTIVITY_BY_AMPK
GO_OSTEOCLAST_DIFFERENTIATION
GO_HIPPO_SIGNALING

GO_REGULATION_OF_HIPPO_SIGNALING
KEGG_CELL_ADHESION_MOLECULES_CAMS
KEGG_ADHERENS_JUNCTION
KEGG_COMPLEMENT_AND_COAGULATION_CASCADES
KEGG_NOD_LIKE_RECEPTOR_SIGNALING_PATHWAY
KEGG_NATURAL_KILLER_CELL_MEDIATED_CYTOTOXICITY
BIOCARTA_TH1TH2_PATHWAY
REACTOME_TNF_SIGNALING
PID_TNF_PATHWAY
KEGG_LEUKOCYTE_TRANSENDOTHELIAL_MIGRATION
GO_SYNAPTIC_VESICLE_CYCLE
KEGG_LONG_TERM_DEPRESSION
GO_PHOTOTRANSDUCTION
KEGG_INSULIN_SIGNALING_PATHWAY
KEGG_PROGESTERONE_MEDIATED_OOCYTE_MATURATION
GO_INTRACELLULAR_ESTROGEN_RECEPTOR_SIGNALING_PATHWAY
KEGG_MELANOGENESIS
GO_PROLACTIN_SECRETION
GO_THYROID_HORMONE_MEDIATED_SIGNALING_PATHWAY
REACTOME_GLUCAGON_SIGNALING_IN_METABOLIC_REGULATION
GO_RENIN_SECRETION_INTO_BLOOD_STREAM
GO_REGULATION_OF_SYSTEMIC_ARTERIAL_BLOOD_PRESSURE_BY_CIRCULATORY_RENIN
KEGG_TYPE_II_DIABETES_MELLITUS
GO_GASTRIC_ACID_SECRETION
GO_PANCREATIC_JUICE_SECRETION
GO_BILE_ACID_SECRETION
KEGG_HUNTINGTONS_DISEASE
BIOCARTA_SALMONELLA_PATHWAY
KEGG_PANCREATIC_CANCER
KEGG_NON_HOMOLOGOUS_END_JOINING
KEGG_HOMOLOGOUS_RECOMBINATION
KEGG_MISMATCH_REPAIR
KEGG_GLIOMA
KEGG_BASAL_CELL_CARCINOMA
KEGG_BLADDER_CANCER
KEGG_CHRONIC_MYELOID_LEUKEMIA
KEGG_ACUTE_MYELOID_LEUKEMIA
KEGG_NON_SMALL_CELL_LUNG_CANCER
LIU_BREAST_CANCER
KEGG_PENTOSE_PHOSPHATE_PATHWAY
REACTOME_REGULATION_OF_KIT_SIGNALING
REACTOME_CELL_CELL_COMMUNICATION
REACTOME_ELASTIC_FIBRE_FORMATION

REACTOME_METABOLISM_OF_NUCLEOTIDES
REACTOME_SYNTHESIS_OF_GLYCOSYLPHOSPHATIDYLINOSITOL_GPI
REACTOME_GLYCOSAMINOGLYCAN_METABOLISM
REACTOME_INTEGRATION_OF_ENERGY_METABOLISM
REACTOME_HEPARAN_SULFATE_HEPARIN_HS_GAG_METABOLISM
REACTOME_GAMMA_CARBOXYLATION_HYPUSINE_FORMATION_AND_ARYLSULFATASE_ACTIVATION
REACTOME_SYNTHESIS_OF_PIPS_AT_THE_PLASMA_MEMBRANE
REACTOME_SPHINGOLIPID_DE_NOVO_BIOSYNTHESIS
REACTOME_NUCLEOTIDE_BINDING_DOMAIN_LEUCINE_RICH_REPEAT
REACTOME_ALTERNATIVE_COMPLEMENT_ACTIVATION
REACTOME_SYNTHESIS_OF_IP2_IP_AND_INS_IN_THE_CYTOSOL
REACTOME_ACTIVATION_OF_TRKA_RECEPTORS
REACTOME_SYNTHESIS_OF_BILE_ACIDS_AND_BILE_SALTS
REACTOME_P75NTR_REGULATES_AXONOGENESIS
REACTOME_BILE_ACID_AND_BILE_SALT_METABOLISM
REACTOME_METABOLISM_OF_WATER_SOLUBLE_VITAMINS_AND_COFACTORS
REACTOME_A_TETRASACCHARIDE_LINKER_SEQUENCE_IS_REQUIRED_FOR_GAG_SYNTHESIS
REACTOME_AKT_PHOSPHORYLATES_TARGETS_IN_THE_CYTOSOL
REACTOME_IMMUNOREGULATORY_INTERACTIONS_BETWEEN_A_LYMPHOID_NON_LYMPHOID
REACTOME_METABOLISM_OF_NITRIC_OXIDE
REACTOME_HS_GAG_DEGRADATION
REACTOME_ENOS_ACTIVATION
REACTOME_SYNTHESIS_OF_LEUKOTRIENES_LT_AND_EOXINS_EX
REACTOME_ARACHIDONIC_ACID_METABOLISM
REACTOME_ABACAVIR_TRANSPORT_AND_METABOLISM
REACTOME_BINDING_AND_UPTAKE_OF_LIGANDS_BY_SCAVENGER_RECEPTORS
REACTOME_DOWNREGULATION_OF_SMAD2_3
REACTOME_TRANSCRIPTIONAL_ACTIVITY_OF_SMAD2_SMAD3:SMAD4_HETEROTRIMER
REACTOME_VISUAL_PHOTOTRANSDUCTION
REACTOME_SENESCENCE_ASSOCIATED_SECRETORY_PHENOTYPE_SASP
REACTOME_ONCOGENE_INDUCED_SENESCENCE
REACTOME_DNA_DAMAGE_TELOMERE_STRESS_INDUCED_SENESCENCE
REACTOME_NON_INTEGRIN_MEMBRANE_ECM_INTERACTIONS
REACTOME_ECM_PROTEOGLYCANS
REACTOME_METABOLISM_OF_POLYAMINES
REACTOME_CLASS_B_2_SECRETIN_FAMILY_RECEPTORS
REACTOME_SEMAPHORIN_INTERACTIONS
REACTOME_DEACTIVATION_OF_THE_BETA_CATENIN_TRANSACTIVATING_COMPLEX
REACTOME_UNFOLDED_PROTEIN_RESPONSE_UPR
REACTOME_GLUCAGON_LIKE_PEPTIDE_1_GLP1_REGULATES_INSULIN_SECRETION
REACTOME_GLYOXYLATE_METABOLISM_AND_GLYCINE_DEGRADATION
REACTOME_PEROXISOMAL_LIPID_METABOLISM
REACTOME_SIALIC_ACID_METABOLISM

REACTOME_REGULATION_OF_INSULIN_SECRETION
REACTOME_SPHINGOLIPID_METABOLISM
REACTOME_PROTON_COUPLED_MONOCARBOXYLATE_TRANSPORT
REACTOME_BIOSYNTHESIS_OF_THE_N_GLYCAN_PRECURSOR_DOLICHOL_LIPID
REACTOME_SYNTHESIS_OF_SUBSTRATES_IN_N_GLYCAN_BIOSYTHESIS
REACTOME_CELL_EXTRACELLULAR_MATRIX_INTERACTIONS
REACTOME_CELL_JUNCTION_ORGANIZATION
REACTOME_ACTIVATION_OF_THE_AP_1_FAMILY_OF_TRANSCRIPTION_FACTORS
REACTOME_O_LINKED_GLYCOSYLATION
REACTOME_N_GLYCAN_TRIMMING_IN_THE_ER_AND_CALNEXIN_CALRETICULIN_CYCLE
REACTOME_ORGANIC_CATION_TRANSPORT
REACTOME_C_TYPE_LECTIN_RECEPTORS_CLRS
REACTOME_FGFRL1_MODULATION_OF_FGFR1_SIGNALING
REACTOME_TNFR2_NON_CANONICAL_NF_KB_PATHWAY
REACTOME_KERATINIZATION
REACTOME_CA_DEPENDENT_EVENTS
REACTOME_FORMATION_OF_THE_CORNIFIED_ENVELOPE
REACTOME_GLUCONEOGENESIS
REACTOME_BRANCHED_CHAIN_AMINO_ACID_CATABOLISM
REACTOME_ER_QUALITY_CONTROL_COMPARTMENT_ERQC
REACTOME_CALNEXIN_CALRETICULIN_CYCLE
REACTOME_MOLYBDENUM_COFACTOR_BIOSYNTHESIS
REACTOME_COMPLEMENT_CASCADE
REACTOME_RUNX1_REGULATES_GENES_INVOLVED_IN_MEGAKARYOCYTE_DIFFERENTIATION
REACTOME_INTERACTION_WITH_CUMULUS_CELLS_AND_THE_ZONA_PELLUCIDA

Table S2: Low grade carcinoma gene sets

Gene Sets
AGARWAL_AKT_PATHWAY_TARGETS
BIOCARTA_RAS_PATHWAY
BIOCARTA_WNT_PATHWAY
CBIOPORTAL_TOP30_AMP_ENDO
CBIOPORTAL_TOP80_AMP_ENDO
HALLMARK_PI3K_AKT_MTOR_SIGNALING
HALLMARK_WNT_BETA_CATENIN_SIGNALING
KEGG_ENDOMETRIAL_CANCER
KEGG_ERBB_SIGNALING_PATHWAY
KEGG_WNT_SIGNALING_PATHWAY
REACTOME_PI3K_AKT_ACTIVATION
SUNG_2014_ENDOMETRIOID
WAMUNYOKOLI_OVARIAN_CANCER_GRADES_1_2_DN
WAMUNYOKOLI_OVARIAN_CANCER_GRADES_1_2_UP
WAMUNYOKOLI_OVARIAN_CANCER_LMP_DN
WAMUNYOKOLI_OVARIAN_CANCER_LMP_UP